ISTANBUL TECHNICAL UNIVERSITY ★ GRADUATE SCHOOL OF SCIENCE ENGINEERING AND TECHNOLOGY

EXPERIMENTAL AND NUMERICAL INVESTIGATION OF REAR AXLE GEAR WHINE

M.Sc. THESIS

Mehmet DEMIREL

Department of Mechanical Engineering

Machine Dynamic, Vibration and Acoustic Programme

MAY 2019

ISTANBUL TECHNICAL UNIVERSITY ★ GRADUATE SCHOOL OF SCIENCE ENGINEERING AND TECHNOLOGY

EXPERIMENTAL AND NUMERICAL INVESTIGATION OF REAR AXLE GEAR WHINE

M.Sc. THESIS

Mehmet DEMIREL
503121408

Department of Mechanical Engineering

Machine Dynamic, Vibration and Acoustic Programme

Thesis Advisor: Dr. Osman Taha SEN

MAY 2019

ISTANBUL TEKNİK ÜNİVERSİTESİ ★ FEN BİLİMLERİ ENSTİTÜSÜ

ARKA AKS DİŞLİ GÜRÜLTÜSÜNÜN DENEYSEL VE NÜMERİK İNCELENMESİ

YÜKSEK LİSANS TEZİ

Mehmet DEMİREL
503121408

Makina Mühendisliği Anabilim Dalı

Makina Dinamiği, Titreşim ve Akustiği Programı

Tez Danışmanı: Dr. Osman Taha ŞEN

MAYIS 2019

Mehmet Demirel, a M.Sc. student of İTU Graduate School of Science Engineering and Technology student ID 503121408, successfully defended the thesis/dissertation entitled "EXPERIMENTAL AND NUMERICAL INVESTIGATION OF REAR AXLE GEAR WHINE", which he/she prepared after fulfilling the requirements specified in the associated legislations, before the jury whose signatures are below.

Thesis Advisor :	**Dr. Osman Taha SEN** İstanbul Technical University	.....
Jury Members :	**Doc. Dr. Ozgen AKALIN** Istanbul Technical University	.....
	Prof. Dr. Muammer OZKAN Yıldız Technical University	.....

Date of Submission : 03 May 2019
Date of Defense : 12 June 2019

To my family,

FOREWORD

I would like to give my deep appreciation to Dr. Osman Taha ŞEN for his technical support and invaluable advice from beginning of study to end.

I would like to thank to Görkem Coşkun for his great help in every step of this project. And I want to thank Nejat Yüksel, Bülent Küçük, Fatih Şahin, Serkan İmren from the Ford Otosan team for their support during the experimental studies.

May 2019

Mehmet DEMIREL
Mechanical Engineer

TABLE OF CONTENTS

Page

ABBREVIATIONS

NVH	**:** Noise Vibration Harshness
TE	**:** Transmission Error
FEM	**:** Finite Element Method
FDR	**:** Final Drive Ratio
CAE	**:** Computer Aided Engineering
HD	**:** Heavy Duty
AWD	**:** All Wheel Drive
RWD	**:** Rear Wheel Drive
ADC	**:** Analog Digital Converter
CAN	**:** Controller Area Network
FFT	**:** Fast Fourier Transform
LHS	**:** Left Hand Side
RHS	**:** Right Hand Side
KIMOS	**:** Klingelnberg Integrated Manufacturing of Spiral Bevel Gears

SYMBOLS

$\mathbf{f_i}$	**:** Mesh Frequency
$\boldsymbol{\omega_s}$	**:** Pinion Shaft Rotational Speed
$\boldsymbol{\eta_p}$	**:** Number Of Pinion Teeth
$\mathbf{TE_{ang}}$	**:** Angular Transmission Error
$\boldsymbol{\theta_1, \theta_2}$	**:** Gear Angles
$\mathbf{TE_{lin}}$	**:** Linear Transmission Error
$\mathbf{r_b}$	**:** Base Radii of Gear Conjugate Gear
$\boldsymbol{\Delta t}$	**:** Time Interval
$\mathbf{M}$	**:** Mass Matrix
$\mathbf{C}$	**:** Damping Matrix
$\mathbf{K}$	**:** Stiffness Matrix
$\mathbf{x}$	**:** Linear displacement
$\boldsymbol{\omega}$	**:** Natural Frequency
$\boldsymbol{\lambda}$	**:** Eigenvalue
$\boldsymbol{\psi}$	**:** Eigenvectors
$\mathbf{X_i}$	**:** Modal Response Matrix
$\mathbf{N}$	**:** Number of Modes
$\boldsymbol{\eta}$	**:** Structural Damping
$\boldsymbol{\phi}$	**:** Mass Normalized Mode Shape

LIST OF TABLES

Page

LIST OF FIGURES

Page

EXPERIMENTAL AND NUMERICAL INVESTIGATION OF REAR AXLE GEAR WHINE

SUMMARY

In last decades, automotive industry is faced with new regulations and high demands of costumers. And, this situation brings new challenges particularly for noise, vibration and harshness (NVH) development of a vehicle. Especially, powertrain systems of the vehicles have crucial effect on noise level of the vehicle and sound quality. Particularly, in the driveline area of vehicles a noise commonly referred as differential gear whine which is a tonal response and becomes apparent in drive conditions. This is one of the key concerns in rear wheel drive commercial vehicles. Although, not a failure state, it is regarded as a quality issue and a source of annoyance, which can lead to warranty concerns.

There are two main noise and vibration issue sourced from gears as gear rattle and gear whine. First one is the gear rattle, also called gear hammering, which is the characteristic noise that produces during impacting gears. The main reason for this influencing is clearance type nonlinearities, which called backlash. Backlash is clearance between two teeth that are engaged and cause to collapse teeth one side or double side and generate impact noise when one gear try to transfer torque to other. There are several reasons for this collision such as engine torsional vibration and torque characteristic of accessory drive especially highly fluctuated. Second one is gear whine which is a high frequency airborne and structure borne noise produced by the vibration due to the imperfect meshing of the gear teeth. Typical frequencies are in the range of 100Hz to 1000Hz depending on the number of the pinion gear teeth. Whine noise that shows pure tone characteristic is annoying for human aural system compared with random noises so that reduction of the gear systems noise level are crucial. A tonal noise emitted at the gear mesh frequency as assigned first the gear mesh harmonic and sound tone at the double of the mesh frequency as assigned the second harmonic, etc. A tonal gear whine noise appears at the gear mesh harmonics that are multiples of the gear mesh frequency. Rear axle whine, also called axle whine is the special case of the gear whine and one of the audible noises in vehicle cabin. Rear axle whine is sourced from the gears in the differential while engaged condition of gear sets and excited by pinion and ring gears at the gear mesh frequency and its harmonics.

In this study, rear axle gear whine investigation was done in two main approaches as experimental and numerical. Firstly, experimental study to investigate rear axle whine was performed as part level test and vehicle level test. Mainly effect of transmission error (TE) of rear axle was investigated in the thesis. Therefore, nine rear axles that have different TE values were produced and four of them tested in the vehicle. As the test vehicle Ford Trucks 1842T was used. The test vehicle was instrumented for vibration, acoustic, temperature, torque, torsional measurements. Then roads were conducted on test track in particular gears. Test data analyzed by

using Campbell analysis and order analysis methods. Vibration data that cut in critical orders was investigated and compared. Another experimental investigation was done by using modal test and analysis. Modal features of powertrain components were measured in conditions free-free and as-installed. Free-free test was done on the rear axle, cut housing rear axle, half shafts, and driveshaft. Afterwards, modal test of powerpack and driveshaft were performed as installed condition. Based on measurement results, natural frequencies, mode shapes and damping values were calculated.

Secondly, multi-body dynamics model of a heavy duty truck's driveline is developed with all the appropriate components. Component flexibility is included for driveshaft pieces, rear axle half-shafts and the suspension elements. The connectivity of the components is accurately modelled such as the floating effect of rear half-shafts, leaf springs, as well as the non-linear effect of tapered roller bearings, supporting the wheel hubs and gears. Purpose of finding the modal parameters of the components, natural frequency analysis was performed via Nastran software. Then the results were used in multi-body dynamic model. By using multi-body dynamic model axle pinion vibrations were calculated and compared with road test data results.

ARKA AKS DİŞLİ GÜRÜLTÜSNÜN DENEYSEL VE NÜMERİK İNCELENMESİ

ÖZET

Son yıllarda, yeni regülasyonlar ve yüksek müsteri talepleri otomotiv sanayiinin aşması gereken durumlar olarak ortaya çıkmaktadır. Özellikle talep ve istekler sonucunda, araçların titreşim ve akustik akustik geliştirmesinde daha zorlayıcı koşullar doğmaktadır. Günümüzde araçların toplam kalite algısında titreşim ve akutik performansı önemli kriterlerden biri haline gelmiştir. Bu durum bütün araç komponentlerinin ve sistemlerinin daha sessiz çalışması gerekliliğini getirmiştir. Araçlarda oluşan ve şikayete sebep olabilecek titreşim ve gürültülerin oluşmasında, motor ve aktarma organları çok önemli bir paya sahiptir. Aktarma organları kaynaklı titreşim ve gürültüler, sorun durumunda, şikayet ve sistem hasarlarına sebep olabildiği gibi garanti işlemi zorunluluğu nedeni ile ekstra maliyetlerde oluşturmaktadır.

Motor ve aktarma organları gürültü ve titreşim kaynaklarının başında dişli sistemleri gelmektetir. Dişli sistemlerinde meydana gelen titreşim ve gürültüler iki ana kategoride toplanabilir. Bunlar dişli tıkırdaması ve dişli vınlaması olarak adlandırılır. İlk olarak dişli tıkırdamasını ele alırsak, bu sorun, dişlilerin kontak duruma gçmesi sırasında meydana gelen çarpma sesi olarak tarif edilebilir. Bu durumun ana sebebi dişli boşluğu (bekleş) olarak adlandırılan düzgünsüzlüklerdir. Bekleş, birbiri ile karşılıklı çalışan iki dişlinin dişleri arasındaki boşluklardır ve bu boşluklar tork aktarımı esnasında ileri yönde, geri yönde veya her iki yönde de darbe oluşmasına sebebiyet vermektedir. Dişli sistemlerinde meydana gelen bu tıkırtı sorununun motor ve aktarma organlarının burulma titreşimleri, sistemlerdeki yüksek tork salınımına sahip sistemler gibi bir çok nedeni vardır. Dişli sistemlerinde görülen ikinci kritik problem ise dişli vınlaması sorunudur. Dişli vınlaması yüksek frekans bölgesine ortaya çıkan, yapısal ve havayolu iletimi ile aktarılan tonal karakterli bir sestir. Bu sorun dişlilerin pinyon dişlisinin diş sayısına bağlı olarak genellikle 100 Hz ile 3000 Hz aralığında gözlemlenir. Vınlama sesinin tonal yapıda olması, insan duyma sisteminde, çok birleşenli seslere oranda daha rahatsız edici bir etki oluşturur. Bu sebeple dişli yapılarında ses seviyesinin azaltılması kritik etkiye sahiptir. Dişli vınlaması, karşılıklı çalışan dişlilerin dişli geçiş frekansı ve harmoniklerinde ortaya çıkar yani geçiş frakansının matematiksek ikinci, üçüncü, dördüncü katlarında da titreşim ve gürültü seviyeleri yüksektir. Arka aks dişli vınlaması da difransiyel dişlilerinin neden olduğu ve araç içierinde duyulabilir olan özel bir titreşim ve gürültü sorunudur. Difrensiyel piyon dişlisi geçiş frekansında ve onun harmoniklerinde ortaya çıkan bu problemin ana nedeni eş çalışan dişlilerdeki iletim hatası. Teoride dişliler mükemmel rijitlikte ve sabit dişli oranına sahiptir fakat gerçek hayatta dişliler de diğer bütün sistemler gibi elastik özelliktedir ve bu nedenle dişli oranı bazı parametrelere bağlı olarak değişkenlik gösterir bu durum dişli sistemlerinde iletim hatası olarak adlandırılır. İletim hatasına dişlilerin tasarımları, üretim kaynaklı hatalar, üretim ve montaj toleransları, dişli geometrisi oldukça etki

etmektedir. Bu sebeple belirtilen parametrelerde yapılan değişiklikler dişli vınlamasına doğrudan etki etmektedir.
Bu tez çalışması kapsamında dişli vınlama problemi deneysel ve nümerik olarak incelendi. Bu çalışmada sorunun oluşmasında ve seviyesinde en önemli parameter olan dişli iletim hatası üzerinden ilerlendi. İlk olarak bu çalıma kapsamında yapılan deneysel çalışmalarında, parça seviyesi ve araç seviyesi olarak testler ve incelemeler gerçekleştirildi. Öncelikle dişli iletim hatasının etkisinin incelenebilmesi amacı ile farklı özellikte arka akslar tasarlandı ve üretildi. Bu akslar farklı geometrik özellikte ve farklı iletim hatası değerlerinde üretildi. Belirlenen kriterlerde dokuz farklı arka aks üretildi. Bu akslardan dört tanesi araç üzerine takılara test edildi. Araç testlerine başlamadan önemli bir adım olarak test edilecek aracın ve parçaların modal testleri gerçekletirildi. Modal parametreler yapıların, parçaların ve sistemlerin dinamik davranışlarının belirlenmesinde önemli bir etkiye sahiptir ve sağlıklı bir değerlendirme için tespiti zorunludur. Bu kapsamda ilk olarak test edilecek arka akslardan bir tanesi Gölcük test merkezinde yumuşak yaylarla asılarak modal testi tamamlandı. Bu testte üç eksenli ICP ivmeölçerler ile sistem cevapları toplanırken tahrik modal çekiç ve şekır yardımı ile sağlandı. Modal test teknigi olarak tek noktadan tahrik çok noktadan sistem cevabı okunması metodu uygulandı. Test sonucunda arka aksa ait doğal frekanslar, mod şekilleri ve kritik sönüm oranları tespit edilmiştir. Arka aks modal testinin ikinci aşaması olarak arka aks kovanı kesilerek iç paraçaların modal incelmesi gerçekleştirildi. Sistem benzer olarak kovaı kesilen aks yaylar ile asıldı. Sonrasında tekerlek akslar, difransiyel içerisinde bulunan dişliler ve braketlere modal test yapıldı. Bu sistemlerin frekans cevap fonsiyonları, mod frekans değerleri ve mod şekilleri tespit edildi. Parça seviyesi ve asılarak arka aks iç şaftları, tahrik şaftının modal incelemesi gerçekleştirildi. Sonrasında araç üzerinde, yeni sınır şartları ve sistemlerin etkisinin tespiti amacıyla motor, şanzıman ve tahrik şaftının modal testleri tekrarlandı. Deneysel çalışmaların diğer aşaması olarak araç testleri geçekleştirildi. Farklı dişli iletim hatasına sahip akslar sırası ile araca takılarak özel manevralarda testler tamamlandı. Araçtan titreşim, gürültü, burulma titeşimi, açısal hız , sıcaklık, tork dataları toplantı. Bu amaçla arka aks ve şanzıman üzerine üç eksenli iki ivmeölçer yerleştirildi, motor volan bağlantısına, şanzıman çıkışı ve difransiyel girişine açılal hız sensörleri yerleştirildi, difransiyel kovanı delinerek sıcaklık sensörü takıldı ve gürültü ölçümü için kabin içerisine mikrofon yerleştirildi. Aracın enstürmantasyonu, aks vınlama sorunun tespiti ve oluşumuna etki eden komponentlerin, parametrelerin tespit ve incelenmesi amacı gözetilerek gerçekleştirildi. Test aracı olarak tek akstan tahrikli, arkadan çekişli bir Ford çekici araç kullanıldı. Bu aracı seçilmesindeki ana neden basit yapıda bir aktarma sistemine sahip olmasıdır. Bu sebeple, transfer patikasının incelenecek ana probleme etkisi minimum düzeyde olacak ve ölçümler arası sağlıklı bir karşılaştıma yapılabilcektir. Yol testlerinde araç tam yüklü olarak, kritik olan viteslerde ve tam gaz (gaz pedalı %100 pozisyonda olacak şekilde) manevrası ile sürülmüştür. Toplanan datalar özel analiz metodları vasıtası ile incelenerek kritik dişli geçiş frekansları ve harmonikleri tespit edilmiştir. Tespit edilen kritik frakans bantlarında data kesilip analiz edilmiştir. Arka aks ivme datarı kritik frakans bantlarında incelenmiştir.

Tez çalışmasının ikinci ayağı olarak arka aks gürültüsü nümerik olarak incelendi. Test edilen araç özellikleri ve sistemlerinin bilgisayar ortamında tasarımı gerçekleştirildi. Sonrasında tasarımı tamamlanan sistemler Nastran programnda aktarılarak modelleme işlemi gerçekleştirildi. Bu kapsamda bağlantı noktaları, kıstılar, sınır şartları, malzeme özellikleri tanımlandı. Modelleme işlemi sonrasında

yine Nastran programı kullanılarak doğal frekans analizi geçekleştirildi. Bulunan sonuçlar ve test dataları sonuçları karşılaştırılarak modelde olan bilgiler güncellenerek korelesyon çalışması yapıldı. Bu analizler sonucu kritik sistem ve komponentlerin doğal frekansları ve mod şekilleri hesaplandı. Paralelde dişlilerin kontak yüzeylerinin ve sonucunda da dinamik dişli rigitlik değerlerinin hesaplanması KIMOS programı yardımıyla gerçekleştirildi. Son olarak diğer programlardan elde edilen bilgiler de kullanılarak sistemin dinamik analiz modeli oluşturuldu. Daha önce modellenen sistem aynı malzeme özellikleri, sınır şartları ve modal özellikleri ile AVL excite programına aktarılarak dinamik model oluşturuldu. Komponentlerin elastik özellikleri ve kontak durumları tanımlanarak dişli kontak, dinamik iletim hatası etkisi tanımlanarak dinamik analiz tamamlandı. Dinamik analiz sonucu arka aks titreşim değerleri elde edilerek bu değerler test sonucunda ölçülen değerler ile karşılaştırılmıştır.

1. INTRODUCTION

In last two decades, total quality perception of a vehicle has become related with noise radiation from powertrain systems and components. So that motivation to investigate different kind of noise, vibration and harshness (NVH) problems which sourced from the engine power stroke related with the firing order, and transferred from crankshaft and then driveline system has occurred. Then the vibrations and noises depending on selected gear transfer from driveshaft(s) and mounts to the vehicle body [1]. One of the important systems causes NVH problem for the vehicles is differential unit and axle. There can be several possible excitation sources for the differential unit and the axle. They are the engine and the transmission sourced linear and torsional vibrations and road excitations which are transferred from wheel hubs and axle casing. Additionally irregularities in differential unit such as transmission error (TE), backlash, and misalignments can be added. Gear whine also called axle whine is a tonal noise sourced from axle and shows higher characteristic at gear meshing frequency and its harmonics. The gear whine noise is often recognized as the whining noise from formula one cars or reversing cars. Additionally, transfer path can be structural borne or airborne according to system characteristics [2]. Whine noise are appear by presence of TE under torque fluctuations sourced from engine power stroke, at the resonance condition [3]. Human perception of audibility is quite sensitive for tonal noises and even if low level vibration and noises can create annoyance [4]. Rear axle gear whine is a component and/or system level NVH phenomenon. And then its propagation can be described with classical source, path and response NVH model approach. The excitation source of axle whine is dynamic gear mesh force induced by transmission error (TE) that is described as fault in the gear ratio of gear set rotation, tooth contact friction, mesh stiffness change, tooth impact, air and lubricant entrapment, etc. [5]. Computer aided engineering and experimental test have been conducted to define dynamic response of the systems coupled in presence of the TE since 1940s. Additionally finite element model which

are multi degree of freedom and complex systems have been presented to define the gear contact interactions of gear drive [6].

Gear whine noise is a factor which becomes even more important when designing transmissions for commercial vehicles. In such applications, the noise generated from the transmission and axle becomes more distinct since internal combustion engines have become quieter. This master thesis is performed in collaboration with the automotive company Ford Otosan. As noise levels are of increasing concern, the main focus is creating an applicable model for axle whine studies and describing the dynamic behavior of rear axle considering transmission error. This study consists of two main chapters. First one is performing part and vehicle level testing were performed to investigate whine levels according to rear axles belongs different transmission error values which were tested on the end of line bench. The second one is building static and dynamic models by using finite element methods(FEM) tools to correlate models with test data and compare analysis results by experimental study results.

1.1 Problem Definition

The acoustic performance of the powertrain is most critical factor evaluating the overall quality of the vehicle. In recent years the vehicles have to decrease overall interior noise level and to provide that noises and vibration sourced from transmission have become very critical components which decides the overall vehicle value. Noise that is sourced by gear systems can be grouped in two headlines as gear whine and gear rattle. Gear rattling noise is the typical noise which sourced from impacts while gear set working. Backlash which is gap between gear sets and also defined type of nonlinearities in the system is the main source for this impacting [7]. While torque transfer from one gear to another, crash of the gear teeth one side or double side sourced from clearance between two engaged gears or backlash propagates noise and vibration. As the reason of this collision torsional irregularities sourced from the engine and highly oscillated drive torque can be defined. Gear rattle is a deep subject and there are many researches on it but it is not the focus of this study.

Rear axle gear whine, also called hypoid gear whine, is one of the common chronic noise and vibration issues for the vehicle and powertrain systems manufacturers.

Static and dynamic TE can be determined as the major source of axle whine. It is presented as error in gear ratio of the gears because of faults in microgeometry and macro geometry, tooth elasticity and manufacturing errors [8]. In theory completely rigid gears provide constant gear ratio so angular speed at the input and angular speed at the output is a constant quantity. However, in real life, gear pairs have flexible teeth and transmission error which are caused gear whine [6]. Major source of rear axle gear whine noise is gear mesh variation in gear working condition in the differential unit. After then vibration that is occurred in differential transfers by the rear axle gear housing and then suspension components, also pass the vehicle chassis reach to cabin interior as an annoying tonal noise [4, 9]. Though axle noise and vibration caused by gear mesh transfer into the vehicle cabin in all gears and rpm range, whereas in particular rpm and speed range noise and vibration are more effective than other ranges. The main reason of this is due to the amplification of the natural frequency(ies) of vehicle components that are on transfer path of the vibration such as driveshaft, sub frame, chassis, and vehicle body matching with the gear mesh frequency [10].

1.2 Objectives

The aim of this study is to investigate effect of transmission error on gear noises and vibrations especially rear axle gear whines. This investigation was done in two main approaches as experimental and numerical. Firstly experimental studies were done as part level tests and system level tests as installed on the vehicle. Nine different rear axles that have different transmission error were produced according to defined gear parameters. After then four of the axles installed to the test vehicle which is Ford Truck 1848T 4x2 heavy duty with 2,67 final drive ratio (FDR). The test vehicle was instrumented from measurement points which are critical to detect axle whine traces and vehicle test was performed in gears 5th to 12th on test track. Based on test data system level whine judgement was evaluated and system level vibration level within entire torque region in X,Y,Z directions along the engine rpm was determined. For all critical powertrain components modal test was applied in free- free condition and fixed condition as installed on the vehicle. Based on modal test data mode shapes were calculated.

Second investigation was done by using computer aided engineering (CAE) tools. Finite element model created via Msc Nastran and it was optimized with test data. Natural frequency analysis was also performed by using Nastran. Multi body dynamic model was built via AVL Excite Power Unit and system level vibrations computed in this model.

Finally submitting the vibration levels of powertrain attachment points to chassis for whine complaint and imrpoved axles so that the Vehicle Teams can analyze the cabin interior whine levels.

1.3 Limitations

In this thesis following limitations have been introduced:

- Measurement points were chosen on powertrain components. Transfer path of the vibration was not investigated.
- During the road test fuel level of the vehicle was not monitored. Mass effect of the fuel was ignored.
- 4x2 heavy duty(HD) vehicle which is less sensitive to axle whine and has less customer feedback about axle whine noise was used as test vehicle to reduce complexity for investigation and modeling
- Bearing stiffness and forces were defined as supplier information in multibody dynamic model. They were not measured for verification and correlation.
- Backlash between pinion and ring gear was ignored for reducing complexity of dynamic model
- Dynamic stiffnesses of all bearings were provided by suppliers but none of the static damping coefficients, or dynamic damping curves
- Modal tests were done only for powertrain components but none of the chasis and body as installed components were investigated as modal characteristic.

2. LITERATURE REVIEW

In this chapter, literature is reviewed and the relevant theories are explained in detail. Firstly, the phenomena of gear whine noise is discussed and followed the concept of transmission error and mesh stiffness. Thereafter follows a revision of signal processing concepts. The last section explains the method of experimental modal analysis.

2.1 Gear Whine Noise

There are many types of defferent noises associated with gears as mentioned previous chapter and rear axle gear whine is one of perceptible noise in vehicle cabin. Rear axle whine is sourced from the gears in the differential while engaged condition of gear sets and vibrations excited by pinion and ring gears at the gear mesh frequency and its harmonics occur as noise [11]. Axle whine noise is a tonal noise generality appears in 100Hz- 3 kHz region matching with the gear mesh frequency and harmonics. Noise that shows pure tone characteristic is quite annoying for human aural system compared with random noises so that reduction of the gear systems noise level are crucial. A tonal noise emitted at the gear mesh frequency as assigned first the gear mesh harmonic and sound tone at the double of the mesh frequency as assigned the second harmonic, etc. A tonal gear whine noise appears at the gear mesh harmonics that are multiples of the gear mesh frequency [12].

Dunn, Houser & Lim [13] are presented that gear whine noise is named according to dynamic responce emitted from source and is described kind of tonal noise that appears at meshing frequency and its harmonics. And mechanism of gear whine generation defined as shown figure 2.1. Equation 2.1 is showing whine frequency related with driveshaft angular speed and pinion teeth.

$$f_i = \omega_{shaft}\eta_{pinion}\frac{i}{60} \tag{2.1}$$

Where $f_i = i_{th}$ mesh frequency in Hz, ω_{shaft} pinion shaft rotational speed, η_{pinion} = number of pinion teeth and i = 1, 2, 3, … for each harmonic.

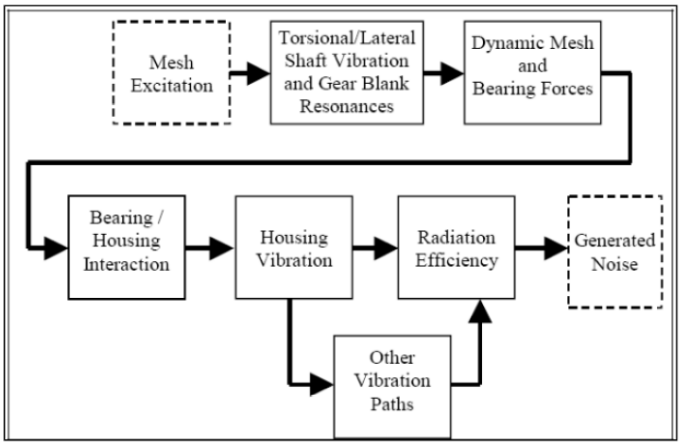

Figure 2. 1: Gears whine generate mechanicm [3].

Many variable affect exciting spreading of the gear whine; mainly they are [2][3]:

- Transmission error
- Variation of meshing stiffness
- Dynamical forces of meshing
- Friction forces
- Detention of air and lubricant between the teeth.

Welbourn [14] is stated that most important factor for gear whine is transmission error (TE) that is introduced as "the difference between the actual position of the output gear and the position it would occupy if the gear drive were perfectly conjugate." And also TE can be expressed differentiation od angular speed between pinion and ring gears. Sum of effects of deflections, geometric errors, and geometric modifications, misalignments bearings, rotational irregularities, linear vibrations, bearings, system resonances take into consideration.

Finite element based model proposed by Sun, Steyer & Ranek[17] that is called block method because components are verified individually and then build up to final model. Main problem of the model by created with the method is unreliable result caused by ignored parameter while individual component validation.

Hirasaka [18] defined a test method to calculate gear connection forces and the dynamic mesh force caused by torsional vibration on the powertrain torsional and to investigate effect of transmission error of gear par on vehicle body and powertrain.

Donley et al. [19] developed a dynamic model of a hypoid gear set for use in finite element analysis of gearing systems. In their gear mesh model, the mesh point and line-of-action are time invariant.

For the investigation of dynamic response of the gear systems dynamic models were improved by researchers, such as [19], [20], [21]. For modeling system response of axle for pressure and angles of the gears, mesh contact point and line action.

Propagation of the whine noise from the differential unit are investigated as three steps excitation, transmission, and radiation. Source of the whine noise is by gear mesh vibrations that are mostly caused by transmission error. The vibrations are transferred thru axle casing from shaft and bearings. Surface of the casing vibrates and energy transmits to air around the system so noise is generated. Based on this information noise can control by making modification on one of the steps. That is presented by MackAldener [15].

Houser [16] is defined that decreasing noise and vibration level by changing on casing is quite hard application by using finite element methods. So modification on

2.2 Transmission Error

In theory, completely rigid gears provide constant gear ratio in the angular velocity of engaged gears. Thus, angular speed at the input and angular speed at the output are constant because of involute gear features [9]. Main thought in this theory is that gears are very rigid and have not any geometrical error but in real life, but they are elastic structures and include different kind of errors that cause irregularities in angular velocity of the gear pairs [3].Transmission error concept is described purpose of the defining irregularities in the angular velocities. Transmission error (TE) is a major contributor of gear noises and vibrations [9]. Additionally Welborn [14] defined TE as the gap between the current position of driven gear and imaginary the position of the output gear with assumption gear teeth are the perfectly rigid gear as assumption.

Another introduction of transmission can be presented by using rotational displacement or linear displacement at the pitch point [9].

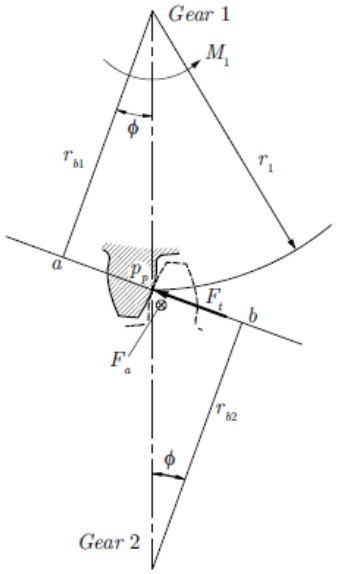

Figure 2. 2: Force elements acting on gear tooth [14].

This difference can be defined a rotational displacement in the position of the gear pair by

$$TE_{ang} = \theta_1 - \frac{r_{b2}}{r_{b1}}\theta_2 \qquad 2.2$$

or as a linear displacement along the line of action according to

$$TE_{lin} = r_{b1}\theta_1 - r_{b2}\theta_2 \qquad 2.3$$

where r_{b1} and r_{b2} are the base radii and θ_1 and θ_2 are the angular positions of Gear 1 and Gear 2 separately can be seen figure 2.3.

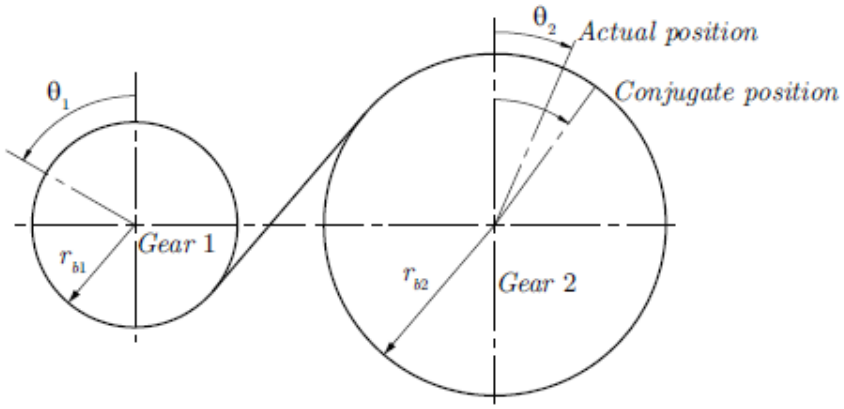

Figure 2. 3: Actual and conjugate positions of gear 1 and gear 2 [8].

Transmitted torque from gear pair is a major factor on the transmission error. When torque value transmitted from gear pair increase, it causes higher distortion on the gear teeth, thus the difference between the current and conjugate position of the driven gear increases due to the elastic feature of the gear teeth. Signal caused by TE can be seen in figure 2.4 [22].

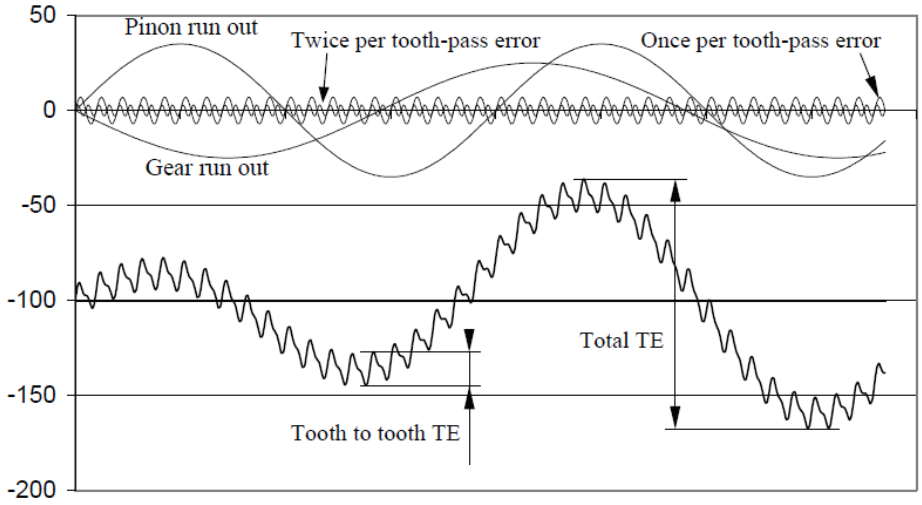

Figure 2. 4: Transmssion error signal [8].

Many factors affect transmission error. The causes of transmission error are deflections, geometrical errors and geometrical modifications [8].

Lee [23] expressed that shape design of the tooth has a major impact on transmission error, Base on measurement results, transmission error value can be decreased nearly

half of current value. Considering tooth profile create nearly perfect coupling of gear pair, transmission error is not possible to be zero because of manufacturing faults in tolerances. Changing on gear tooth shape and surface bring the positive contribution to reduce TE on gear sets have been seen by test and simulations. Additionally those studies define transmission error under load caused by production process. Another important factor to TE is contact ratio that can be introduced mean of total gear teeth number in touch while gear pairs working. Variable tooth mesh stiffness over the rotation angle since teeth meshing and leaving process. Chung et al [24] showed correlation between total averaged gear contact ratio and noise level as shown in figure 2.4.

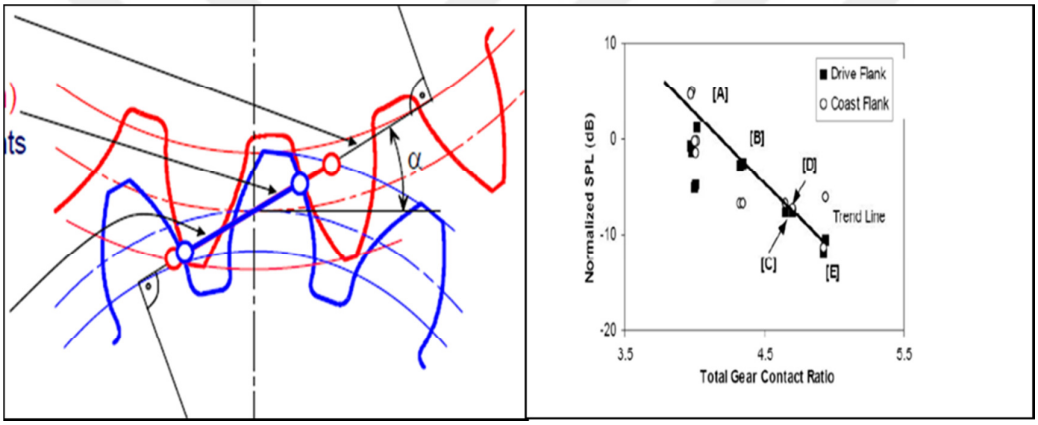

Figure 2. 5: Gear contact and noise level relation [20].

Misalignment in powertrain system is crucial for all wheel drive (AWD) and rear wheel drive (RWD) vehicles so misalignments are conserved with load, tooth profile as the design parameters. On the other hand, in the low load condition gear meshing geometry cannot be ideal so it can create whine noise in acoustic frequency range. Harris [25] defined an experiment to show that contact surface of gear mesh decreases in case to be misalignment sourced by toot profile or montage faults in the driveline system and it cause gear impacts. In addition, same results as reducing contact of gear mesh seen when lead crowning applied.

Maki [26] stated that gear whine cannot totally be prophesied despite gear profile is conserved in analytical model of gear system. Therefore, those macro-misalignments such as teeth deflections and gradient are included the analysis model as shown in figure 2.5. Additionally the model presented that inclination error sourced from teeth deflections and gear mesh as shown figure 2.6 have a major effect on transmission

error when TE difference produced by gear profile and mesh contact does not take in to account.

Transmission error can be measured in different conditions as static loaded or static unloaded, dynamic loaded or dynamic unloaded. Transmission error in condition static unloaded is mostly chosen method to detect production errors and define gear. Test in condition static loaded also contains the gear bias. Transmission error measurements in conditions dynamic loaded and dynamic unloaded are the most appropriate method for NVH assessment. While the dynamic measurement, system have to be as installed condition to define effects of other components such as bearings, casing and shafts that are critical contribution on TE [12].

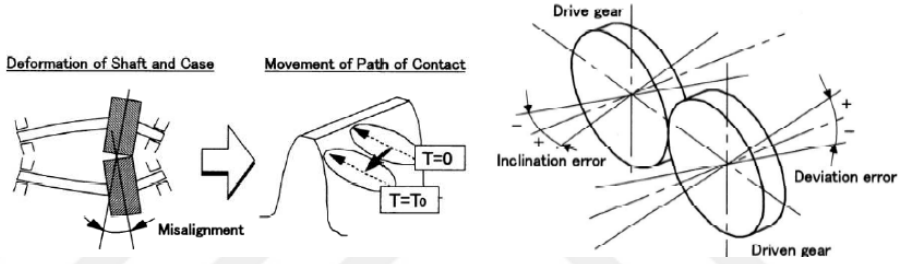

Figure 2. 6: Changing of contact position and gear pair misalignment [26].

2.3 Signal Processing

Digital signal processing is interested with transferring information in the signals and their operations by using number and symbols. Purpose of the digital signal processing is to asses and filter time variant raw analogue signals. Analogue to digital transformation of a signal have to be done with an especial converter also named analogue to digital converter that uses. The raw signal is converted to numbers that is with a 'Δt' time interval. Main goal of the transform from analogue to digital signal is to control the data by using opportunity mathematical calculations and additionally recusing data size [27].

Flow of analogue to digital transform multiplies the signal by a square wave function which is zero around the 'Δt' time and has a value of unity at each 'Δt' producing a noncontagious digital signal at too small time depending on the sampling rate 'Δt' can be seen in figure 2.7 and figure 2.8. Sampling rate is too critical to take reliable analogue signal [27].

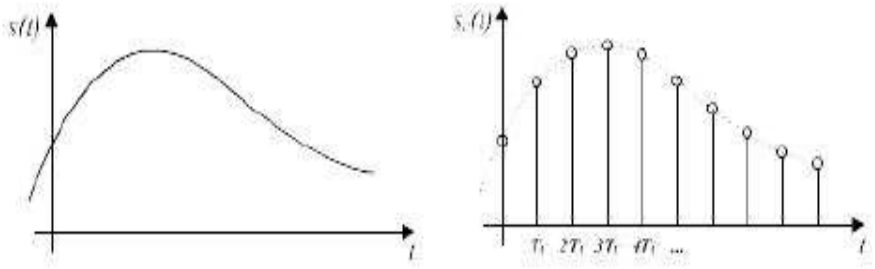

Figure 2. 7: Analogue to digital signal conversion with time sampling period T [27].

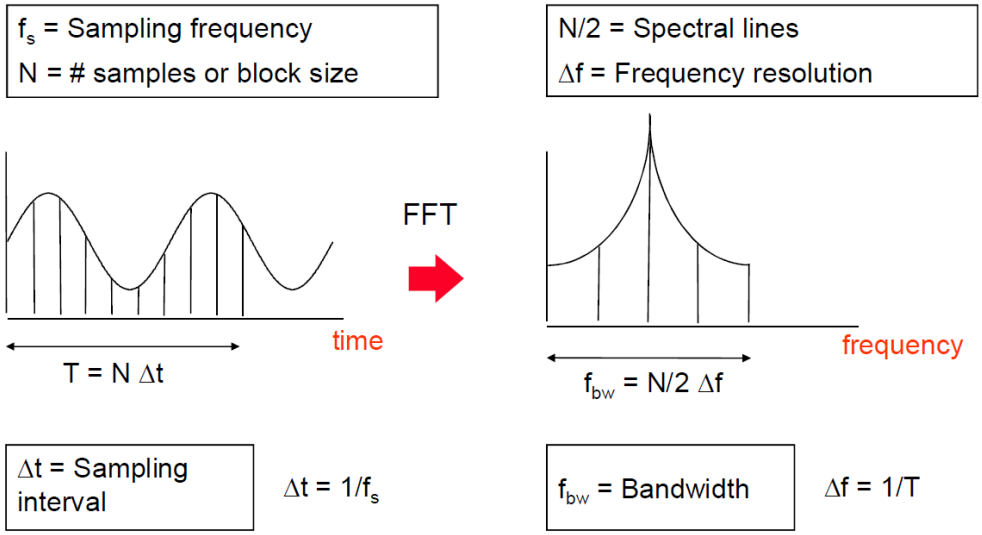

Figure 2. 8: Fast fruer transformation from time domain to frequency domain [28].

Aliasing is an expression which defines as signal comprising high frequency content to seem as low frequencies as depicted in figure 2.9. Main reason of this situation is to sampling rate. Concept of aliasing can be introduced by Nyquist sampling theorem. Actually Nyquist sampling theorem states that an analog signal can be completely rebuilt as an order of samples when the sampling rate is chosen two times more samples per cycle from the highest frequency of related signal as shown in figure 2.9 [27].

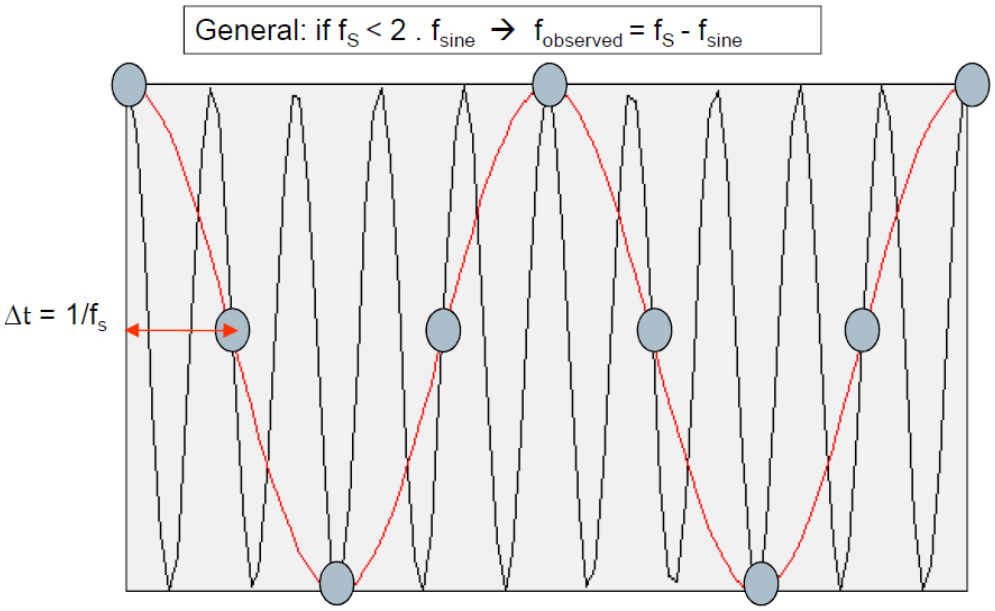

Figure 2. 9: Digital Signal Processin aliasing problem [28].

In theory two times sampling rate of the highest frequency of the interested signal is enough to digitalize that signal. But in real life to make correct analogue to digital conversion spectral mirroring takes into account so forty percent of sampling frequency is defines as alis-free region can be seen in figure 2.10.

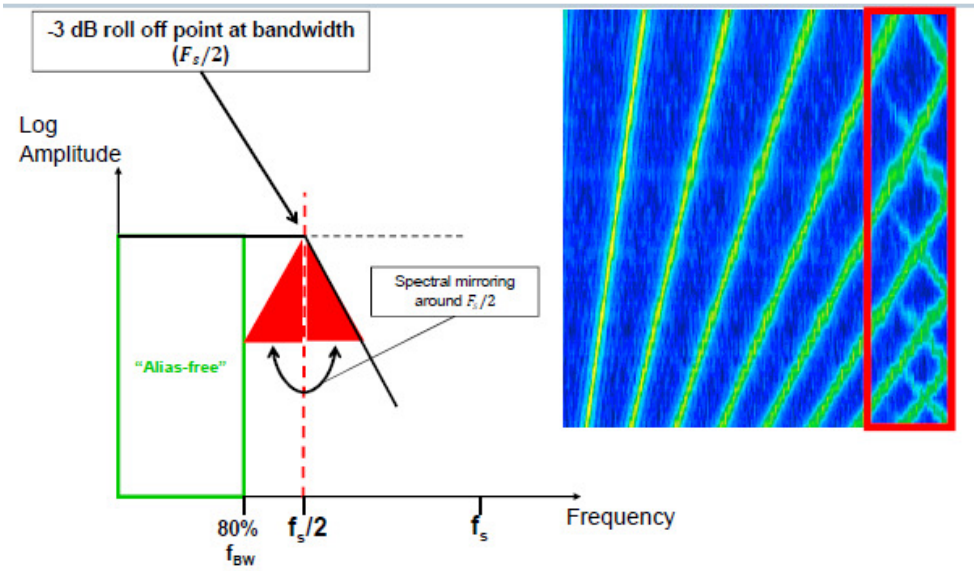

Figure 2. 10: Aliasing – spectral mirroring [28].

Fourier transform is described for periodic waveform and the conversion can be accomplished for periodic signal. Consequently, a signal qualified in particular time interval can be described by sum of sine function and cosines functions. In case of

non-periodicity, another analogue to digital conversion problem which is called as leakage can occur because of failure in splitting the signal at particular integral multiples of its period. As a result of that incorrect frequencies become visible in digital window of the signal as smearing of spectral content to neighbouring lines as shown figure 2.11. As Fourier Transforms assumes that a signal is periodic within the sample record length.

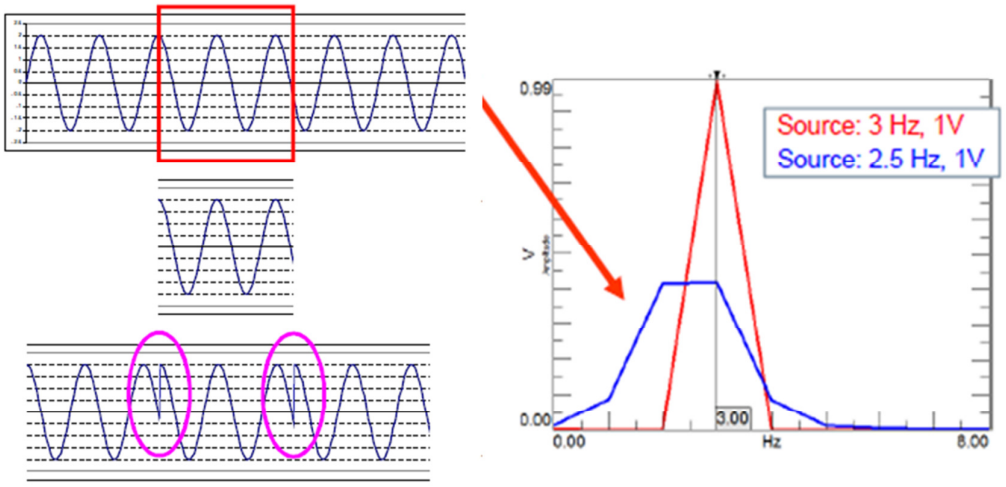

Figure 2. 11: Analoque to digital signal conversion leakage issue [28].

Nonetheless leakage can be reduced or totally prevented with the use of windowing functions. For the random characteristic and continuous applications generally Hanning windowing function seen in figure 2.12 is suggested. It is a mathematical function that brings the signal to zero values at the starting point of signal and ending point of the signal.

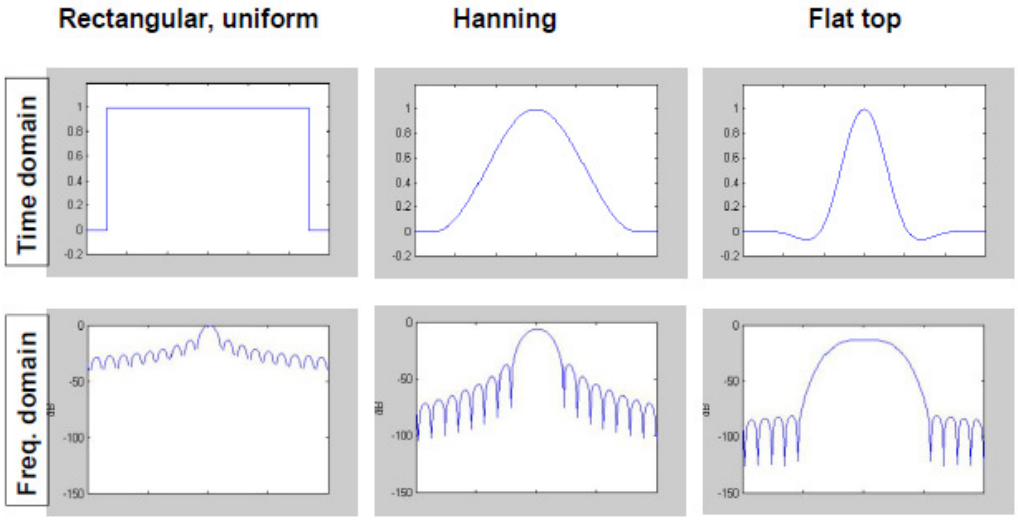

Figure 2. 12: Signal processing windowing functions [28].

2.4 Modal Analysis

In recent years, modal testing and modal analysis are popular topics that are studied by researchers and engineers so it has shown big improvement. In industry modal testing methods are used in wide area to support development and manufacturing sides for solving complicated structural vibration problems.. Modal analysis is a technique to define dynamic response of the structures with doing vibration test and extracting the modal parameters including mode shapes, natural frequencies, critical damping by setting mathematical model of system. In another word it describes transfer functions of structures between source and receiver can be seen in figure 2.13. Despite modal analysis methods and applications have shown great progress in time, knowledge gained from previous experiences states that test setup of modal analysis has major effect on the data quality. Some elements of modal test are hard to include in modal testing though importance of the elements have to be take into account for modal testing. The elements which can be introduced in three titles as hanging method of structure, selection of driving point and selection of measurement points are mostly accepted as ideal in modal test theory [29].

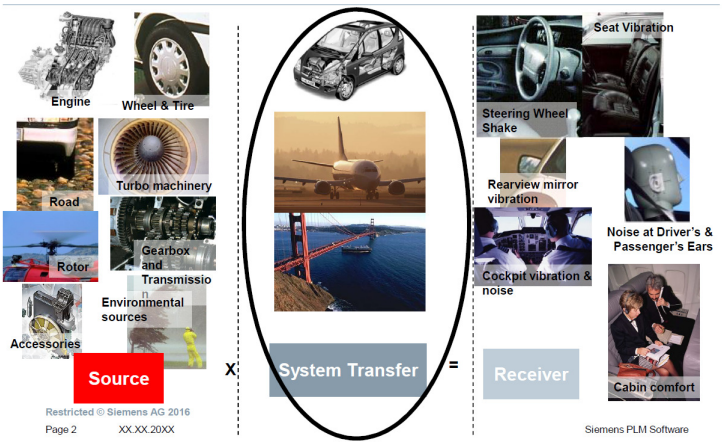

Figure 2. 13: Method of modal testing to calculate transfer function [30].

D.J.Ewins [29] defined the spatial model that is representation of the physical model of structure in form of its mass, stiffness and damping properties as shown in figure 2.14. Furthermore, modal model is introduced as explanation the dynamic response of the structures in terms of natural frequencies, mode shapes including critical damping parameters as seen in figure 2.14. Last method of explaining the dynamic behavior of samples can be done by using response model which is including set of frequency response functions (FRFs) can be seen figure 2.13.

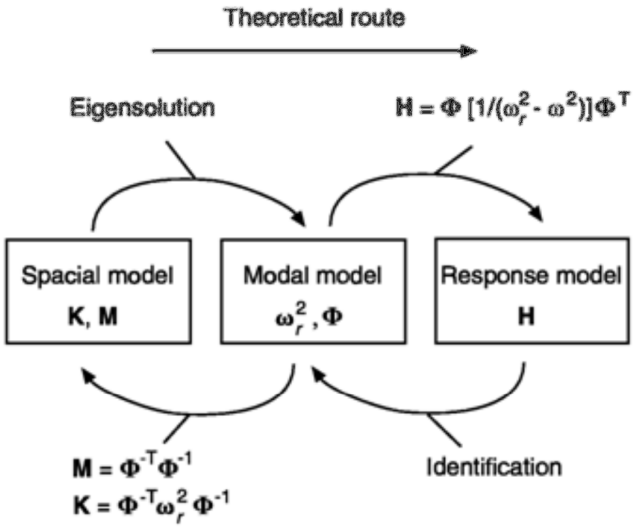

Figure 2. 14: Theoretical route of modal analysis [29].

Modes can be described as vibration pattern of a structure and total dynamic response of system. Additionally they include important information to define vibration character, physical models of dynamic behavior of the structures. Modes of vibration system are calculated by figuring out the eigenvalue problem extracted

from the mathematical model. There are some solution techniques for eigenvalue problems and they are generally named as the theoretical modal analysis

The spatial model contains m as mass, c as damping and k as stiffness as mentioned before to create the modal model. For a given n degree of freedom system, the governing differential equation of motion of a vibration system is defined as the second degree matrix equation. The governing equation of multi-degree of freedom system is shown by,

$$[M]\{\ddot{x}\} + [C]\{\dot{x}\} + [K]\{x\} = 0 \qquad 2.4$$

For solving the free vibration of the response apart from forcing function, the form of equation (2.4) is turned into an eigenvalue problem. The eigenvalues λ and the eigenvectors ψ can easily be calculated as

$$([K] + i\omega[C] - \omega^2[M])\{X\}e^{i\omega t} = 0 \qquad 2.5$$

In the solution of the equation **(2.4)** turns back eigenvalues as the squares of natural frequencies. Therefore replacing any of the natural frequency back into the eigenvalue equation yields a corresponding set of relative values for $\{X\}$ that is named as mode shape equivalent of corresponding natural frequency. Thus, eigenvectors introduces the mode shapes of the corresponding natural frequency of the system and then the solution of equation (2.5) returns the vibration pattern of the system. Eigenvalues and eigenvectors obtained from the solution can then be used to obtain FRF as,

$$\alpha_{ij}(\omega) = \frac{X_i(\omega)}{F_j(\omega)} = \sum_{r=1}^{N} \frac{(\emptyset_{ir})(\emptyset_{jr})}{{\omega_r}^2 - \omega^2 + i\eta_r{\omega_r}^2} \qquad 2.6$$

Where, N indicates the number of modes, ω indicates the square root of eigenvalue λ, η is the structural damping term and ϕ indicates the mass normalized mode shapes.

3. EXPERIMENTAL INVESTIGATION

In this chapter, the experimental studies of gear whine are presented. Description of the test vehicle and preparation in order to operate the vehicle test, the test conditions and axle which is test on the test vehicle are given in details. The data acquisition systems and instrumentation to measure vibration, torsional vibrations, axle dynamic angles, differential oil temperature, and drive shaft torque are introduced. Data acquisition and signal analyzing process is presented. The modal analysis of the driveline system and components are investigated.

3.1 Introduction

Axle whine becomes visible in specific engine speed range in AWD and RWD vehicles. Whine Noise appears in all gear whereas it is more audible in higher gears because of the lower background noise. For the axle whine noise, cruising on motorway is most critical condition since excitation range of the whine is too wide. When the engine speed is in particular range for all gears, it comes harshly and turns off in higher engine speed range as shown in figure 3.1.

The goal of the experimental investigation firstly is to define axle whine in heavy duty commercial vehicles as well as to identify effect of axle microgeometry and TE on axle vibration. Axles which have different TE and gear microgeometry are tested as installed on the vehicle and numerical models are compared with the results. Mechanical vibrations can be measured by transmission and axle pinion accelerometers at locations where previous experimental studies have been realized.

Secondly the experimental investigation can be used to detect the modal characteristic of the powertrain components and systems. The relation between naturals frequency(ies) and axle vibration can be used to understand the reasons of axle whine for the specific cases

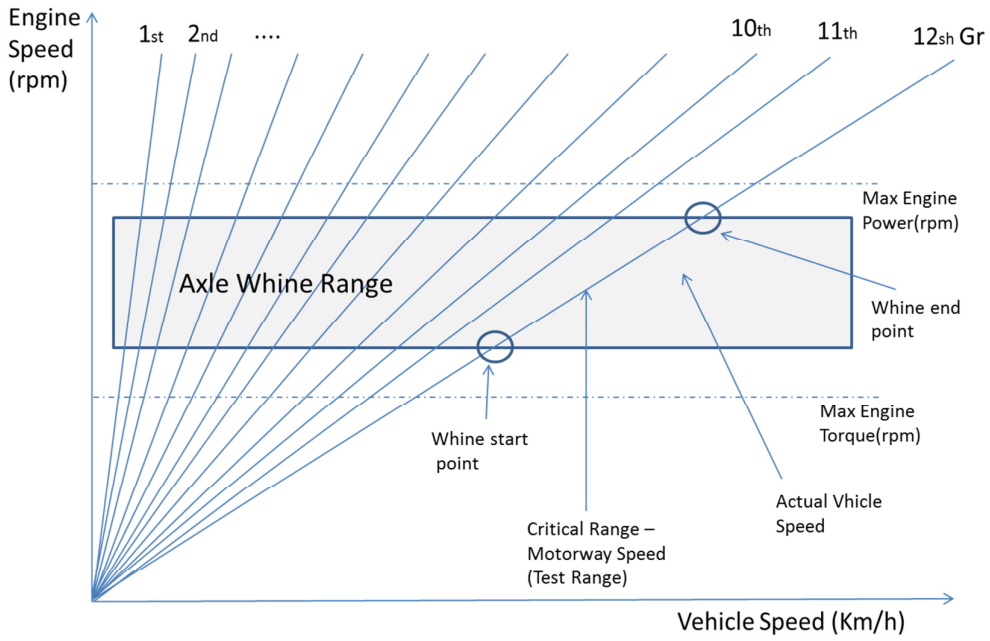

Figure 3. 1: Gear whine effective region.

Experimental investigations results finally can be used to validate the numerical models and verify the dynamic analyze results. In this study, axle whine prediction models can be developed for further projects and issues.

3.2 Test Specifications

3.2.1 Test Vehicle

For the experimental investigation, Ford Trucks 1848T model vehicle which is shown in figure 3.2 is used. It is a 4x2 RWD tractor that is seen in figure 3.3. So it is a single rear wheel and has short chassis vehicle for medium load carrying capacity. Previous works is showed that higher level of axle whine noise in long chassis construction type and road type trucks when they are under full load. Nevertheless, the tests are performed by using a tractor instead. The main reason of this is to reduce complexity. Tractor 1848T has one piece driveshaft and no central bearing. Addition to that effect of chassis installed components is limited. On the other hand, construction and road trucks have driveshaft that is more than one piece and one (or two) central bearing(s). Besides variation of chassis and body configurations are too much. So these factors make more difficult to collect pure whine signal for experimental evaluation and building an axle whine model according to test data

become more complicated. The basic mechanical characteristics of the test vehicle Ford Trucks 1848T is shown in table 3.1 and 3.2 below.

Figure 3. 2: Test Vehicle Ford Trucks 1848T [31].

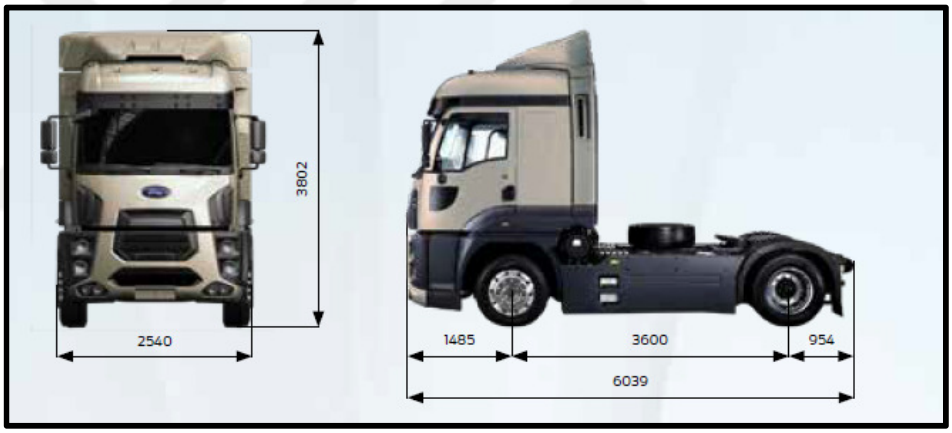

Figure 3. 3: Ford Trucks 1848T Dimensions [31].

Table 3. 1: Ford Trucks 1848T Mechanical Features [31].

Vehicle VIN	**NM0KCXTP6KFU94365**
Overall length	6039mm
Overall width	2540mm
Overall height	3802mm
Wheelbase	3600mm
Chassis width	866
Turning Radius	7500mm
Loads	
Gross Vehicle Mass	18000 Kg
Mass	7675Kg
Front Axle Mass	5490Kg
Rear Axle Mass	2185Kg

The engine is six cylinders in line, 12.7l diesel with turbocharger and intercooler. It has single overhead camshafts, 24 valves in cast iron cylinder head. Direct injection integrated with high-pressure common-rail system for fuel delivery and multipoint fuel injection. Finally, it has a 430mm single mass flywheel. Its characteristics are as shown in Table 3.2.

Table 3. 2: Engine Characteritics [31].

Engine Model	Ecotorq 12.7 L H566
Emission Level	Euro 6
Engine Capacity	12700 cc
Max Power	480 PS (353 kW) / 1800 rpm
Max Torque	2500 Nm / 1000-1400 rpm

The engine is linked to an automated 12-speed transmission with gearbox code ZF 12 TX 2620 AMT excepting reverse. The gearbox combines synchromesh mechanisms to all gears. Its gear ratios are as follows in table 3.3.

Table 3. 3: Gear ratio values for ZF 12 TX 2620 AMT [31].

Gears	Gear Ratio
1. Gear	16,529
2. Gear	12,801
3. Gear	9,832
4. Gear	7,614
5. Gear	5,839
6. Gear	4,522
7. Gear	3,655
8. Gear	2,831
9. Gear	2,174
10. Gear	1,684
11. Gear	1,291
12. Gear	1,000

Engine power transferred from gearbox to differential by one-piece driveshaft. Then, power is driven to the gear set pinion inside the differential unit, which has a 2,67 final drive ratio. Then it passed on the rear wheels, which have 3150 mm diameter. Leaf springs and air springs supported on the axle housing.

3.2.2 Tested Rear Axles

In automotive industry many types of different axles deign had been used. It has shown variation according to vehicle type and load capacity. The vehicle used for this investigation had banjo type rear axle can be seen in figure 3.4.

Figure 3. 4: Banjo type rear axle [32].

The main gear parts for the rear axle applications were chosen as spiral bevel- and/or hypoid gears in automotive vehicles. Rear axle gears can be classified to offset of axes. If there is no offset between driver and driven gears it called as Spiral Bevel Gear but if there is an offset between gear axes, it called as Hypoid Gear. Since there is an offset between pinion and ring gears:

- Connection axis of driveshaft can be changed to improve angles of U/J.
- More teeth can be in contact position and higher contact ratio can be obtained to provide better NVH characteristics.
- More durable and large gears can be designed, since spiral angle of pinion can be designed as higher than ring gear's spiral angle.
- As higher durability life can be provided compared to spiral bevel gears, higher final drive ratios can be chosen during design phases to use on the vehicles which have higher GVM.

Microgeometry and macro geometry are important parameters to show gear total performance such as durability, NVH, dynamic performances. So geometrical information of a gear set NVH performance can be predicted and optimized.

Based on prevous measurements and analsis the best whine solution proposal is the combination of a stiffer tooth macro-geometry allowing minimumn bending under higher torques, with a flank mıcro-geometry allowing maximum contact surface during tooth to tooth rubbing. as shown in figure 3.5.

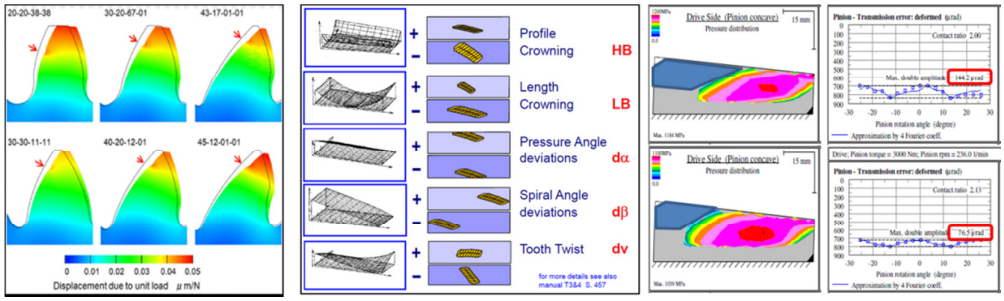

Figure 3. 5: Gear tooth geometric design parameters.

For this study axles which have different geometrical features according to desired criteria as shown in table were defined. Geometric features that used as choosing criteria are TE, gear runout, pinion runout (RO), pitch deviation (Fp) of pinion and gear. Considering the geometrical parameters nine different combination of pinion and gear set were determined as shown in table 3.4.

Table 3. 4: Combination table of rear axle according to defined criteria.

#	Criteria1	Criteria 2	Criteria 3	Criteria 4	Serial Numbers
1	min pinion RO	min gear RO	min TE Drive	-	[Pinion SN 183 & Gear SN 216]
2	min pinion RO	min gear RO	**max** TE Drive	-	[Pinion SN 194 & Gear SN 141]
3	**max** Pinion RO	min gear RO	min TE Drive	-	[Pinion SN 297 & Gear SN 334]
4	min Pinion RO	**max** gear R.O.	min TE drive	-	[Pinion SN 305 & Gear SN 007]
5	min pinion Fp	min gear Fp.	min TE drive.	Gear run outs to be kept same	Pinion SN 130 & Gear SN 240]
6	min pinion Fp	min gear Fp.	**max** TE drive.	Gear run outs to be kept same	[Pinion SN 235 & Gear SN 031]
7	**max** Pinion Fp	min gear Fp.	min TE drive.	Gear run outs to be kept same	[Pinion SN 240 & Gear SN 022]
8	min Pinion Fp	**max** gear Fp.	min TE drive.	Gear run outs to be kept same	[Pinion SN 383 & Gear SN 271]
9	**max** PinionFp.	**max** gear Fp.	**max** TE drive.	Gear run outs to be kept same	[Pinion SN 193 & Gear SN 264]

Afterwards maximum and minimum limits were defined according experience obtained from previous studies and generic values which suggested in literature can be seed in table 3.5.

Table 3. 5: Defined the max and min values of mentioned parameters based on measurements results.

1	min T.E.	between 30-40µrad/sec	**max**T.E“	betweeen 60-71µrad/sec
2	min pinion Fp.	<7micron	**max** Pinion Fp	>17micron
3	**max** Pinion R.O.	>22micron	min pinion R.O	<12micron
4	**max** gear Fp	>22micron	min gear Fp	<12micron
5	**max** gear R.O.	>87micron	min gear R.O.	<50micron

Finally rear axles were produced in supplier company FUWA as defined features can be seen in table 3.5. All of the nine rear axles were measured end of the production line in load-free condition. After then they were transferred from supplier to consider end of the line phasing, balancing and misalignments.

Table 3. 6: Produced axles and their properties after lapping process.

#	Gear Serial Numbers	Differentail serial No	Pinion Fp	Gear Fp	Pinion Run-out	Gear Run-out	TE /drive
1	[Pinion SN 183 & Gear SN 216]	18D260290048	5.4	13	8	28.9	38.44
2	[Pinion SN 194 & Gear SN 141]	18D260290049	7.4	13.5	7.7	29.9	70.97
3	[Pinion SN 297 & Gear SN 334]	18G190100003	7.6	9.4	12.3	39.4	38
4	[Pinion SN 305 & Gear SN 007]	18G190100004	5.8	16.5	5.7	81.9	36.94
5	Pinion SN 130 & Gear SN 240]	18D260290047	3.6	9.8	13	35.5	32.32
6	[Pinion SN 235 & Gear SN 031]	18G180100001	5.8	10.6	4.2	46.1	60.86
7	[Pinion SN 240 & Gear SN 022]	18G190100006	16	8.4	19.3	34.2	34
8	[Pinion SN 383 & Gear SN 271]	18G190100005	6.1	23.4	14.2	77.8	31
9	[Pinion SN 193 & Gear SN 264]	18G180100002	8.2	21.8	13.2	62.8	63

Firstly rear axle which has differential number 18D260290049 was installed the test vehicle. After than rear axles 18G180100002, 18D260290048, 18D260290047 were installed the test vehicle and road test was performed.

3.2.3 Conditions of tests

The vehicle test took place on a test track for NVH studies at the Ford İnönü Plant as shown in figure in Eskisehir. The test took place with no sound barriers at the test track. The external temperature was nearly 22 degrees and humidity at 25%. Test was performed on Durability Performance Track that has special surface for NVH testing.

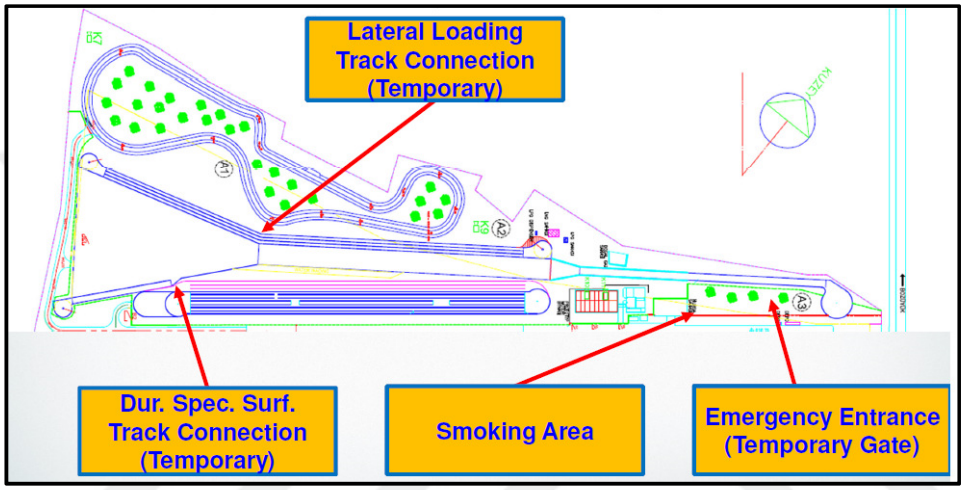

Figure 3. 6: Ford Otosan İnönü Test Track Sketch [33].

Figure 3. 7: Ford Otosan İnönü test track top view [33].

3.3 Test Instrumentation and Data Acquisition

3.3.1 Introduction

For the experimental investigation, the test vehicle is instrumented for vibration, torque, dynamic angle, torsional vibration, oil temperature measurements. Instrumentation locations are selected taking into consideration previous studies to define axle whine characteristic and effect of powertrain systems on axle vibrations as seen in figure 3.8.

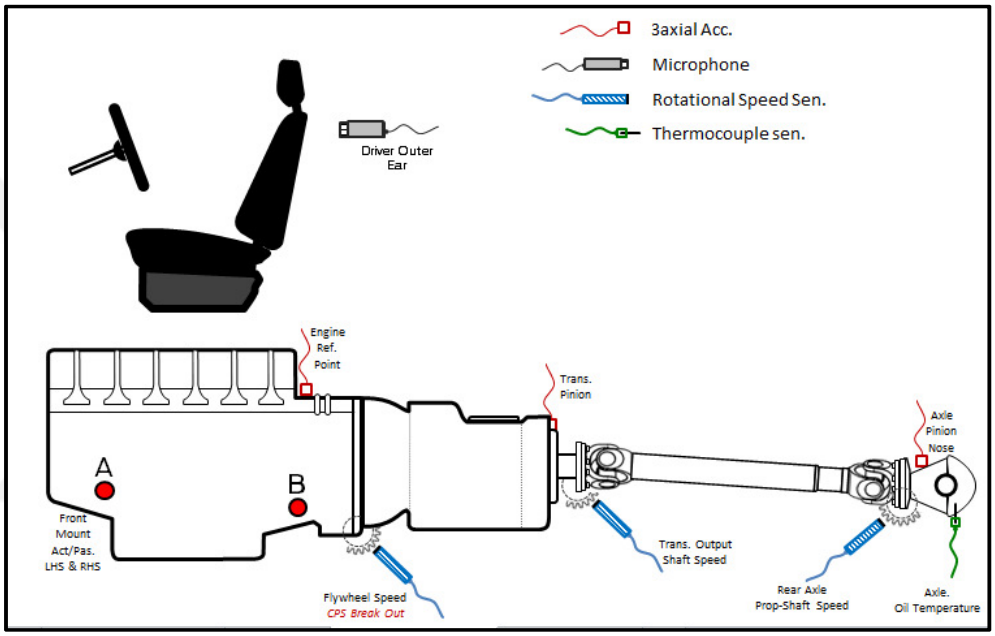

Figure 3. 8 Instrumentation locations on the test vehicle.

3.3.2 Vibration measurement

The structural vibration from engine, transmission and rear axle is collected by using Kistler 8766A500BA type accelerometer. It is a triaxle IEPE accelerometer, which wide operating frequency range and stable sensitivity to temperature changing. It is in miniature and lightweight triaxial accelerometer family and convenient for structural analysis of light and small components, test structures in aviation, space, and automotive industries. It has 500g measurement capacity and durable for vehicle level testing. Dimensions is shown in figure 3.9.

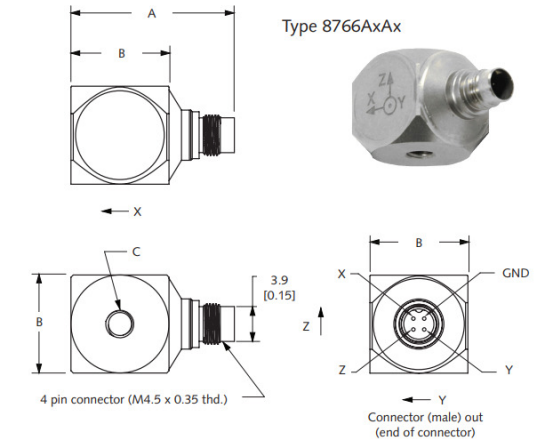

	Type 8766A050/100Ax	Type 8766A250/500/1K0Ax
A	21.1 [0.83]	18.2 [0.72]
B	12.5 [0.49]	10.9 [0.43]
C	6-32 UNC-2B mtg. thd., Typ. 3	5-40 UNC-2B mtg. thd., Typ. 3

Figure 3. 9: Kistler accelerometer properties [34].

3.3.3 Acoustic measurement

Brüel& Kjær 4188 type free field microphone as shown in figure 3.10 which is pre-polarized and is used for sound recording. It used with corrector for random incidence feature. Mechanical specification of the microphone is given as below;

- Sensitivity: 31.6 mV/Pa
- Frequency: 8 Hz to 12500 Hz
- Dynamic Range: 15.8 to 146 dB
- Temperature: –30 to +125 °C (–22 to +257 °F)
- Polarization: Prepolarized

Figure 3. 10: B&K 4188 microphone and 2671 pre-amplifier [35].

3.3.4 Oil temperature measurement

Fluke type K thermocouple placed in differential housing by drilling oil drainage plug of the differential unit. Installation process carefully performed to not touch the metallic walls of the unit to avoid faulty readings Fluke 80 TK thermocouple module was used for conversion of thermocouple signal to 1mV Degree or Fahrenheit. Module signal was directly connected data acquisition hardware by BNC connection as seen in figure.

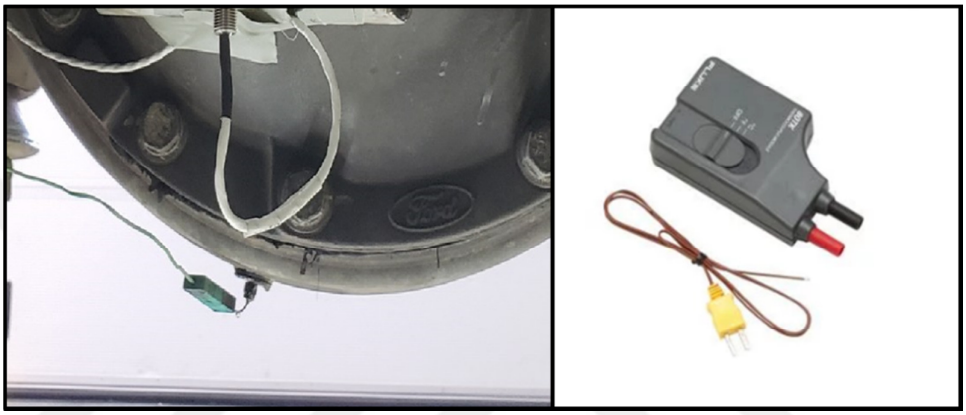

Figure 3. 11: Modified oil drain plug to accept thermocouple [36].

3.3.5 Angular velocity measurement

One of the critical parameters for axle vibration is dynamic angle changing in driven condition. Therefore, angular velocities in 3-rotation axis were measured while the test was performing. Dytran 7576A type six degree of freedom (6DOF) sensor was used for this measurement. Fully analog six degree of freedom (6DOF) sensor incorporates three MEMS–based single axis accelerometers and three MEMS–based gyros. The sensor will provide the end user X, Y, Z acceleration as well rotational information (roll, pitch, yaw expressed in degrees/sec) around those three orthogonal axes

Figure 3. 12: Dytran IMU sensor [37].

3.3.6 Data acqusition

Siemens LMS Recorder as shown in figure 3.13 was used as data logger hardware to collect data simultaneously from 20 analog channels as acceleration, sound pressure, rotational speed temperature and angular velocity and digital vehicle control unit parameters (e.g. engine rpm, vehicle speed, gas pedal position)

Figure 3. 13: Siemens lms scadas recorder [38].

It has 72 channels analog input and reliable signal conditioning towards environmental effects. In addition, ultra-quiet operation without fan cooling so it is ideal for acoustic measurements. The data acquisition system can use Up to 204.8 kHz sampling rate per channel and has 24-bit analog digital converter (ADC) technology (150 dB dynamic range). High-speed Ethernet host interface uses to connect computer.

Different module types can be integrated with LMS SCADAS data acquisition systems with inclusion of any combination of signal conditioning modules. Combined signal conditioning and direct connection to the inputs of each transducer actually clear the multi channels problems. In this study, LMS V8-E data acquisition card was can be seen in figure 3.14 used for accelerometer, microphone and gyro measurements. The entire measurement chain is continuously Eight-channel voltage / ICP / TEDS input module. Input range up to ±10 V, a wide range of signal conditioning modules monitored during testing for open or short circuits. Voltage and ICP input types are eligible per channel. Overload checks from several places are applied in the signal paths, including full bandwidth checks in front of the antialiasing filters. 24-bit ADC with up to 204.8 kHz sampling frequency per channel can support.

For the rotational vibration measurements, four channel input module RV4 is used. It can support analog tacho, torsional vibration and angular position information,

incremental encoder. It can measure simultaneous and synchronic acquisition of rotational signals and normal analog signals up to 200 kHz. Real-time correction for missing pulses or double pulses feature.

Figure 3. 14: Siemens LMS data acquisition card V8-E [38].

PLM LMS Test Lab 17A software was used for data acquisition from the hardware. LMS Testlab supports wide range of test based engineering by combining solutions for data acquisition, structural testing, signal processing, modal analysis and data reporting tools. Data acquisition parameter and signal conditioning parameter are defined by user. For the vehicle measurement, sampling rate, measurement time and spectral lines number are applied based on sensor limits and range of critical whine excitation.

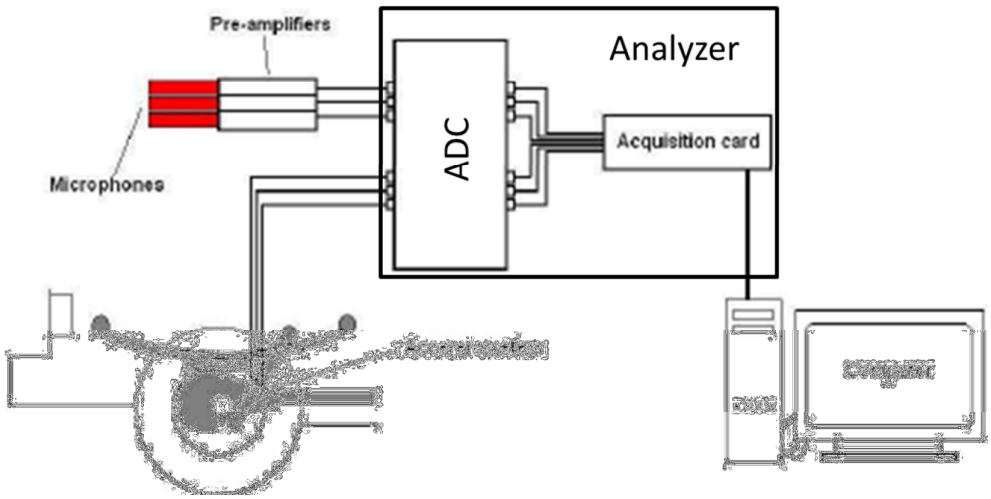

Figure 3. 15: Data flow from the sensor to the computer.

3.4 Testing Methodology

After the vehicle is given sign-off for mechanical and electrical components, sensors were fitted on the location where had been identified form previous studies. First triaxial accelerometer was fixed to engine reference point where is top of third bolt of the engine head connection. Second one is installed on transmission rear nose as seen figure. And last one is put on the differential pinion nose as given in figure 3.16. Directions are recorded according to global vehicle coordinate system that is the z-direction (vertical vibrations), the y-direction (lateral vibrations) and the x-direction (longitudinal vibrations) as shown in figure. Loctite 454 type glue was used to fit the accelerometers. Differential oil temperature was taken from differential oil drainage bolt with K type thermocouple. After Fluke thermocouple module and analyzer conncetion is done in the vehicle.

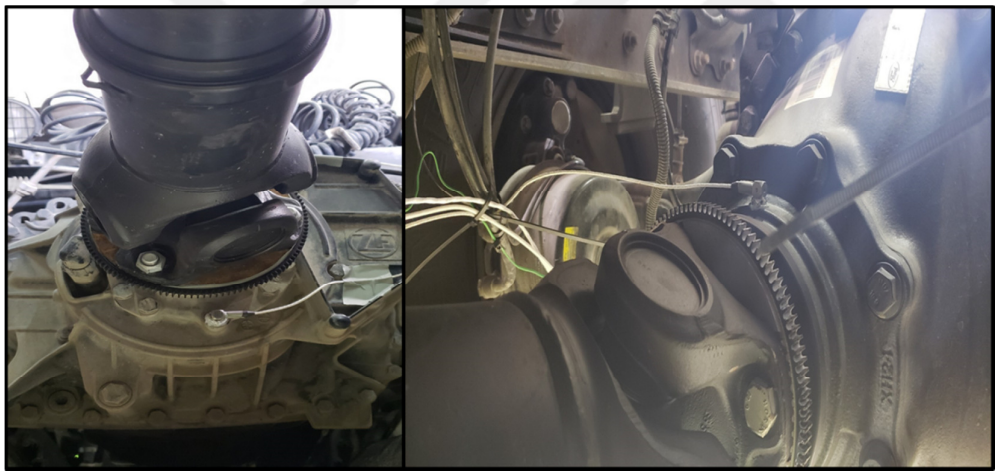

Figure 3. 16: Accelerometer instrumentaiton on transmission output and rear axle pinion.

Secondly, driveshaft was removed and two metal gear rings were fitted from transmission side and differential side of universal joints flanges as shown in figure. And then, rotational speed sensors were installed by the help of brackets to measure torsional vibrations acting transmission output and differential input. The ring gears have 120 teeth so speed sensors were measured 3 degree angle rotational resolution with 120 pulses per driveshaft rev. when the vehicle reach maximum engine speed that is 2400rpm, powertrain systems, that conjugate 1st order of the crank shaft, work at 40Hz. Therefore rotational sensors have to collect data up to 4800 Hz for the first order of the system. Powertrains with 6 cylinder engine as the test vehicle have higher excitations at 3 order of crank shaft as firing order. For this reasons, sampling

frequency of the torsional sensors have to be chosen covering all critical orders. For this study, sampling rate is defined as 104k for tacho or torsional measurement channels.

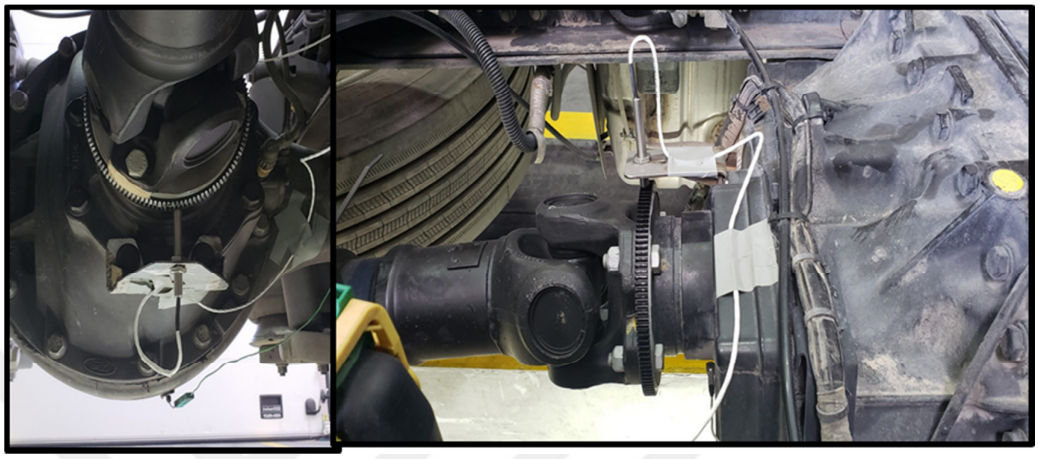

Figure 3. 17: Instrumentation of torsional vibration measurement.

As mentioned in previous section, one of the important parameters on axle vibrations is dynamic angle changing in driven condition. So Dytran 6 dof sensor fixed on rear axle with special glue is called X60 as seen in figure 3.18. It need external power supply for measurement for this reason a special cable was made for the sensor as 6 bnc outputs for analog measurements (3 linear and 3 angular velocities) and the last one is for power feed from the vehicle 12V plug.

Figure 3. 18: IMU sensor connection.

Lastly, microphone is put for sound recording. It is located at driver seat outer ear. Acoustic data was collected with 50k sampling frequency based on Nyquist theorem

to cover the human audio range 20Hz - 20kHz. For this study, sound recording has second importance since 1848T (4x2) type has less sensitivity for axle whine audibility and it is hard to catch whine traces clearing from vehicle noise at interior noise data.

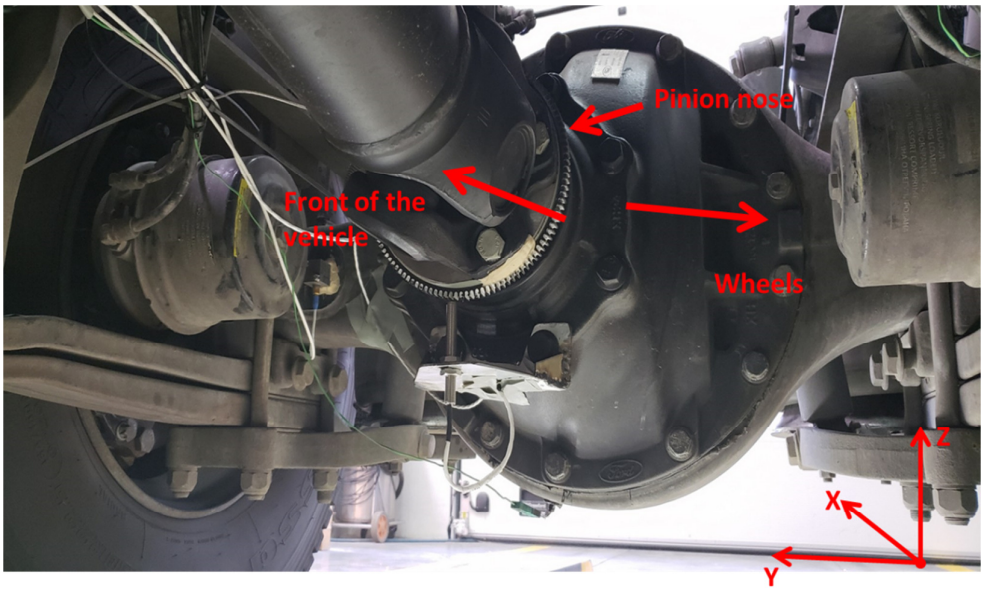

Figure 3. 19: Global vehicle coordinate system.

After instrumentation of the vehicle was completed, road test was started. Firstly, the vehicle warmed up process was done. It is controlled from engine temperature parameter in CAN-Bus and thermocouple plugged into differential housing. The test maneuvers were started up to engine temperature 80 Degree Celsius and the differential oil temperature 40 degree Celsius.

Road test was conducted based on Ford Motor company procedures [30]. Data acquisition software is set for vibration measurement as sampling rate 12800 Hz and acoustic measurements 52400 Hz. The vehicle was driven in maneuver wide open throttle (wot) in all gears. Test was performed as given below;

- In 5^{th} gear, maneuver was started at 700 rpm engine speed and engine run up in % 100 throttles until 2400 max engine rpm. It was repeated 5 times checking test repeatability.
- Same maneuvers were repeated in $5^{th,}$ 6^{th}, 7^{th}, 8^{th}, 9^{th}, 10^{th}, 11^{th}, 12^{th} gears.
- In 11^{th} and 12^{th} gears, maneuvers can be done until maximum vehicle speed as 90 km/h because of speed limit at motorways.

- In 11th and 12th gears are more critical for whine assessment as seen figure 3.1.
- Torque fluctuation is very critical so torque values compared and checked. Maneuvers were chosen for data analysis by torque curves that collected from CAN Bus with relating parameters can be seen in figure 3.20 and figure 3.22.

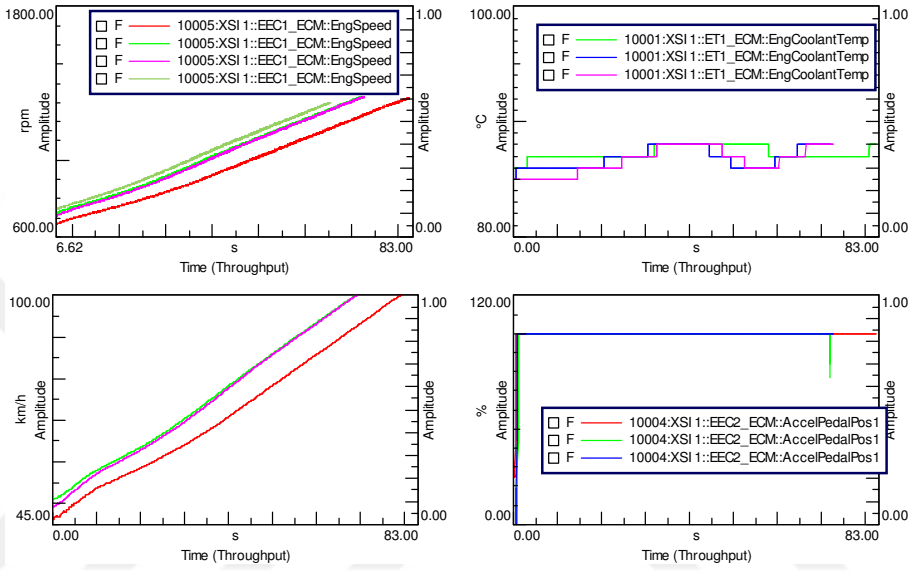

Figure 3. 20: Vehicle CAN Bus parameter such as vehicle speed, gas pedal position.

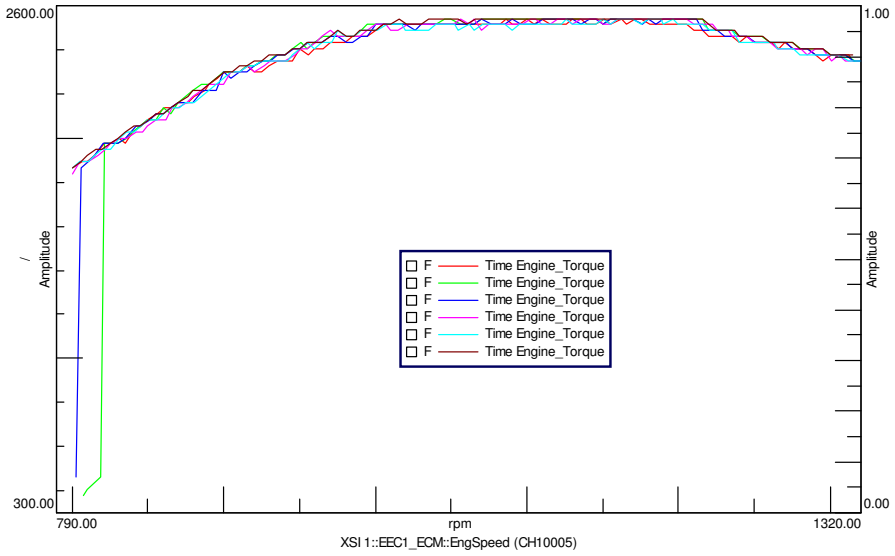

Figure 3. 21: Torque comparison between different runs.

After test maneuvers were done, data check has to be done to be sure collecting reliable and correct data. This was done by using LMS Test Lab software Navigator and Time Data Selection modules. Firstly time data such as reear axle pinion nose

data as shown in figure 3.23 for all channels were checked according to procedures [30].

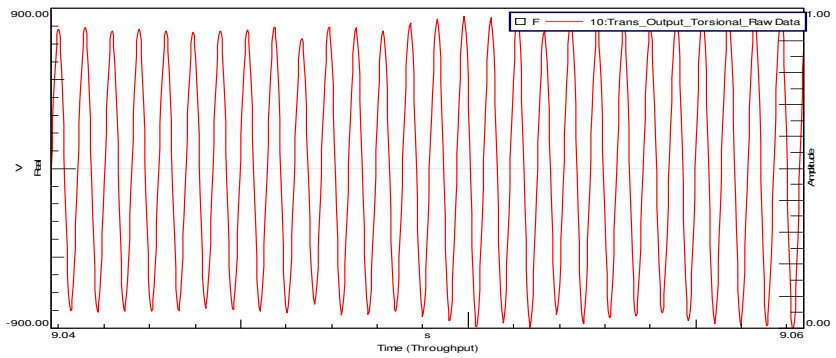

Figure 3. 22: Transmission output shaft rotational vibration signal.

Transmission output data as shown in figure 3.22 and differential input torsional signal investigated in time domain considering signal rates, levels and electrical noises

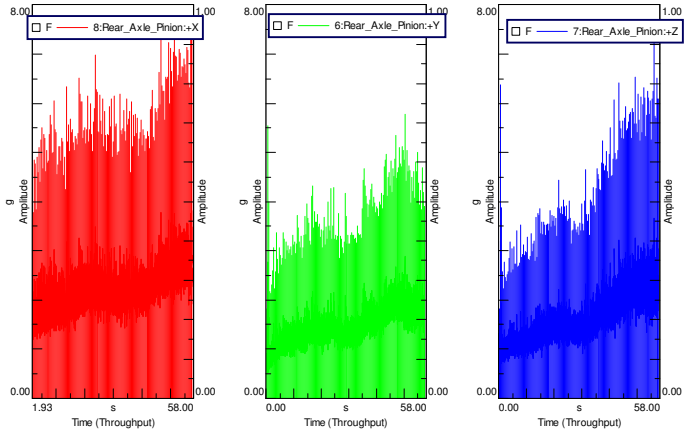

Figure 3. 23: Rear axle pinion nose accelremeter data.

Then Fast Fourier Transform (FFT) vs Time spectrums were calculated to detect engine order traces and acceleration traces of the systems, which data collected from the vehicle. Campbell plots also used as seen in figure 2.24 purpose of check excitation of vibration orders in frequency domain.

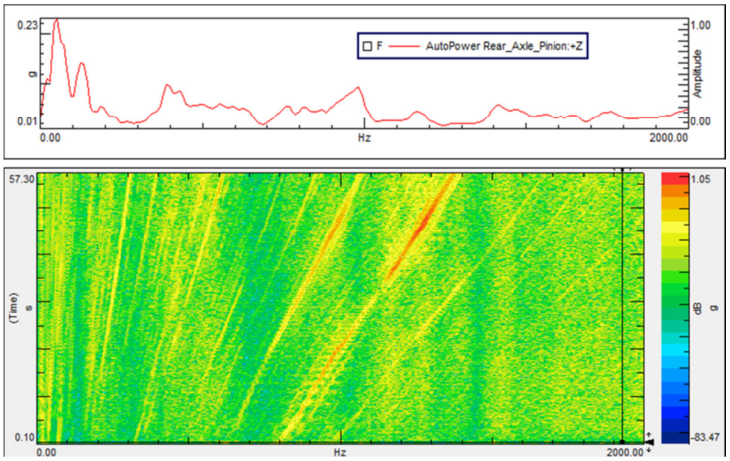

Figure 3. 24: 2D FFT plot and Campbell plot.

Described flow in this section was done for all four-rear axles, which have different gear features and transmission errors. One installed them to the vehicle on and road test performed for each one. In this investigation, main purpose was to detect effect of TE on differential housing and meshing frequencies so whine noises. After subjective and objective evaluations showed that axle gear whine noise inside the vehicle was not clearly detectable. In this section, experimental investigation steps were introduced with introductions of tested system and used equipment, sensor and software.

3.5 Experimental Modal Test and Analysis

In this section, studies were introduced on modal test performed on powertrain systems. Main goal of this investigation is to determine dynamic response of components and systems in excited condition. After then use the result for test data analysis and FEM correlation. Calculations and analyses were done by using LMS Test Lab. Structural testing and Polymax modal analysis modules. Brief presentation of the theory used by LMS Test Lab can introduce as below:

Equations governed for the multi degree of freedom systems as shown in figure 3.25 frequency response function

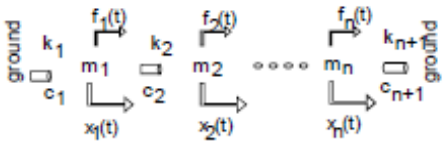

Figure 3. 25: Multi degree of freedom vibration system.

$$X(\omega) = H(\omega)F(\omega) \tag{3.1}$$

Here $X(\omega)$ is the responce function, $F(\omega)$ is the foce function and $H(\omega)$ is the transfer function of the system. Rewriting the transfer function in terms of mass, damping, and stiffness;

$$H(\omega) = [-\omega^2 M + j\omega C + K]^{-1} \tag{3.2}$$

Here M is mass matrix of the system, C is the damping matrix of the system and K is the stiffness matrix of the system.

$$H(\omega) = \sum_{k=1}^{n} \frac{A_k}{j\omega - \lambda_k} + \frac{{A_k}^*}{j\omega - {\lambda_k}^*} \tag{3.3}$$

Where, called as A_k modal constant and

$$A_k = Q_k\{\phi_k\} < {\phi_k}^T > \tag{3.4}$$

$$\lambda_k, {\lambda_k}^* = -\xi_k\omega_k \pm j\sqrt{1 - {\xi_k}^2}\omega_k \tag{3.5}$$

Here, ω_k are eigenfrequencies, ξ_k is damping ratios, $\{\phi_k\}$ are the modes shapes and Q_k are modal scaling factors.

After governing equation of modal model, LMS Test Lab uses curve-fitting algorithm as seen in figure 3.26 and stabilization diagram to solve modal parameters.

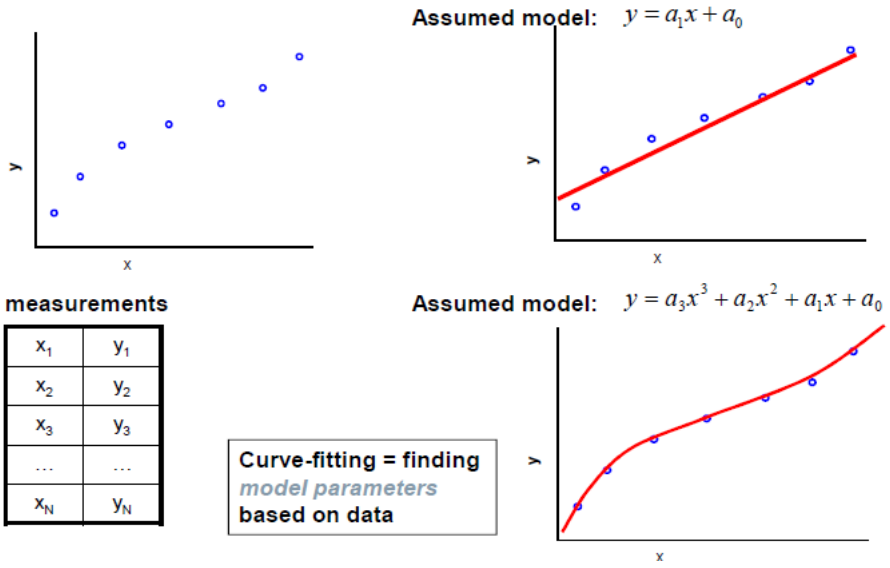

Figure 3. 26: Curve fitting process of LMS Polymax.

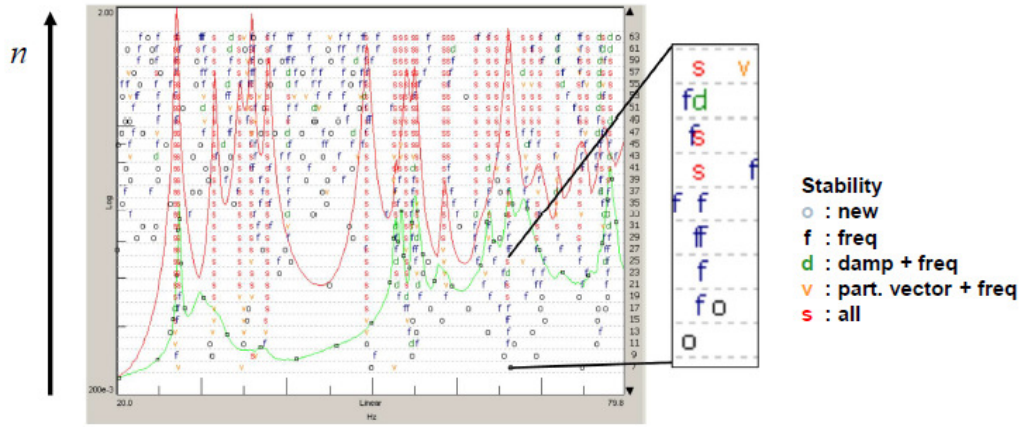

Figure 3. 27: LMS Polymax stabilization diagram.

After then modal parameter estimation are done with Polimax tool. Method is reliable for heavily and lowly damped structures. It can be used for broadband, high-order analysis and has very clear stabilization diagrams. Calculation is done in the z-domain (complex & discrete domain).

Matrix- fraction model in Laplace domain

$$[H(\omega)] = [B(\omega)][A(\omega)]^{-1} = \frac{[\beta_p](j\omega)^p + [\beta_{p-1}](j\omega)^{p-1} + [\beta_0](j\omega)^0}{[\alpha_p](j\omega)^p + [\alpha_{p-1}](j\omega)^{p-1} + [\alpha_0](j\omega)^0} \quad 3.6$$

Matrix- fraction model in z- domain (used in Polymax)

$$z = e^{j\omega\Delta t} \quad 3.7$$

$$H(\omega) = [B(\omega)][A(\omega)]^{-1} = \frac{[\beta_p]z^p + [\beta_{p-1}]z^{p-1} + [\beta_0]z^0}{[\alpha_p]z^p + [\alpha_{p-1}]z^{p-1} + [\alpha_0]z^0} \quad 3.8$$

These studies were done at different boundary conditions and test conditions. Test can be grouped in two main categories as part level tests and vehicle installed tests.

3.5.1 Part level modal tests

3.5.1.1 Rear axle modal test

Another step of the experimental investigation was modal test and modal analysis. For the purpose of define the dynamic behavior and material features of the rear axle, free- free modal test is performed. The axle was hanged with soft springs as seen in figure 3.28. One of the axles that is installed the test vehicle was test in Ford Otosan Gölcük Test Center.

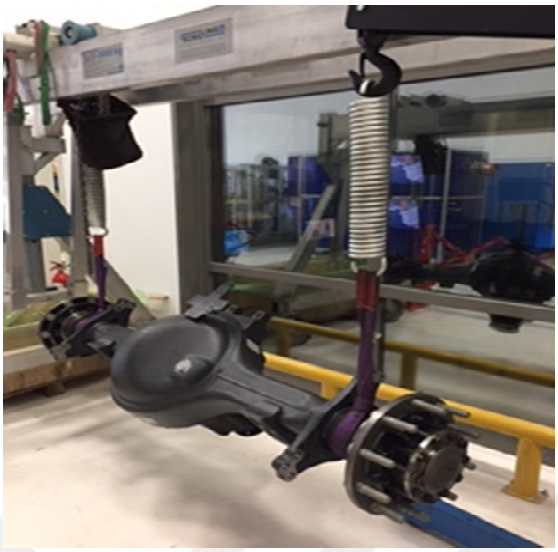

Figure 3. 28: Rear axle supended with soft springs.

As excitation method, both impact hammer and shaker were used. First investigation showed both excitation methods gives similar ford this system. After that the test continued with impact hammer method by reason of fast and easy application. Totally, 13 accelerometers on response points were used for the test as shown in figure 2.29.

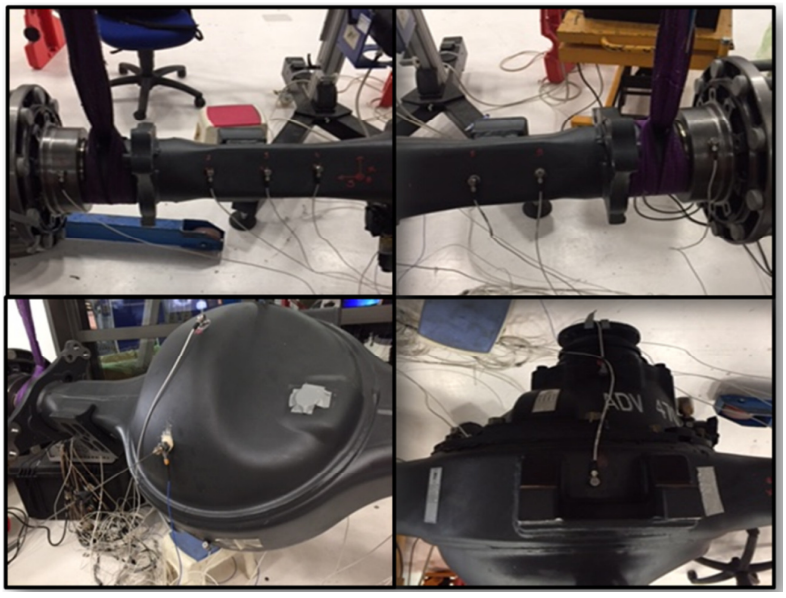

Figure 3. 29: Rear axle intrumentation locations.

Local coordinate system was defined using orientation of Global Vehicle coordinate system. Origin of geometry was chosen as arbitrary point on axle and other points coordinate was determinate in LMS geometry as shown in figure 3.30.

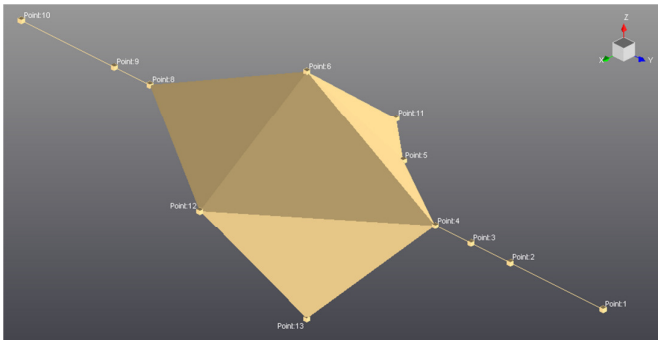

Figure 3. 30: LMS Test lab model of rear axle test.

Selection of right excitation points were another important step. Excitation points were chosen on vertical and longitudinal surfaces of the axle consistent with driving point measurement results. Lastly, the axle was excited from chosen point and measured frequency response functions as seen in figure 3.31.

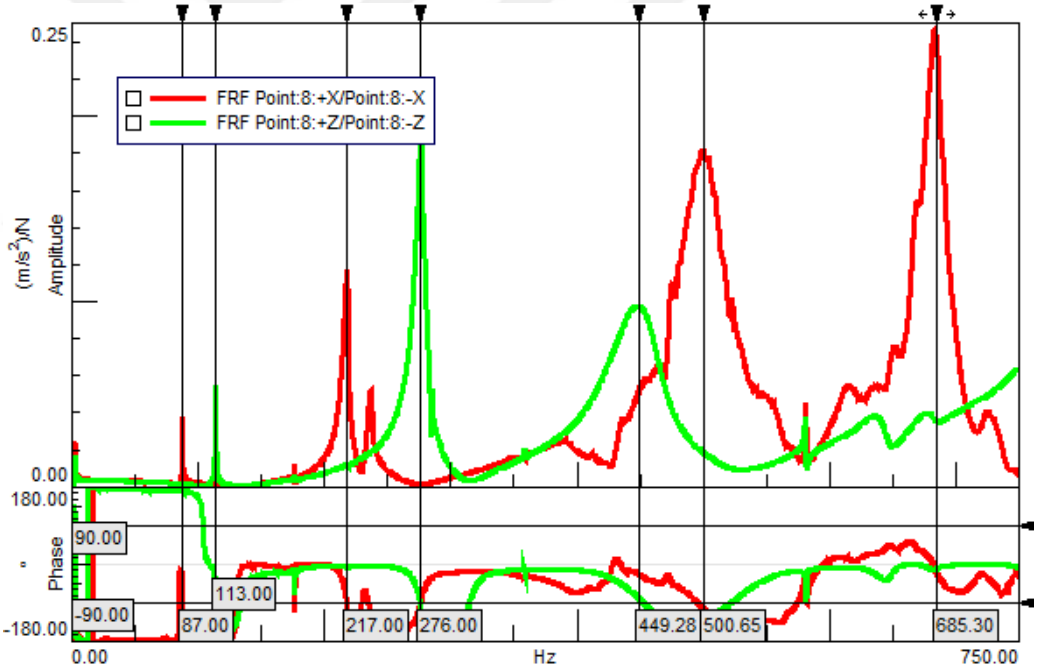

Figure 3. 31: FRF results of rear axle test.

3.5.1.2 Rear axle cut housing modal test

Firstly, the full rear axle that was all components mounted in housing was tested. After then housing of the axle was cut as shown in figure 3.32 to determine dynamic responses and modal features of the axle components in mounted condition. Cut houing axle was hanged by soft springs for free-free assumption

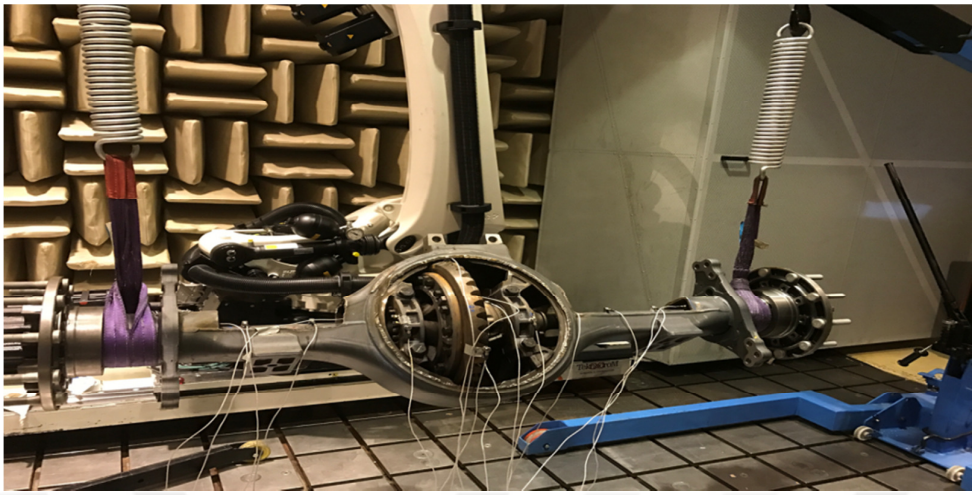

Figure 3. 32: Cut housing rear axle.

Local coordinate system was defined using orientation of Global Vehicle coordinate system same as uncut axle test. Similarly, beginning point for geometry was chosen arbitrarily on axle and LMS geometry as seen in figure 3.33 was created in this coordinate system

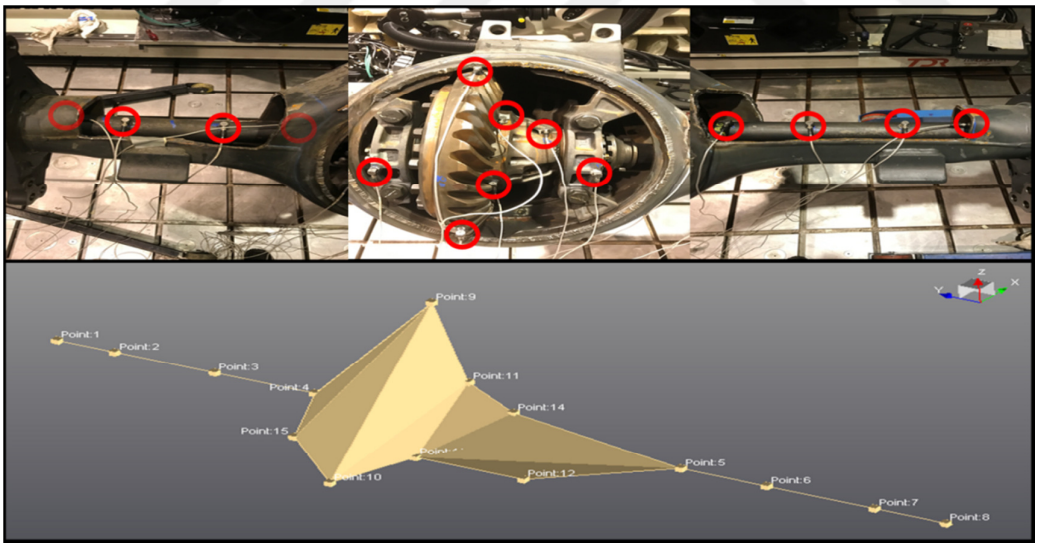

Figure 3. 33: Instrumentation locations and LMS Test Lab model.

Instrumentation and excitation points were determined from the inner part of the axle such as gears, inner shafts. Completely 15 triaxial accelerometer was fitted as response points as indicated in figure 3.34.

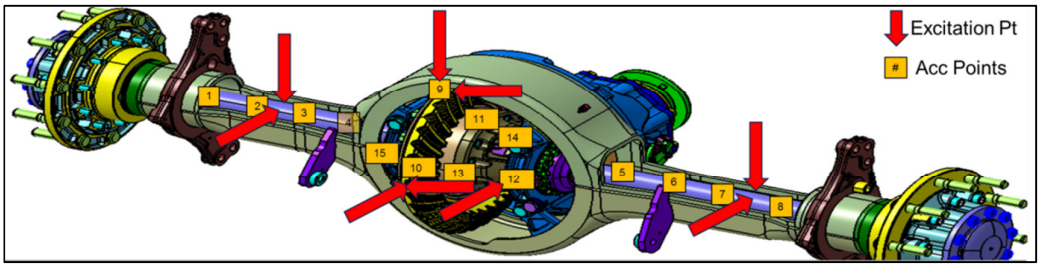

Figure 3. 34: Excitation points.

Structure was excited from points, which are on right and left hand side inner shafts, ring gear, bearing bracket from longitudinal, lateral and vertical directions. Response as FRF was read from measurement point as shown in figure 3.35.

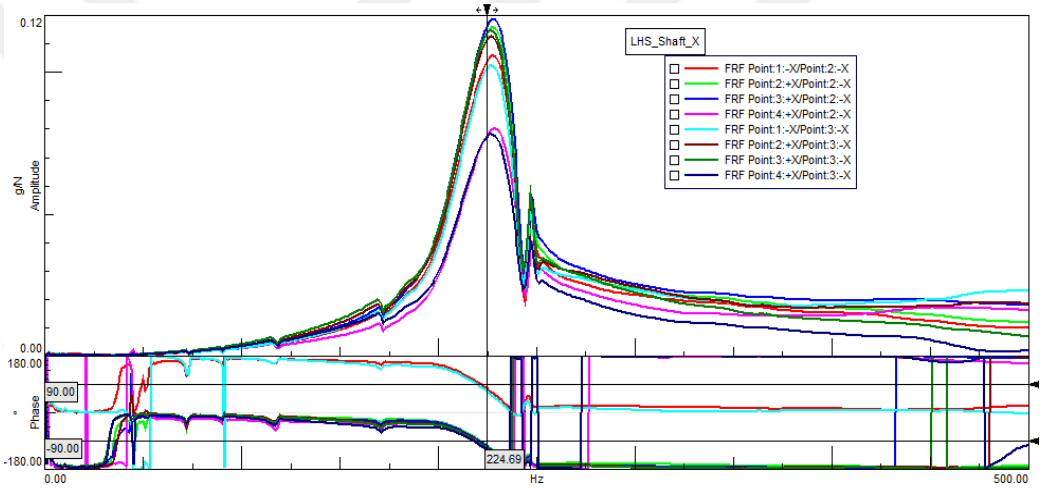

Figure 3. 35: FRF results.

3.5.1.3 Rear axle inner shaft modal test

Next step for the rear axle modal investigation was on right and left hand side inner shaft test. Same test procedure was applied with previous ones. In total 14 measurement point for RHS shaft and 15 measurement points for LHS shaft were determined as seen in figure 3.36.

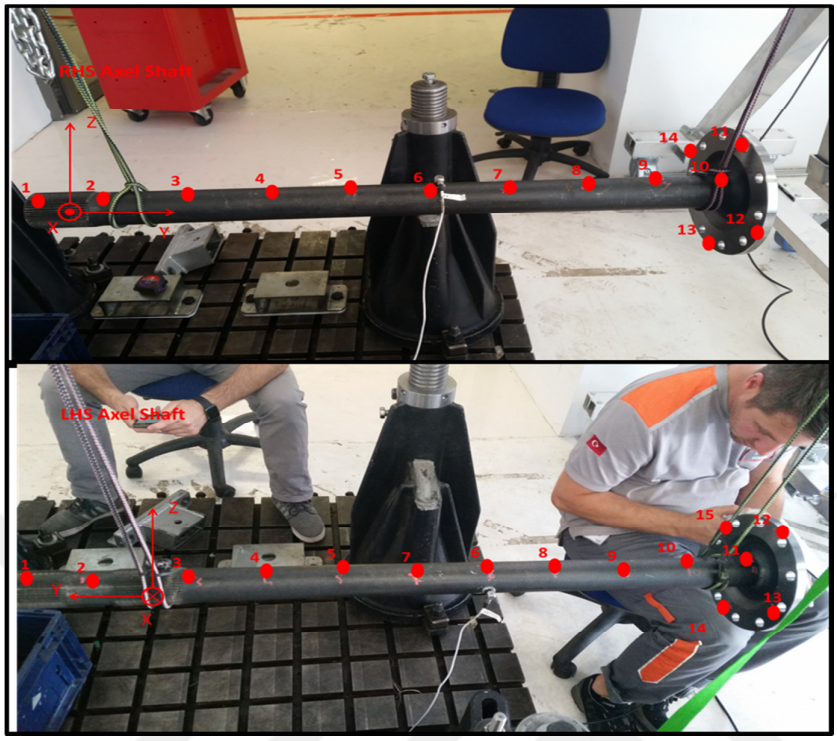

Figure 3. 36: Intrumentation locations of rifht and left inner shafts.

Structures were suspended in free-free condition with soft cords. Rowing hammer method was applied and structure was excited from all measurement points. On the other hand, only one triaxial accelerometer was used on measurement point 6 for collecting responses. FRFs were collected as shown in **figure.** Results in detail are showed in results section.

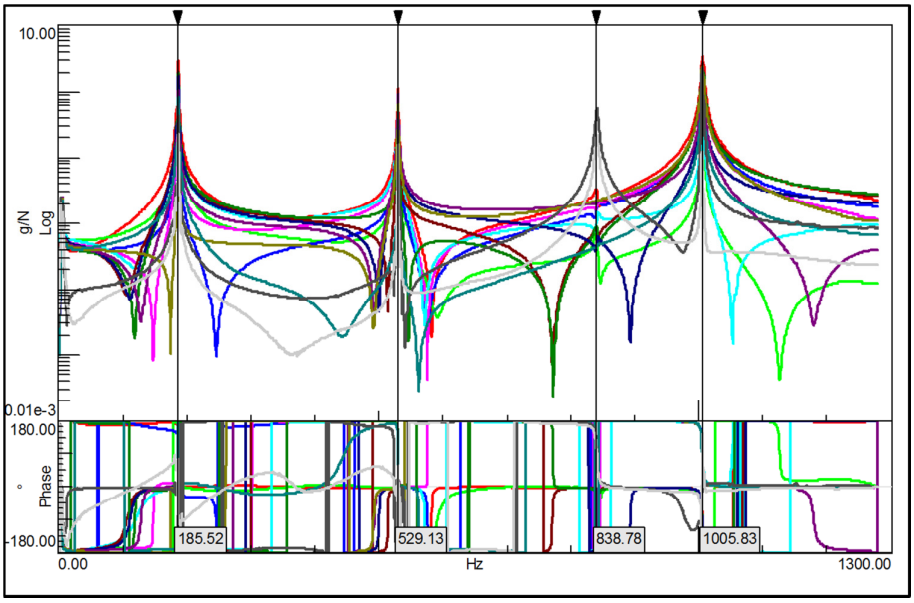

Figure 3. 37: Inner shafts FRF results.

3.5.1.4 Drive shaft housing modal test

Another structure, which investigated in terms of modal features, is driveshaft. Similar test methodology was applied for this part. Only difference is that structure was modeled in three dimensions as seen in figure 3.38 because of detecting high frequency mode shapes. Especially breathing modes of the driveshaft could be critical for high frequency region. For this purpose, measurement points were chosen to symbolize circular shape in LMS model**.**

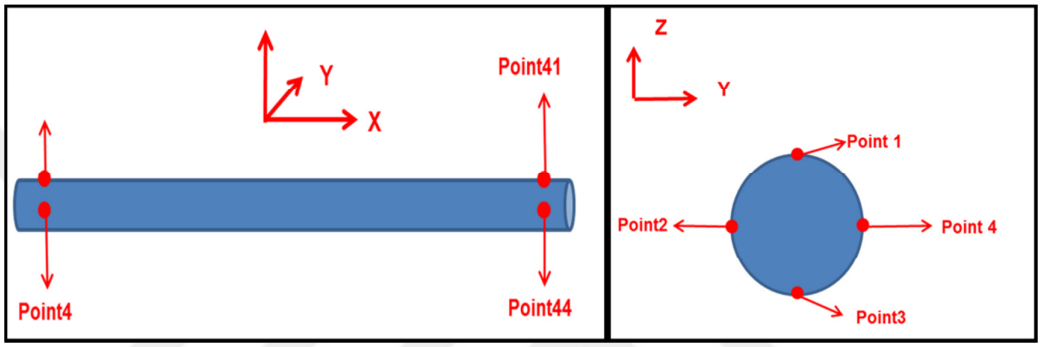

Figure 3. 38: Instrumentation points of driveshaft test.

Test condition can be summarized as given below:

- Driveshaft was hanged by soft springs like free-free
- As coordinate System, Global Vehicle coordinate system was defined. An arbitrary point on center of front surface of shaft was detected as origin.
- Totally 40 measurement points were determined. Rowing accelerometer method was used for 40 responce points.

Structure was excited and investigated up to 2000 Hz as shown in figure 3.39**.** Results in detail are given in results section.

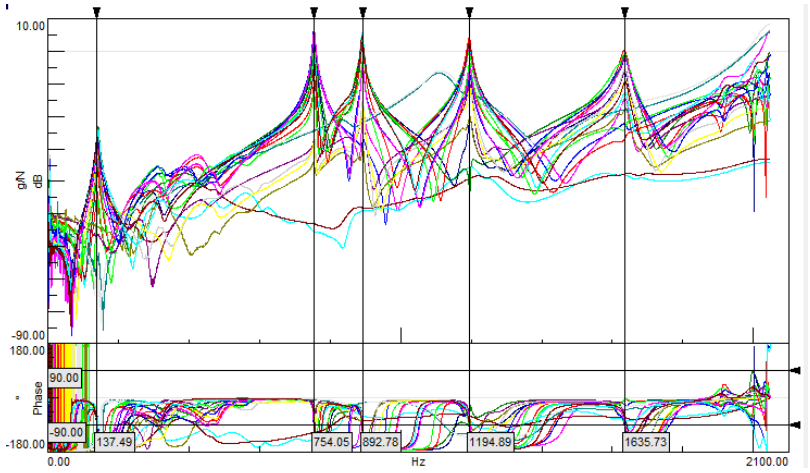

Figure 3. 39: Frequency responce functions collected on driveshaft.

3.5.2 Vehicle level modal tests

3.5.2.1 Power pack (engine and transmission) modal test

In this section modal test study on power pack (engine and transmission) was presented as installed condition. For this purpose the engine was instrumented to define rigid body modes and flex modes mounted condition on vehicle chassis. Totally, 16 measurement points were detected and instrumented with Kistler triaxle accelerometers can be seen in figure 3.40.

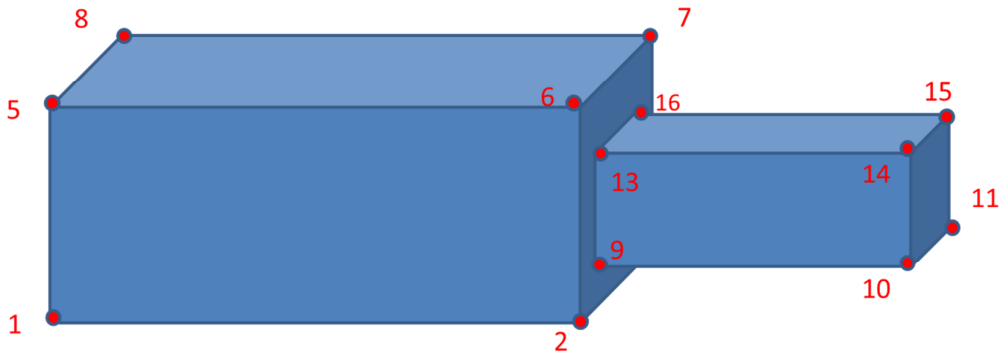

Figure 3. 40: Intrumentation locations of powerpack

PCB 086D20 type modal sledge (hammer) was used for excitation. Excitation points were chosen more than one to detect bending modes in vertical and lateral directions. Transmission and shaft connection was analyzed in detail to see interaction.

4. NUMERICAL INVESTIGATION

In this chapter, numerical investigation of gear whine is discussed. Firstly, finite element model elements are described. After then It is followed a statement of process of the natural frequency analysis. Afterwards gear contact and mesh stiffness analyses for dynamic transmission error is introduced. Finally, multi body dynamic model and analysis are presented.

4.1 Finite Element Model

Firstly, static modeling of the powertrain system and components individually are created for the numerical investigation of gear whine. As finite element modeling software Msc Nastran was used. For purpose of this, models which are previously created for Ford Otosan projects in CatiaV5 were utilized. All systems and sub-systems such as inner shafts, bearings were modeled in details.

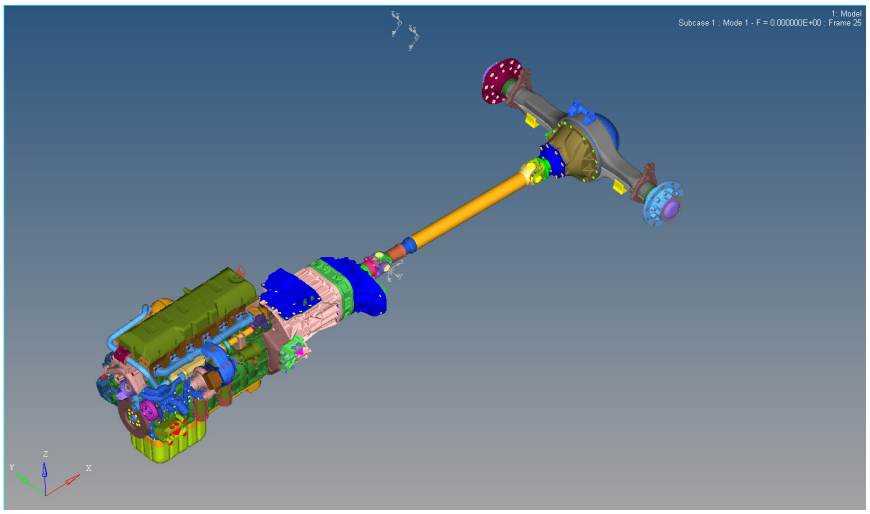

Figure 4. 1: Nastran model of driveline system.

Mechanical features like component materials, elasticity, and thermal expansion coefficients were defined. Defined materials for the rear axle can be seen in figure 4.1 and mechanical properties as shown in table 4.1.

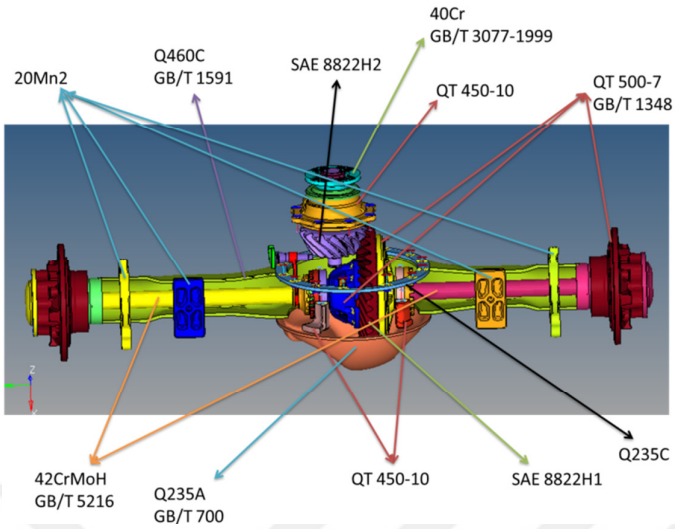

Figure 4. 2: Rear axle model used materials for components**.**

	Modulus of Elasticity,	Poission Ratio	kg/m^3
42CrMoH GB/T 5216	2.12x10^11Pa	0.28	7.85E+03kg/m^3
Q235A GB/T 700	2.12x10^11Pa	0.288	7.86E+03kg/m^3
QT 450-10	1.69 x10^11Pa	0.257	7.06E+03kg/m^3
Q235C	2.10x10^11Pa	0.274	7.83E+03kg/m^3
QT 500-7 GB/T 1348	1.62x10^11Pa	0.293	7.00E+03kg/m^3
40Cr GB/T 3077-1999	2.11x10^11Pa	0.277	7.82E+03kg/m^3
Q460C GB/T 1591	2.06x10^11Pa	0.280	7.85E+03kg/m^3
20Mn2	???	???	7.81E+03kg/m^3

Figure 4. 3: Mechanical features of modeled components.

4.2 Natural Frequency Analysis

Afterwards completion of the static modeling of the systems and components natural frequency analyze were performed with the models. Results of this analysis are one of the critical inputs for multi body analysis. Effects of natural frequencies in whine critical region need to be considered for dynamic investigation. Msc Nastran Software ran frequency response functions and mode shapes analyze. The software are used Lanczos Method while doing calculations. Cornellius Lanczos [39] presented this method in 1950. It is an iterative method to solve the eigenvalue problem.

Lanczos method can be used for the solution of the standard eigenvalue problem:

$$Ax = \lambda x \tag{4.1}$$

Results can be rewritten after Lanczos recursion

$$Tq = \lambda q \tag{4.2}$$

T is a tridiagonal matrix and α_i's on the diagonal and β_i's on the off-diagonal in the matrix

$$T = \begin{bmatrix} \alpha_1 & \beta_2 & & \ddots \\ \beta_2 & \alpha_2 & \beta_3 & \ddots \\ \vdots & \beta_3 & \alpha_3 & \beta_4 \end{bmatrix} \tag{4.3}$$

1. Initialization

a. Choose a starting vector v_1 , where v_1 is normalized, $|v_1| = 1$.

b. Set $\beta_1 = 0$ and $v_0 = 0$.

2. Iteration

for i =1,2,3 .... m as follows;

$$w = Av_i - \beta_i v_i - 1 \tag{4.4}$$

Then,

$$\alpha_i = v^T{}_i w - \beta_i v_i - 1 \tag{4.5}$$

$$c = w - \alpha_i H v_i \tag{4.6}$$

$$\beta_{i+1} = [c^T Hc]^{1/2} \tag{4.8}$$

$$v_{i+1} = c/\beta_{i+1} \tag{4.9}$$

where for the vibration cases H is M (mass matrix), H, w and c are temporary vectors. The vectors v_1, v_2, v_m are the set of Lanchos vectors.

The order of A could be more than 10000 when order m is generally same or up to twice the number of wished eigenvalues and eigenvectors.

Calculation of eigenvector consisting eigenvalue λ of T_m can be done

$$T_m q = \lambda q \tag{4.10}$$

Moreover, frequencies computed by

$$\omega^2 = \sigma + 1/\lambda \qquad 4.11$$

In this study, Ford Motor Company's High Speed Computing system was used for calculating the eigenvalues of the tridiagonal matrix.

Mesh models were created with all boundary condition for all individual components and subsequently response and excitation points defined in Msc Nastran software can be seen in figure 4.2.

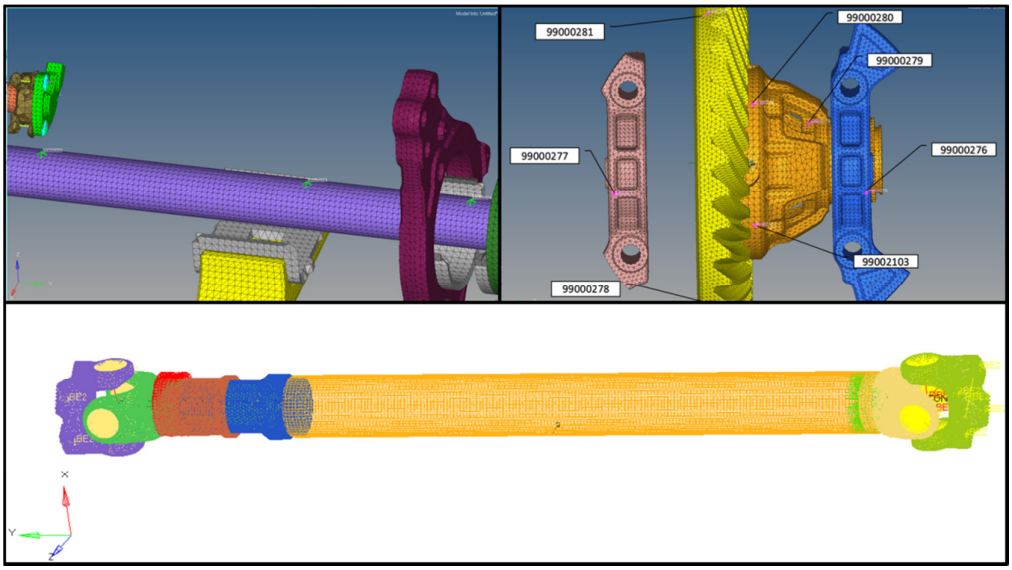

Figure 4. 4: Mesh model of driveline components for natural frequency analysis.

By using, the eigenfrequencies and their respective eigenmodes could be extracted and a number of eigenmodes could be included in the substructure

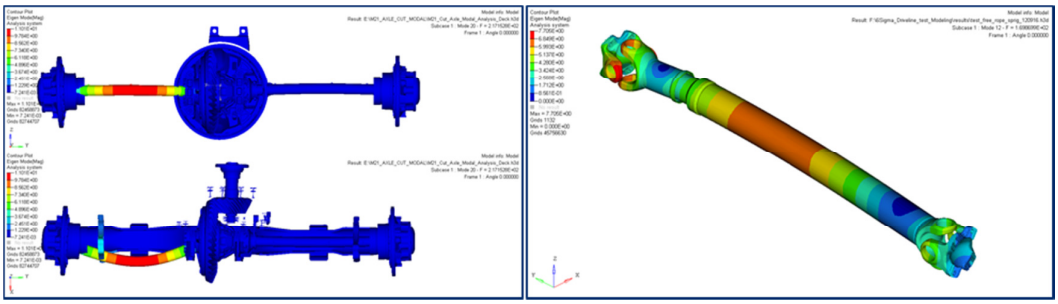

Figure 4. 5: Natural frequency analysis results.

4.3 Mesh Stiffness and Contact Analysis

Another important parameter dynamic model for gear whine investigation was dynamic mesh stiffness and transmission error calculation. Therefore, gear contact need to be determined and loaded gear features could be estimated. Mesh stiffness value and dynamic transmission error in the loaded gear condition were calculated by using KIMoS (Klingelnberg Integrated Manufacturing of Spiral Bevel Gears). KIMoS is special software for Geometry dimensioning, macro geometry inspection based on common standards, simulation of the manufacturing process, tooth contact analysis for load-free and under load for bevel gears for various gear structures. In This study, gear parameters were determined via KIMoS and optimized according to manufacturing opportunities and errors. By using the software, geometry including macro & micro geometries of the gear was defined as shown in figure 4.4 to calculate gear contact surfaces and pressure maps.

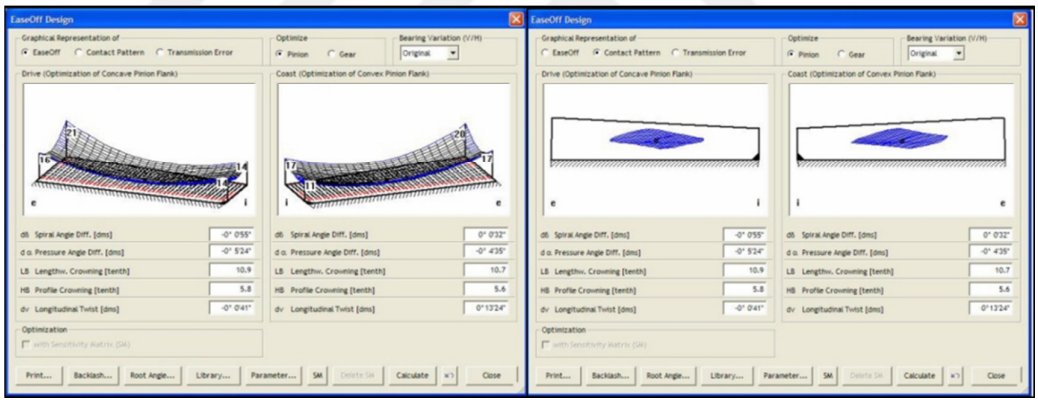

Figure 4. 6: Gear geometry design in KIMoS.

The transmitted error curve along pinion rotation angle changes significantly with driving torque as shown in figure 4.5 , however suppliers E.O.L can measure the T.E. At a very low torque value (50Nm) which doesn't represent real life torque spectrum of complaint whine region at reear axle (acc to the gear and FDR 2000-4000Nm) Currently a computation via KIMOS is used to estimate the T.E under related Torque values, but these KIMOS results are also not verified directly with measured T.E under varying drive torque.

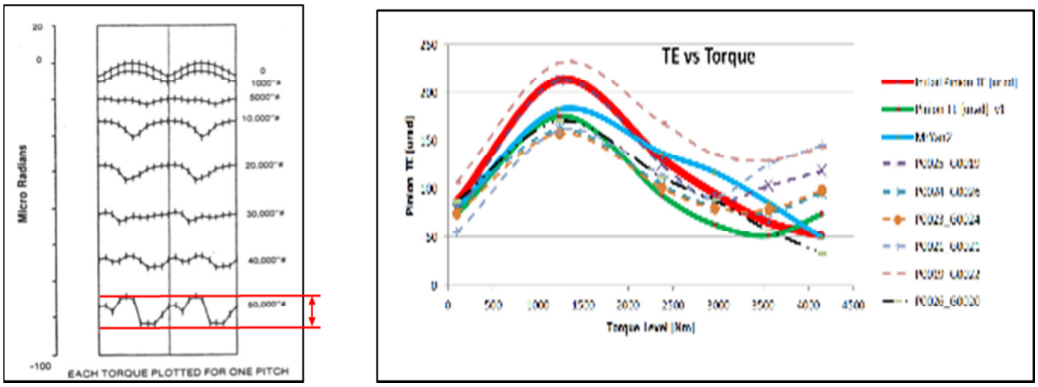

Figure 4. 7: Effect of torque fluctuations on transmission error.

In this study flank pressures are displayed alternatively as distribution within the active tooth flank or along the path of contact i.e. within the angle of pinion rotation during mesh. Tooth root bending stresses are alternatively displayed as the respective maximum across the face width or along the path of contact i.e. within the rotation angle of pinion during mesh. And then the full geometry including macro & micro geometries of the gear sets a stress and tooth contact analysis under load were calculated for either with load deflections. Based on this results mesh stiffness curve can be seen in figure 4.6.

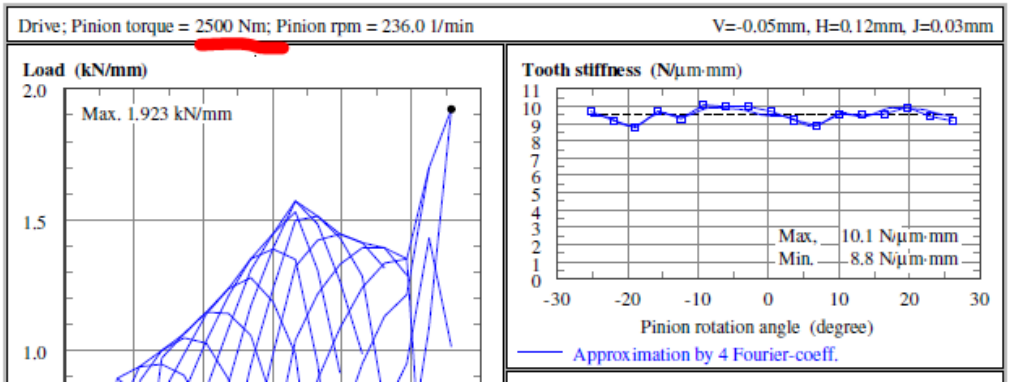

Figure 4. 8: Toot mesh stiffness curve under load.

Bewel and hypoid gears get into multiple teeth contacts at a given time to each other. The number of teeth in contact changes from 2 to 3 then back to 2 as the pinion rotates, while the varying contact area and stresses sweeps along the tooth flank with the pinion rotation. The resistance of a single tooth against being bent under the contact force is called «tooth mesh stiffness», which is a varying curve along the pinion rotation angle. Every time that 3 teeth get in contact, this resistance gets

higher, and the curve makes an upper peak.When it drops back to 2 teeth in contact, the resistance gets lower and the curve draws a lower peak.

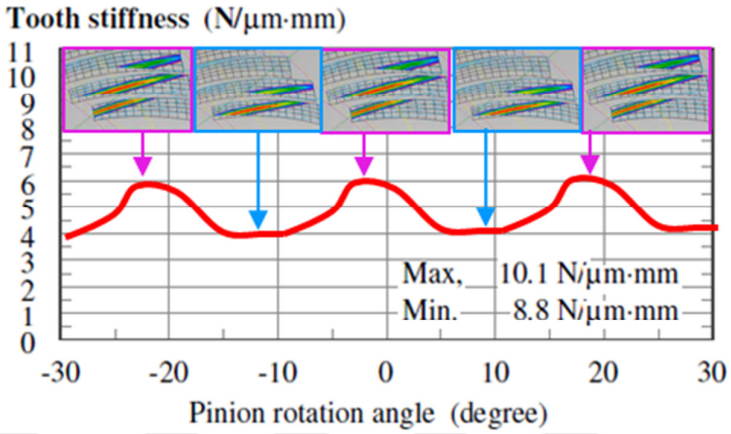

Figure 4. 9: Contact surface and mesh stiffness relation.

4.4 Multi Body Dynamic Analysis

In order to investigate dynamic response of the rear axle, multi body dynamic model tools become more important over the last decade since effect of a changing on design or process can easily be observed without physical prototype. For that, reason building a correlated dynamic model can be critical element for further development process and issue resolution. For this investigation, multi-body dynamic model was built via AVL Excite Power Unit SHYP module. The Hypoid Gear Mesh (SHYP) joint is used for modeling meshes between two bevel gears with non-intersecting axes. Hypoid gear meshes are based on a rather complex geometry. Considering this in detail would cause a lot of effort, which may significantly influence calculation performance. For that reason, several simplifications and assumptions are made for the SHYP joint.

All structure models were used in the AVL Excite dynamic model were imported from Msc Nastran with created constraints and boundary conditions. In detail only powertrain components such as driveshaft and differential was investigated but full vehicle model was built in this investigation to catch undesired errors sourced from other vehicle components. AVL Excite 3D dynamic model as shown in figure 3.8 was created. Global vehicle coordinate system same as experimental studies was used as coordinate system for all analyses in component level and system level. The

origin of the coordinate system was used as powertrain origin, which is at the center of the crankshaft main bearing on rear side of the engine block.

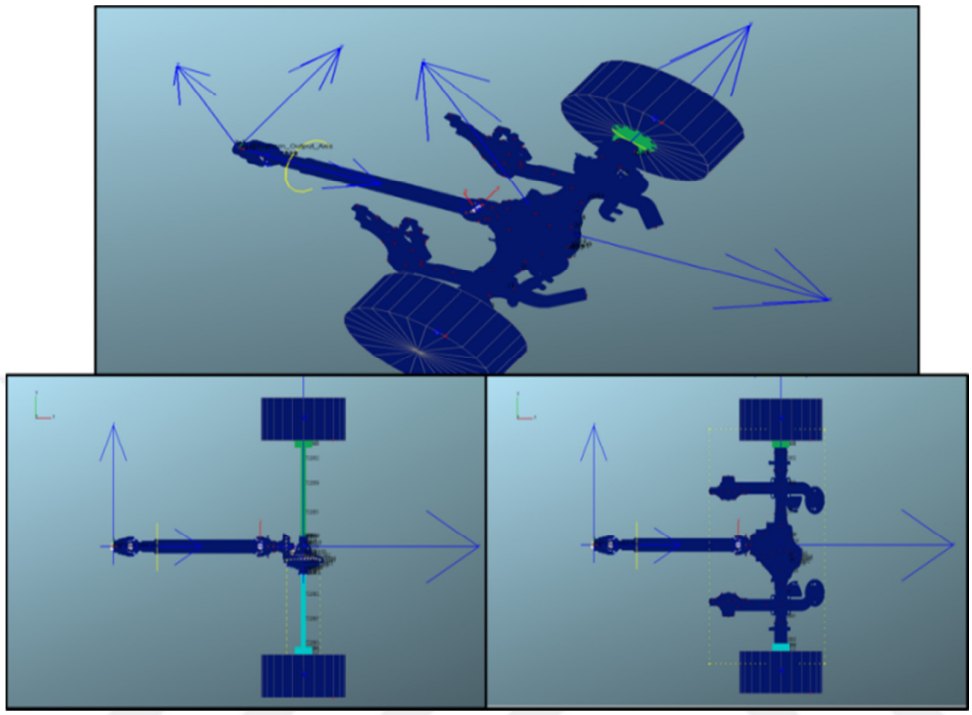

Figure 4. 10: 3D view of AVL Excite model.

Tooth mesh stiffness and transmission error inputs were imported from KIMoS results. Modeling of the contact surfaces and contact forces were also calculated by using KIMoS. Modeling of bearings was done information that was received form supplier. Mechanical features and stiffness valued were defined according to supplier specifications that were not verified with test in Ford Otosan. Based on information was collected from other finite element models and manufacturers AVL Excite model in 2D can be seen in figure 4.9 was created.

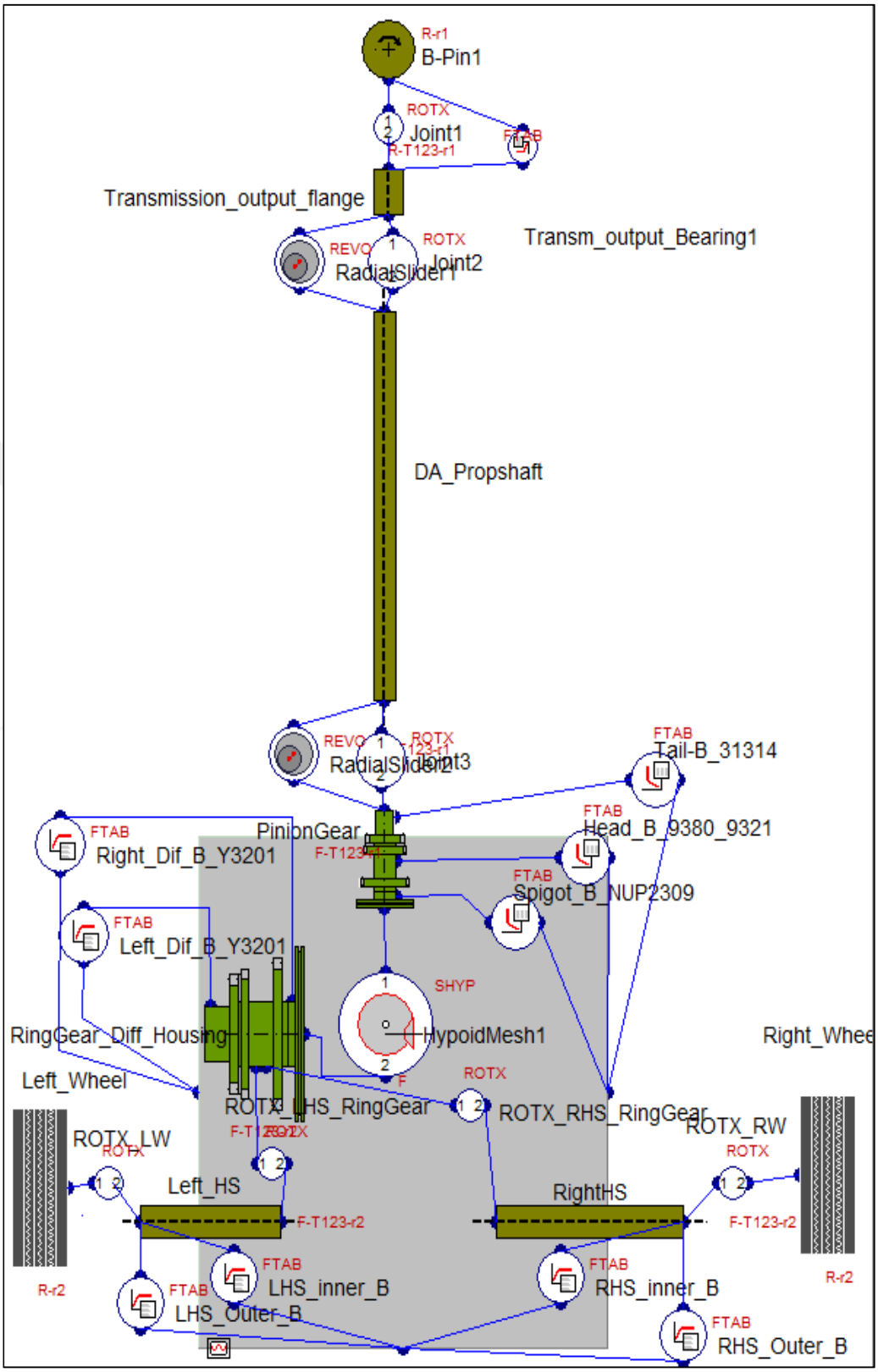

Figure 4. 11: 2D view of AVL Excite multi body dynamic model of driveline system.

In the model connections, constraints and mechanical features such as material, density, and stiffness were defined. The structure modeled as flex body so frequency responses and mode shapes are introduced in model by using output of Nastran.

First step of the dynamic model was that importing Nastran model with its defined mechanical features such as material, mass, density and modelinng setting like mesh models, boundy conditions, constrains and additionally model including natural frequencies and mode shape informations .Then general settings as number of teeth, helix angle, etc as seen in figure 4.10.

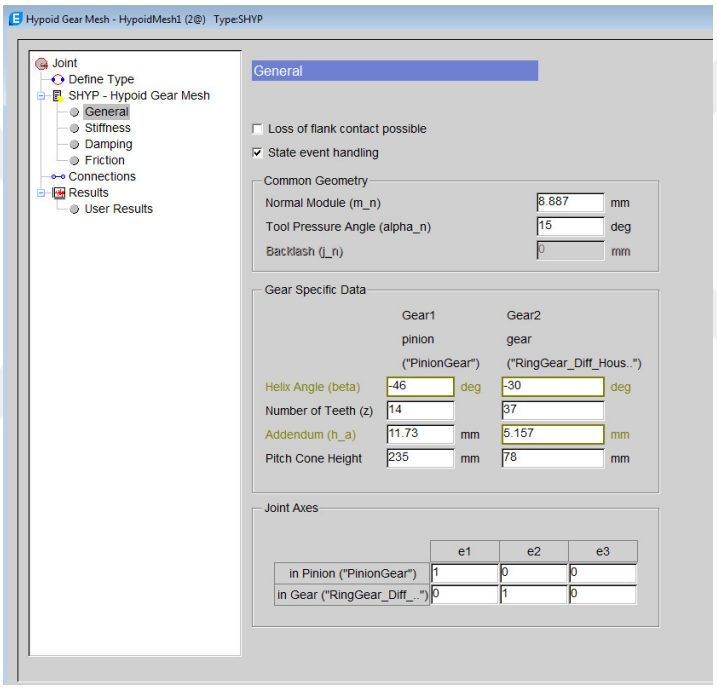

Figure 4. 12: AVL Excite screen for general settings.

Secondly tooth mesh stiffness curve and gear contact force curve were introduced can be seed in figure 4.11. Mesh stiffness values introduced according to pinion rotation angle which was calculated via KIMoS. And then contact forces which were also computed by using KIMoS were defined in range 0 to 15 kN with additional load dependency. Addition to contact forces, stiffness were also determined as shown in previous section TE dependent to load so after calculating contact force for one torque value the others were defined with normalization.

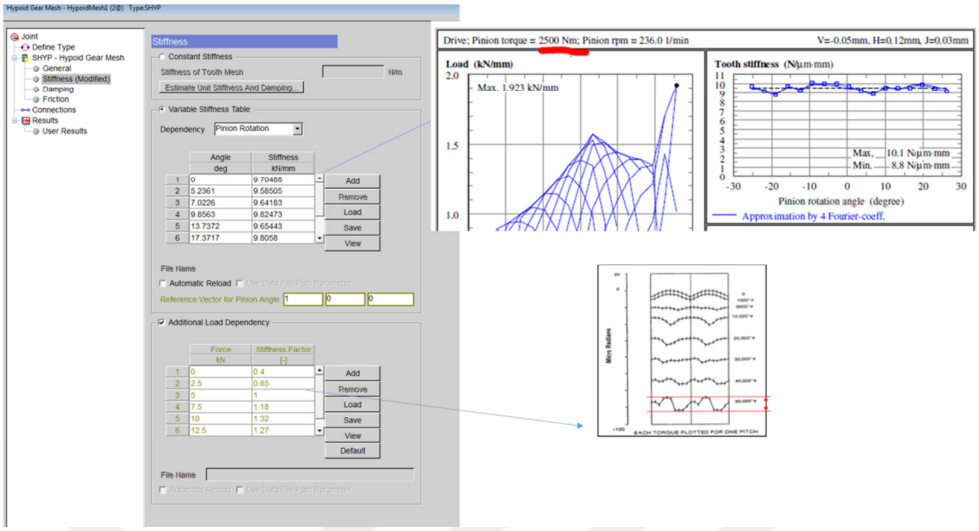

Figure 4. 13: AVL Excite force and stiffness setting screen.

Lastly, damping and friction values were defined in the model in the dynamic model. Damping value was used a constant damping value that was suggested for the cases similar with this one as shown in figure. For the friction factor also defined as constant value, which was calculated by KIMoS as 0,084, can be seen in figure 4.12

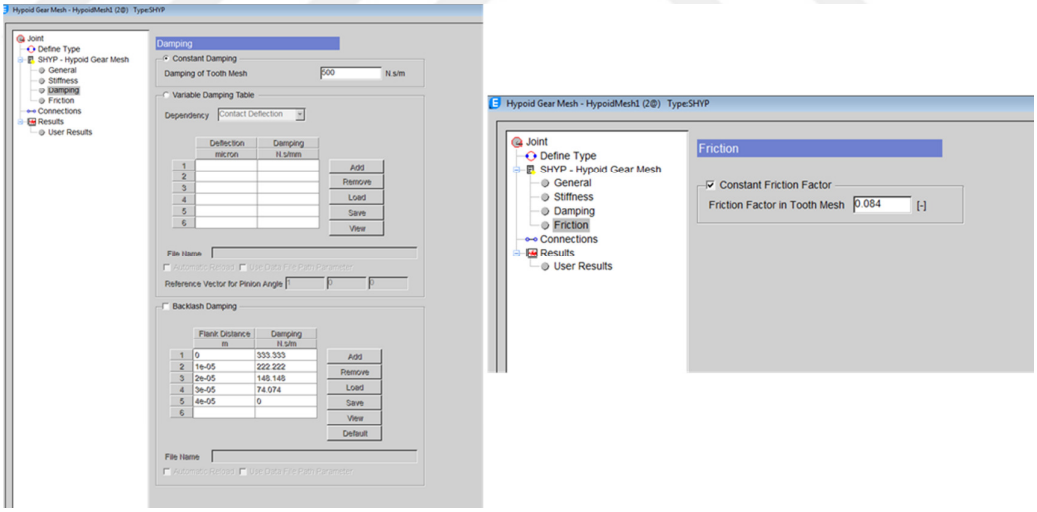

Figure 4. 14: AVL Excite damping and friction setting screen.

5. RESULTS AND COMPARISONS

In this chapter, results including vibration tests and modal tests introduced. Firstly, vehicle vibration test and data analysis results presented. Then comparison results between vehicle data and numerical tools vibration data are discussed. Lastly, model test results shared.

5.1 Vibration Test Results

5.1.1 Experimental test results

For this study, vehicle tests were performed with four different rear axles as given in details in chapter 3. Signal in time domain collected during the vehicle test were converted to physical quantity via LMS hardware and software. Sampling frequency was defined for vibration channels is 12800 Hz and for acoustic channel is 52400Hz. To prevent leakage, Hanning window was used as the windowing function. Then vehicle test was run in gears from 5th to 12th. Purpose of the increasing cycle number, minimum five runs were done for every test gear. After the measurements, data checked in time domain and compared to be sure data repeatibility and see run-to-run variations as shown in figure 5.1.

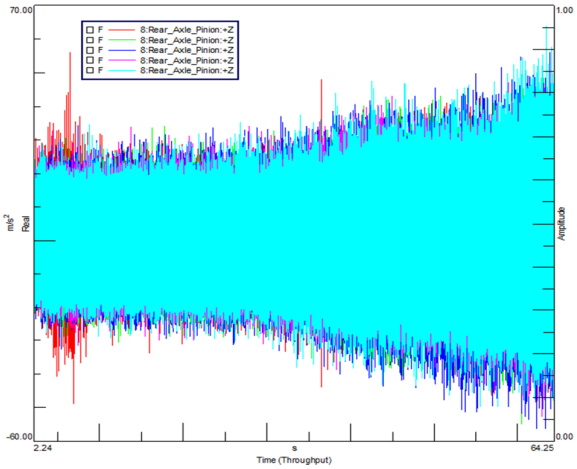

Figure 5. 1: Time data comparison to check run-to-run variations.

Second step before the post processing was that compared test data collected in different gears to define the most critical gear. As the most critical gear, 12th (maximum gear value for that transmission) gear detected based on subjective and objective assessment as expected. Then data post processing steps started. For the data post process, LMS Test Lab Time Data Processing module was used. Firstly, torque curves of runs collected in 12th were compared as shown in figure 5.2 to choose proper run for this study because torque fluctuations have important effect on gear whine.

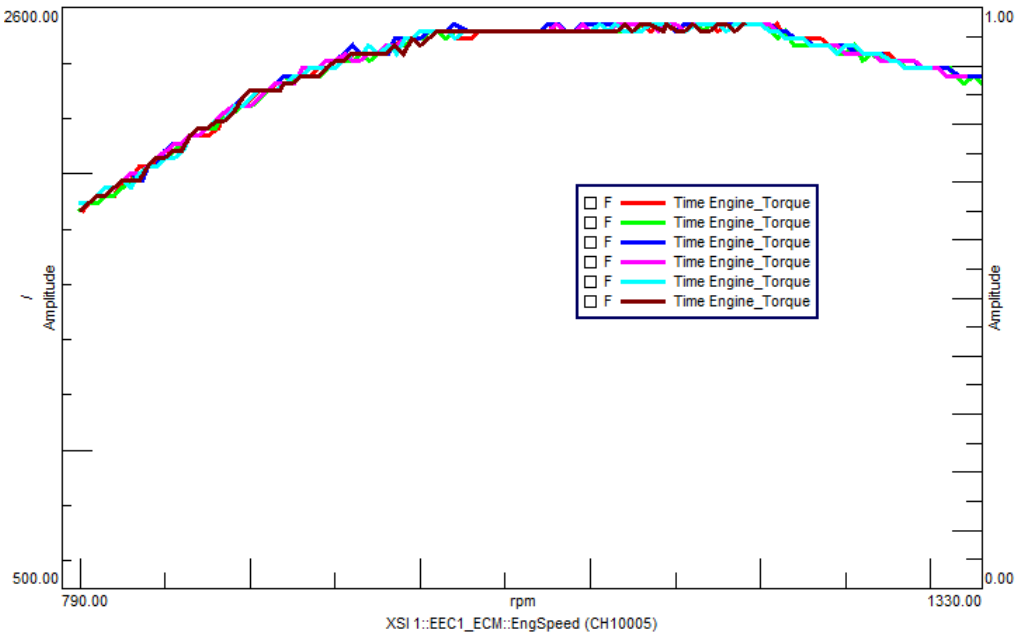

Figure 5. 2: Torque curves comparison.

As the second step, raw data was processed according to engine rpm purpose of choosing critical orders from waterfall and Campbell plots. Normally meshing orders for this axle should be 14th engine order and its harmonics. Whereas meshing orders can shift or side band can be higher amplitude. Critical orders were detected according to the processed data collected from the road test as shown in figure 5.3.

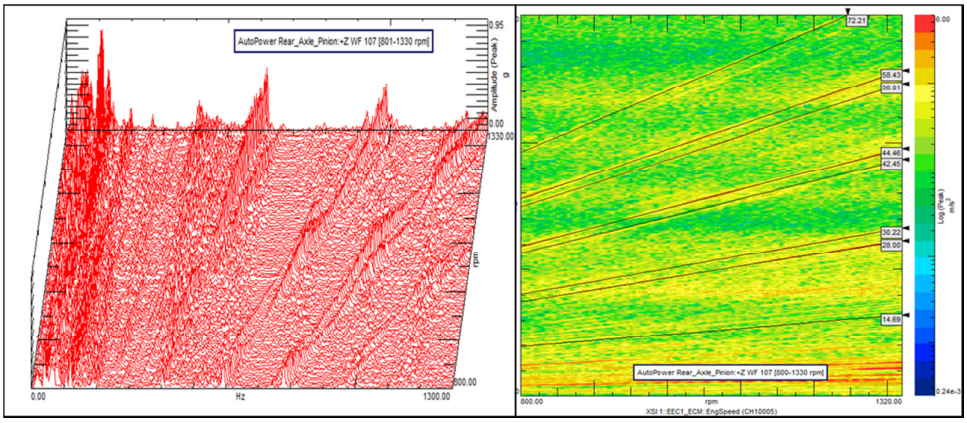

Figure 5. 3: Watefall plot and Campbell plot of axle 48 data to obtain the critical meshing orders.

Campbell and waterfall analyses performed for test data collected from the vehicle test with different axles. And then crtical orders determined due to the gear mesh orders that are show higer amplitude level in campbell diagram as seen in figure 5.4. Last two digit of serial number was used to define axles during the test and data processes.

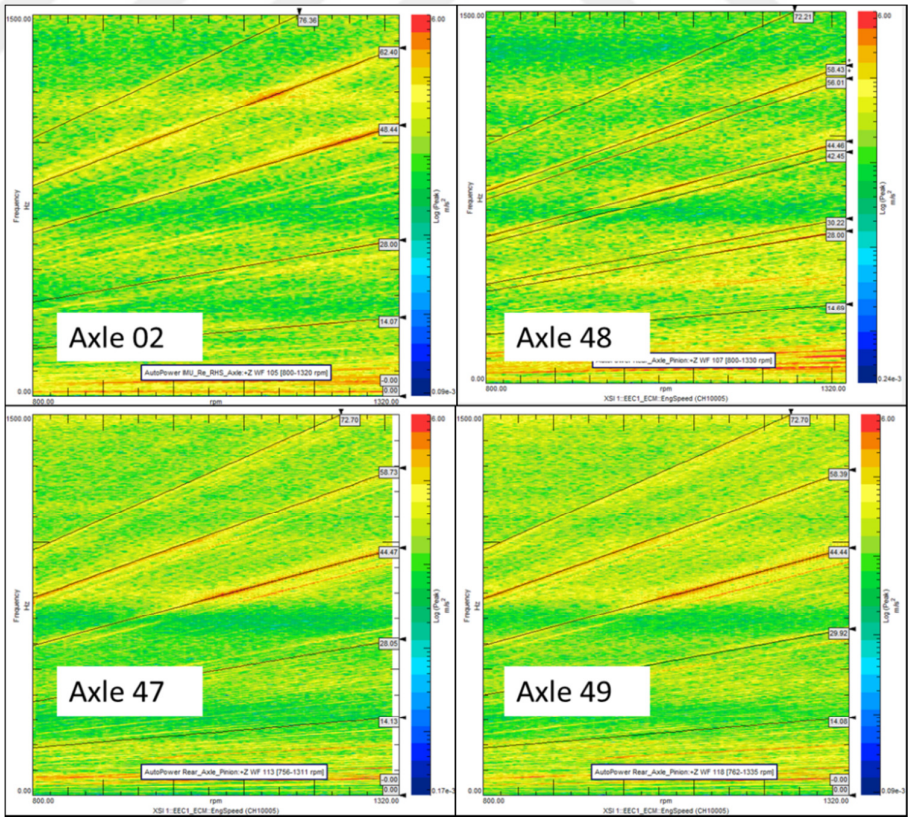

Figure 5. 4: Critical order selelection plots of all tested axles.

Firstly, the data collected from axle 49 vehicle tests was analyzed and critical orders 14.8th, 29.9th, 44.2th, 58.4th, and 72th engine order as excitation order for differential vibrations. Based on previous experiences and data comparison, vibration in z direction had higher amplitude and effect on whine noise. So that vibration levels cut in defined orders were presented in figure 5.5.

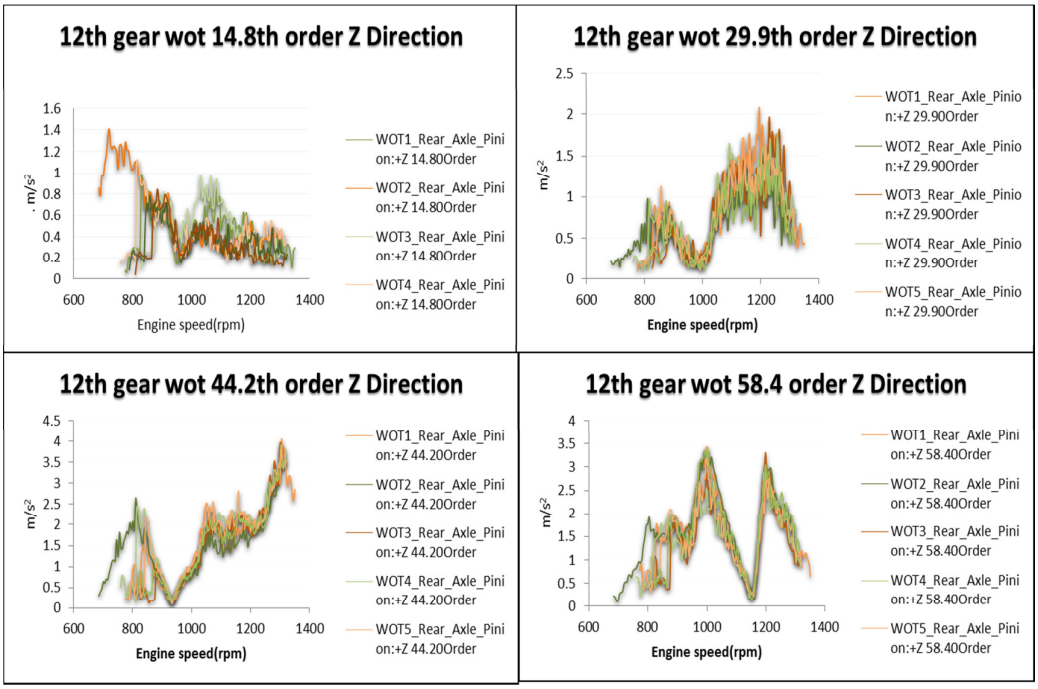

Figure 5. 5: Pinion nose vibration levels o in critical orders that was calculated with order analysis of axle 49.

For the axle 48, data analyzed by using FFT and Campbell analyses methods and critical orders obtained as 14th ,28th,30th,42th,44.5th , 55.90th,58.3th,72th engine orders. Here some of the orders were not harmonics of meshing order 14th order. As mentioned before, it caused by sideband orders that are mainly sourced from manufacturing errors or shifting main meshing order. As seen in figure 5.3 some of the selected orders have lower amplitude therefore 14th and 72th engine results were not used in data investigation. Vibration levels are calculated and presented below in figure 5.6.

Data collected from the vehicle test with axle 47 and 02 analyzed with same processing tools and vibration levels are investigated. For the axle 47, data analyzed by using FFT and Campbell analysis's methods and critical orders determined as 15th, 27.95th, 30.2th, 44.38th , 58.3th, 72.3th engine orders. Pinion nose accelerometer data in z direction analyzed in selected orders cut. As seen in figure 5.7, vibration

levels are presented in the plots that are vibration level in y-axis and engine speed in x-axis.

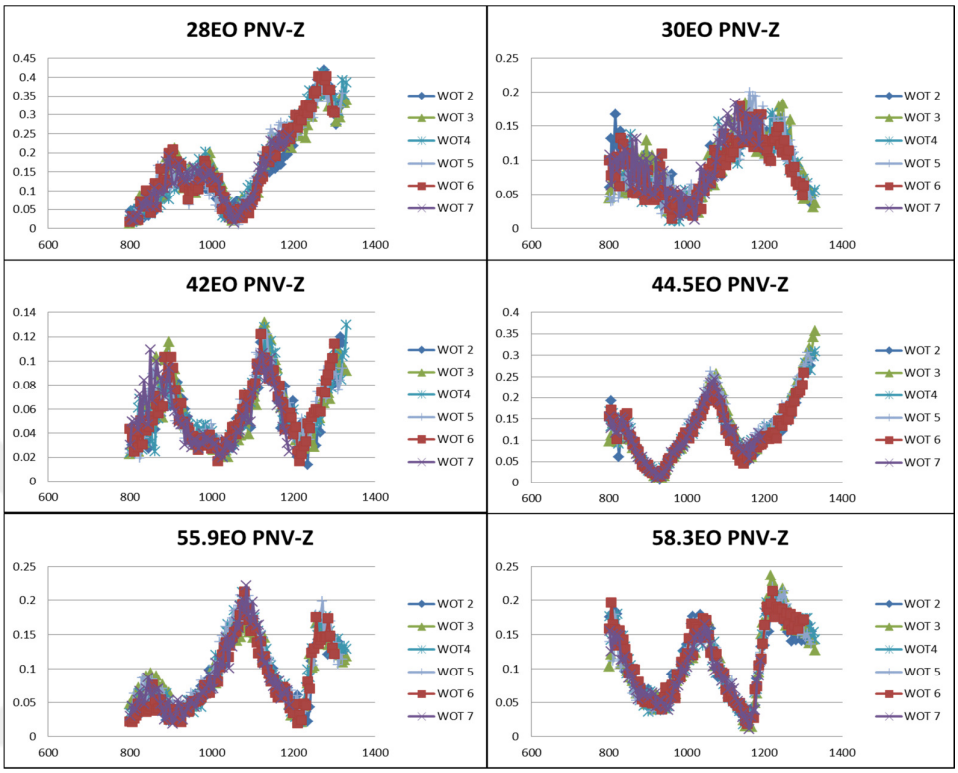

Figure 5. 6: Pinion nose vibration levels(m/s^2) according to engine speed (rpm) in critical orders that was calculated with order analysis of axle 48.

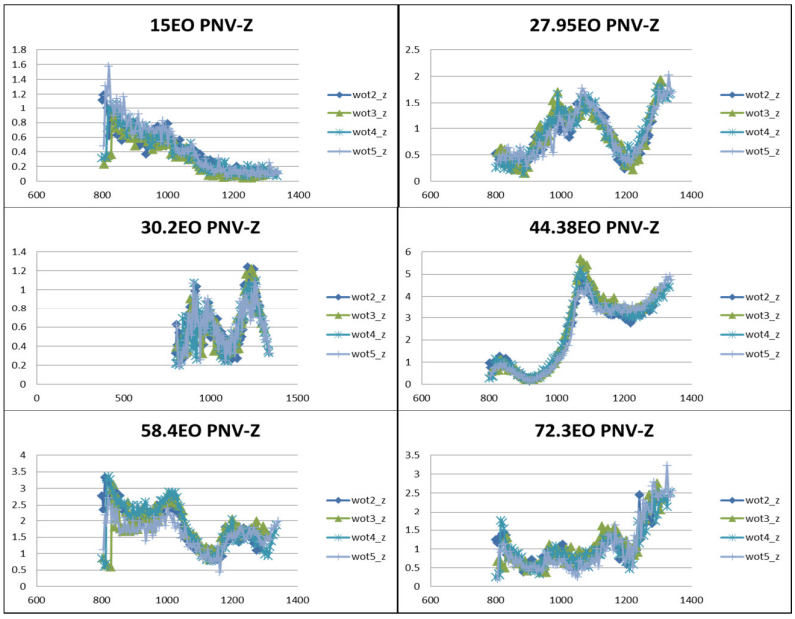

Figure 5. 7: Data results Pinion nose vibration levels(m/s^2) according to engine speed (rpm) for the axle 47, analyzed by using order analyses methods.

Similarly, road data belongs to axle 02 was analyzed and critical orders 14th, 28th, 48.5th, 62.5th, 76.5th were determined. Pinion nose vibration investigated as given below in figure 5.8.

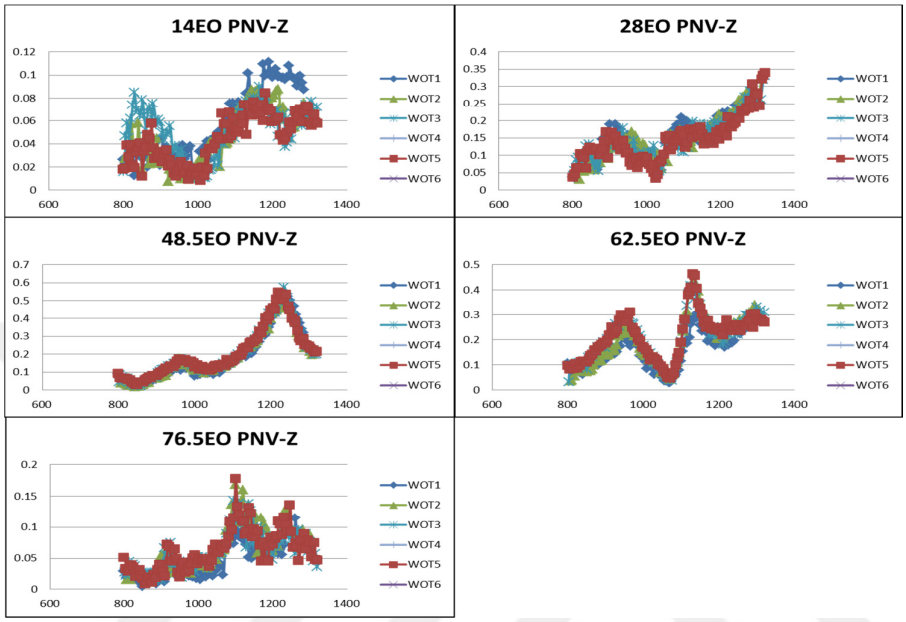

Figure 5. 8: Pinion nose vibration levels (m/s^2) according to engine speed (rpm) in critical orders that was calculated with order analysis of axle 02.

Tosional vibration data of the sensors on transmission output and differential input was processed by using order anylsis in 3rd engine order bcause of important effect of the engine on rotational fluctuations. Then results presented as seen figure 5.9 and figure 5.10.

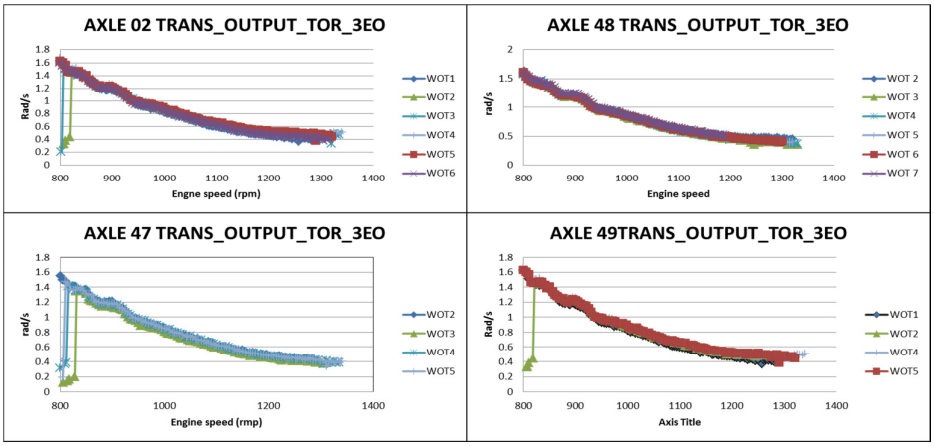

Figure 5. 9: Anaysis results of transmission output torsional vibration data in 3rd engine order.

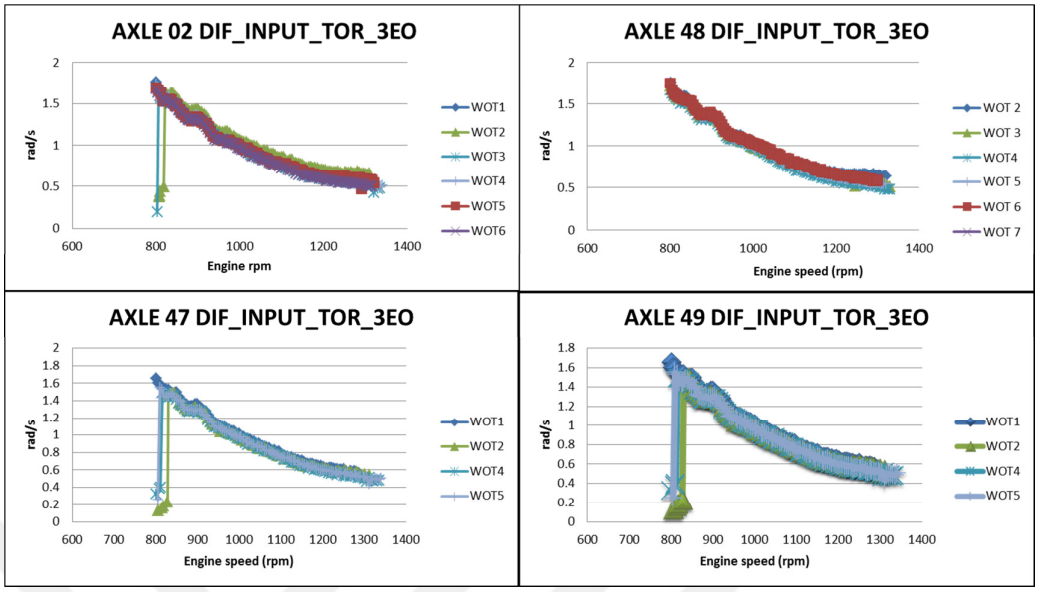

Figure 5. 10: Anaysis results of differantial input torsional vibration data in 3rd engine order.

5.1.2 Numerical study results

Purpose of the numerical investigation of the gear whine, multi body dynamic model was create by using AVL Excite as details mentioned in chapter 4. By using this model some iterations were performed to understand whine mechanicm.

Firstly effect of mesh stiffness on pinion nose vibrations are investigated as seen in figure 5.11. The corelation status of different mesh curves of the same pinioın-ring gear couple (difference occurs by entering different tooth combinations of each gear into KIMOS) vary less in curvature (modal sensitivity) more in amplitude, depending on the order population (%) of the mesh stiffness curve calculated by KIMOS. Physically, 14 pinion teeth can come in combination with 37 ring teeth (518 tooth combinations). Neither Klingelnberg measurement sytsem, nor KIMoS indicate the worst combination in terms of T.E, neither give the list of all possible combinations for that installed condition. So results can vary by used combination. Additionally, amplitude of mesh stffness has critical importance o vibration levels. By changing the amlitude levels of mesh stiffness, vibration levels can investigated as shown in figure 5.12.

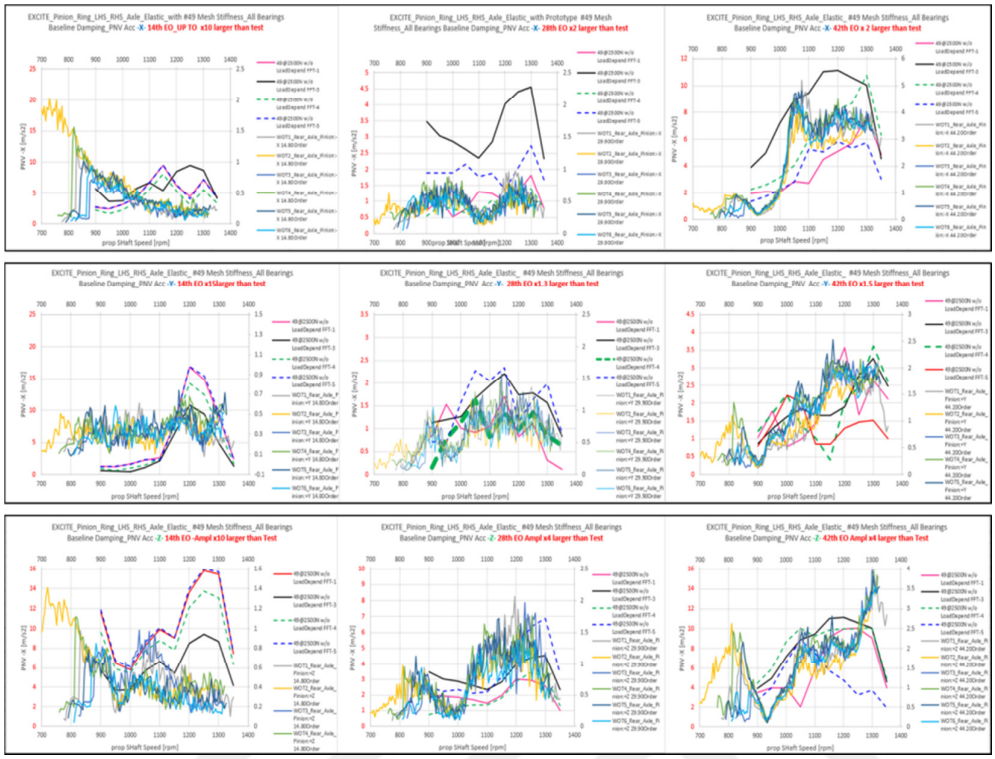

Figure 5. 11: Effect of mesh stiffness curve of different tooth combinations on rear axle vibrations in cirical orders.

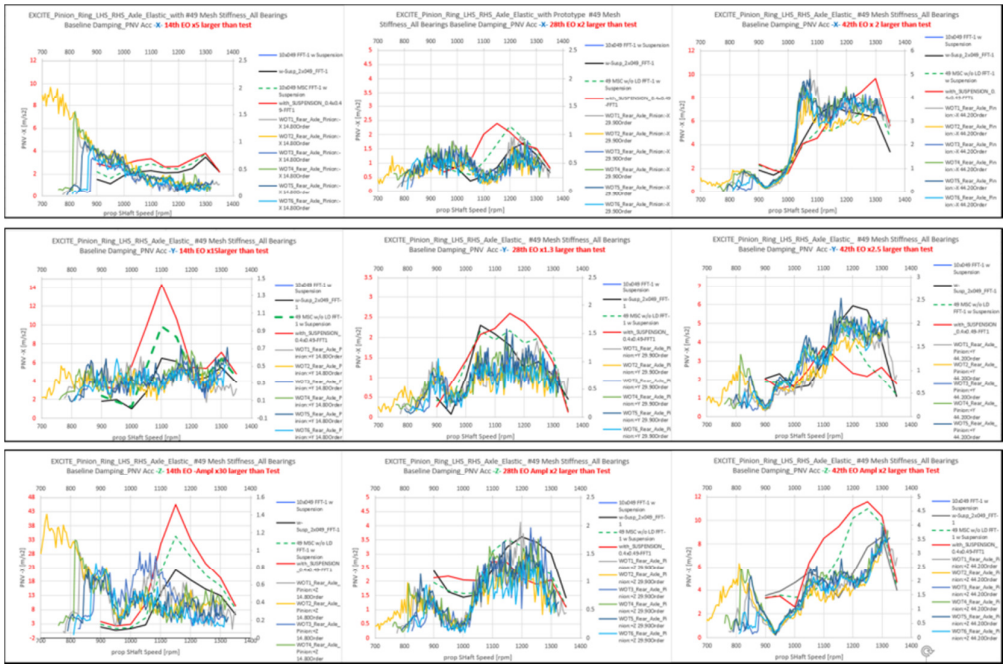

Figure 5. 12: Effect of mesh stiffness curve amplitude on axle vibrations.

Second iteration was done in dynamic model by changing driveshaft inclination. The corelation of inclined vs straight propshaft vary, in terms of curvature and amplitude, according to the order and direction.

Physically inclination of propshaft and its angle cause secondary tangential forces in U-Joints and lead to tooth contact area differences between pinion and ring gear, as well as dynamic mode differences, which both act on pinion-ring whine significantly

The extreme gap in 14th mesh order between test and CAE that twenty times (x20) is due to the mode at 250Hz. The gaps in x and y directions are related with the 1st order population of FFT.

Last iteraion with dynamic model was done to determine and optimize the effect of chasis and its conccestions. The mass effect of chassis, front suspension and cabin is superfluous. The amplitudes CAE vs Test dropped to 0.2x smaler in 14th Order, in 0.05 smaller in upper harmonics 28 and 42th Orders. With the new modes coming from Chassis the CAE curve characteristic doesn't even come close to the test results.

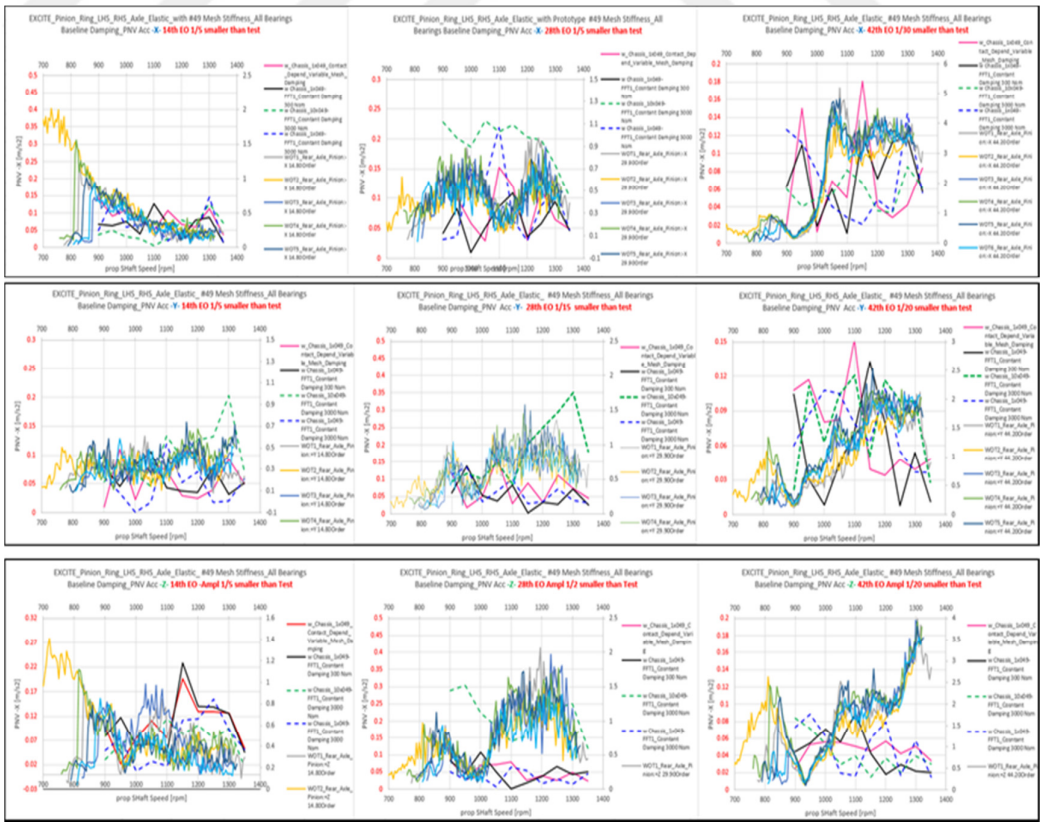

Figure 5. 13: Effect of chassis with varying mesh stiffness and damping factors**.**

5.2 Modal Test Results

5.2.1 Rear axle modal test results

Rear axle modal test process are presented in dails in chapter 3. In this section test results are introduced . Summary of test condition and frequency response functions in figure 5.14 are as given below;

- Both Impact and Shaker Tests are performed.
- 13 acceloremeters are used to generate mode shapes.
- 1st and 2nd bending modes are calculated.

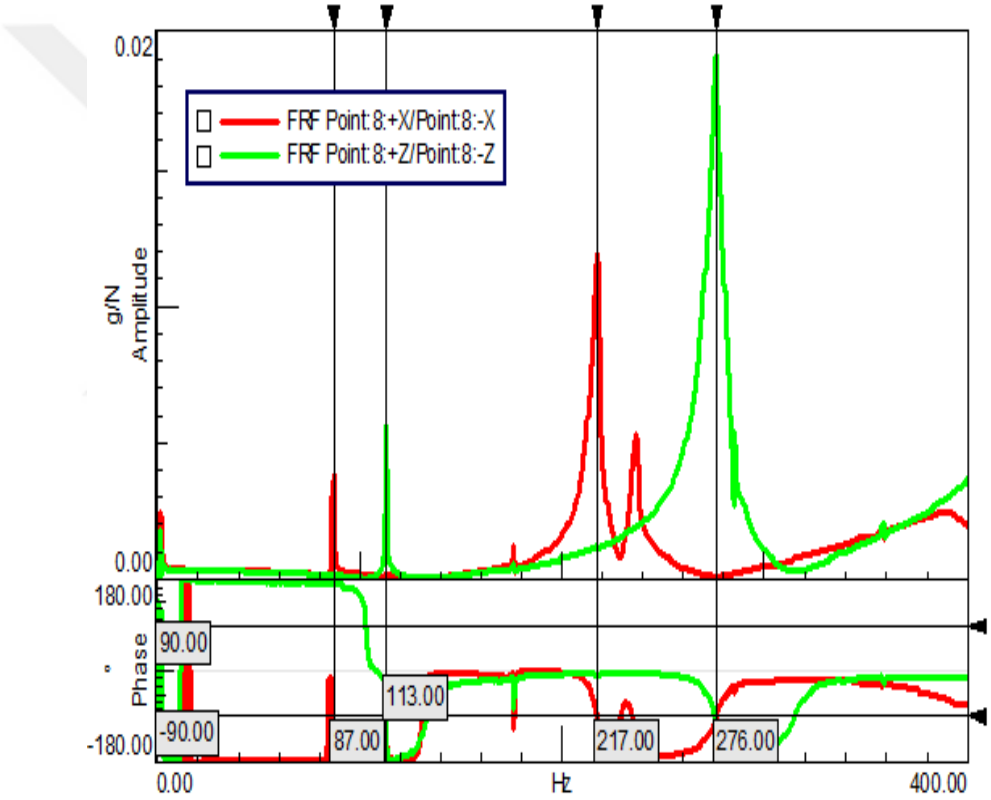

Figure 5. 14: Frequency response function measured from rear axle.

Then mode shapes calculated by using LMS Test Lab. Modal analysis module. Moreover, result compared with finite element analysis results in figure 5.15 and figure 5.16.

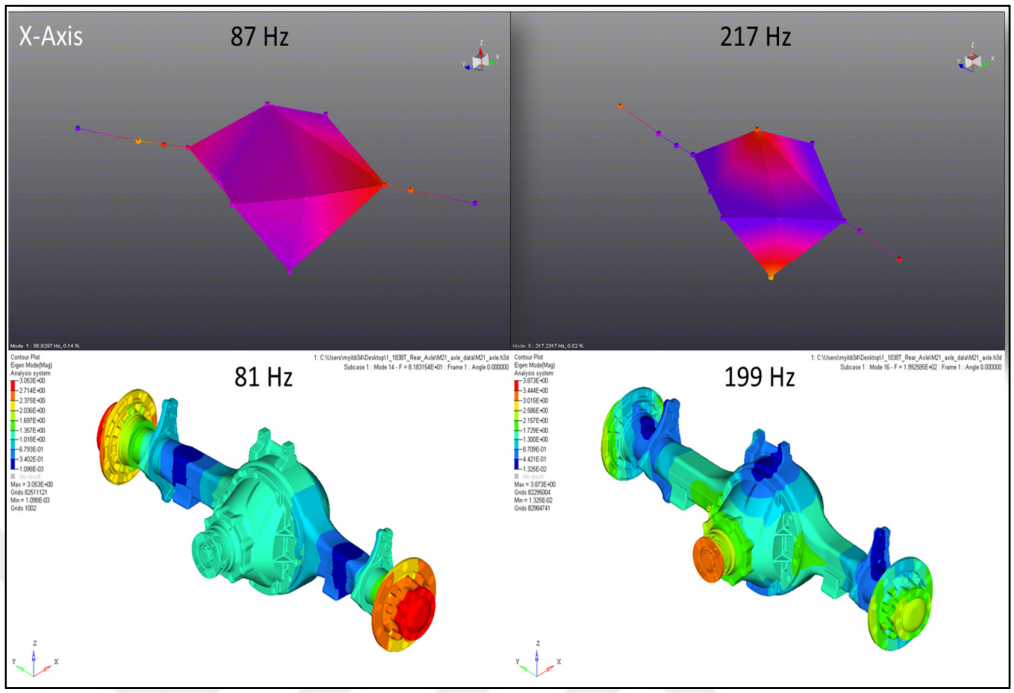

Figure 5. 15: Rear axle mode shapes results of both test and finite element analysis in x- direction (accoring to global vehicle coordinate system)

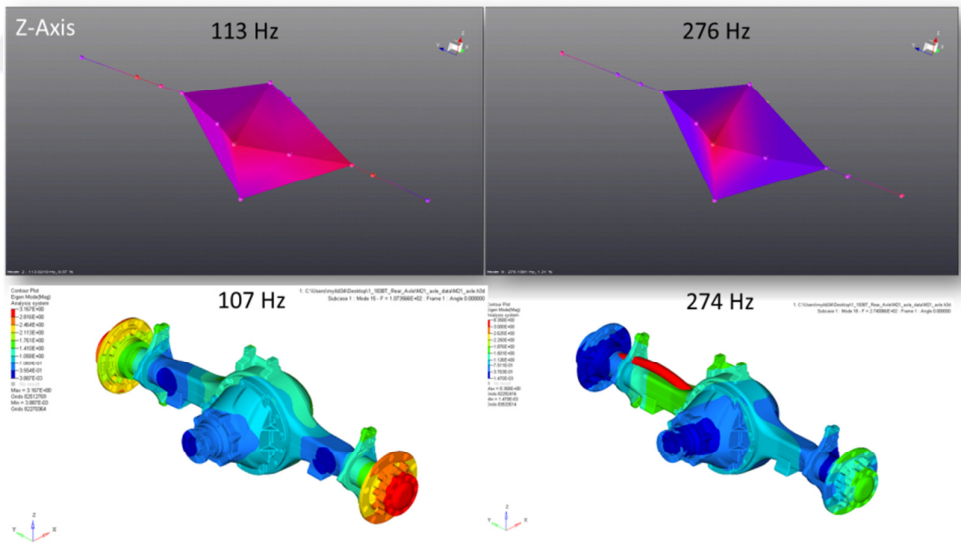

Figure 5. 16: Rear axle mode shapes results of both test and finite element analysis in z- direction (accoring to global vehicle coordinate system).

5.2.2 Rear axle cut housing modal test

As second step of the rear axle, modal test was that cut axle housing and test done on inner components. For this study, housing of the axle was cut and instrumented as given in chapter 3. Firstly half shafts were testes and LHS half shaft frequency response functions as shown in figure 5.17 were collected and mode shapes were calculated can be seen in figure 5.18.

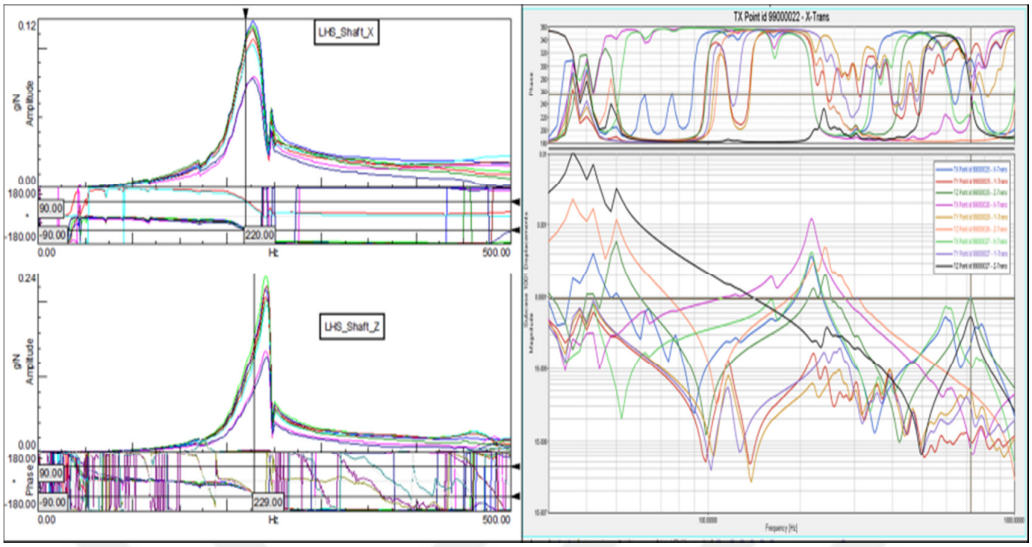

Figure 5. 17: Frequency response functions which obteined by test (left) and finite elements method tools (right) of left half shaft .

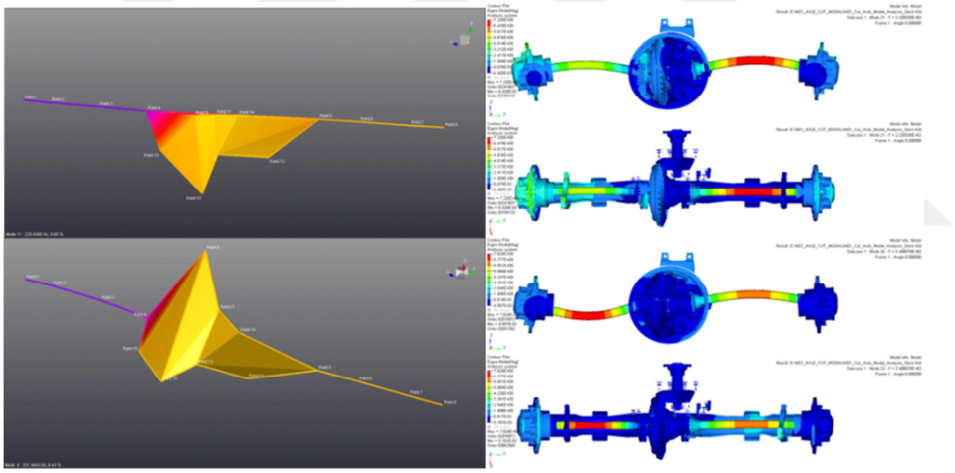

Figure 5. 18: Mode shapes calculated with test data (left) and finite element method tools (right).

Similarly modal analysis was applied to RHS half shaft with test and CAE tools and FRFs collected as seen in figure 5.19 and mode shapes were calculated can be seen in figure 5.20.

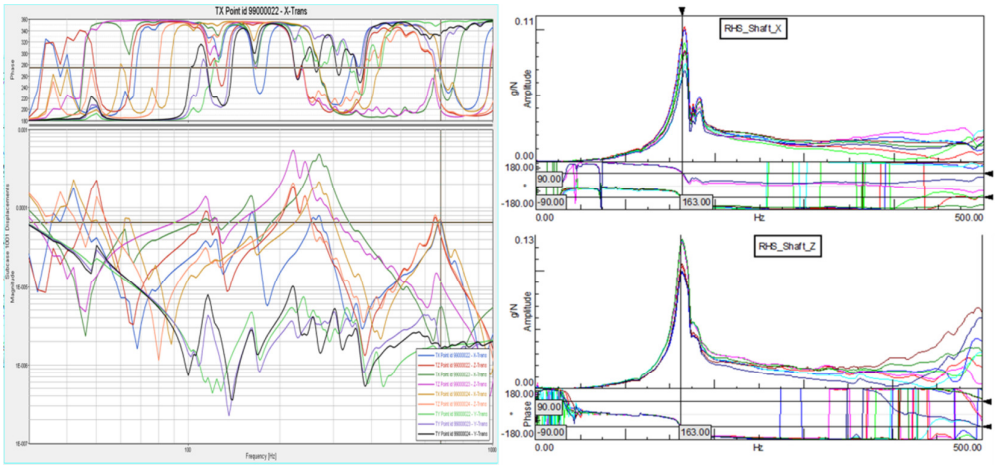

Figure 5. 19: Frequency response functions which obteined by test (left) and finite elements method tools (right) of right half shaft .

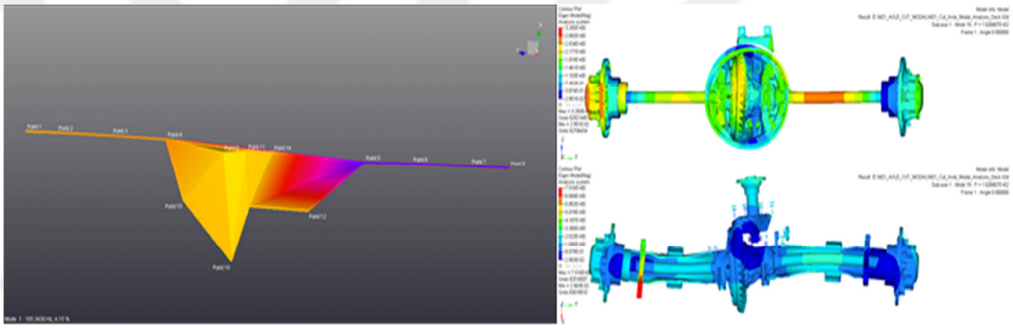

Figure 5. 20: Mode shapes calculated with test data (left) and finite element method tools (right).

Then test and CAE analysis were applied to define mode shapes of the gear set as seen in figure in 5.21.

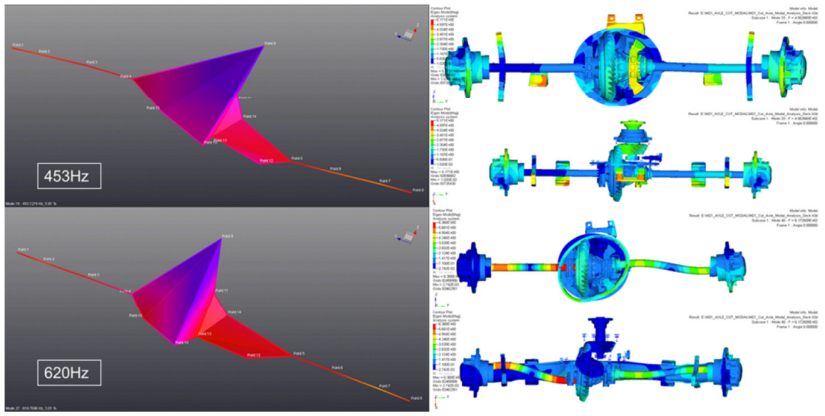

Figure 5. 21: Mode shapes calculated with test data (left) and finite element method tools (right).

5.2.3 Inner shaft modal test results

Nest step for the modal test was for inner half shafts as free-free condition. Right and left shafts tested one by one and frequency response functions measured can be seen in figure 5.22.

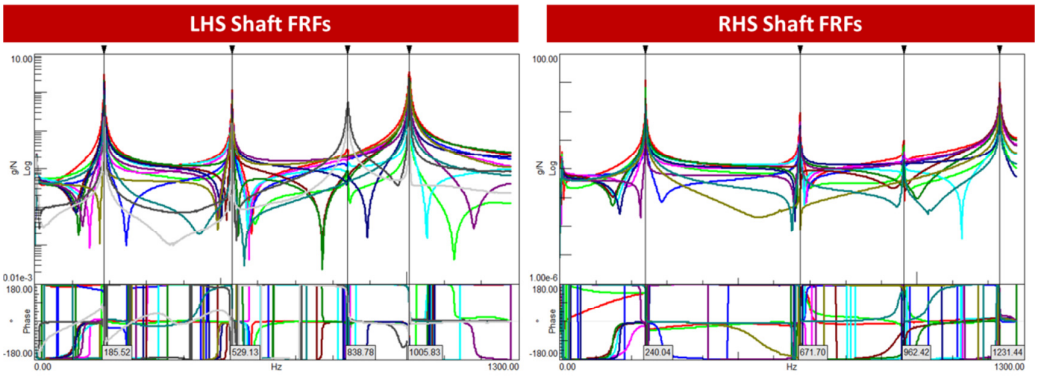

Figure 5. 22: Frequency response functions which obteined by test (left) and finite elements method tools (right) of rear axle inner shafts.

Based on measured FRFs mode shapes were determined with LMS Test Lab and then natural frequency analysis was performed in Msc Nastran and mode shapes calculated as shown in figure 5.23.

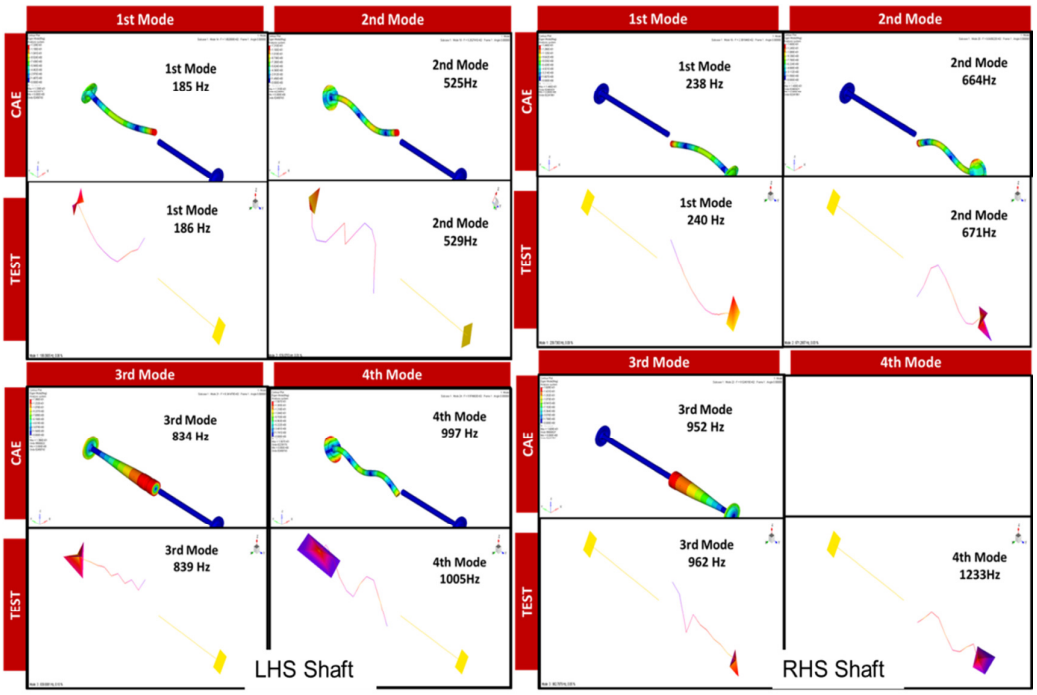

Figure 5. 23: Mode shapes measured by test and finite elements method tools of rear axle inner shafts.

5.2.4 Driveshaft modal test results

Drive shaft is the ctirical part on the transfer path of the gear whine. So modal features, FRFs were determined in free-free condition by using test method and FEM tool as seen in figure 5.24.

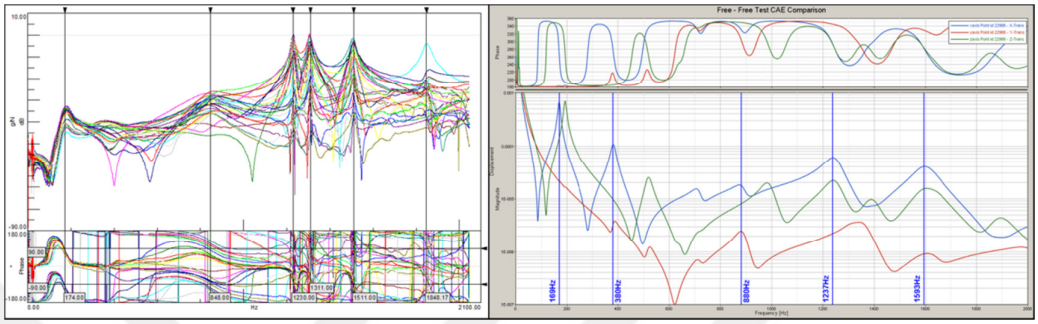

Figure 5. 24: Driveshaft FRFs which obteined by test (left) and finite elements method tools (right).

Then calculations of the modal parameters were done in both test method and FEM. As a result, natural frequencies and mode shapes were obtained as shown in figure 5.25.

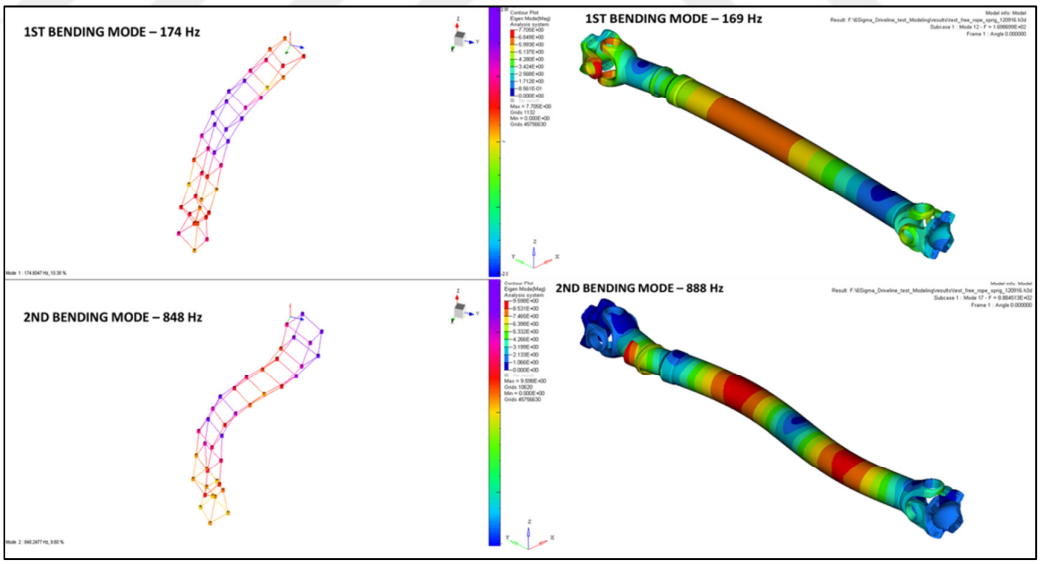

Figure 5. 25: Drive shaft's natural frequency values and mode shapes.

6. CONCLUSIONS

In this study, rear axle gear whine is studied as noise and vibration concern in two main approaches experimental and numerical. Firstly, experimental study was conducted as modal analysis and road test. Before the vehicle level test, modal characteristics of driveline components that have crucial effect on rear axle vibrations were investigated in free-free condition and as installed condition. Thereafter, road tests were performed with the Ford Trucks vehicle, which is 4x2 RWD with 2.67 FDR. Four prototype axles that are designed and produced considering to the different parameters of the micro and macro geometry of gear teeth so they have different TE values were measured in critical gears. Secondly, numerical investigation of the axle whine studied. For this, finite element model in NASTRAN was built. Then dynamic transmission error and mesh stiffness curves were calculated by using KIMOS. As the final step, multi-body dynamic model of driveline system was created by using AVL Excite. Vibration data collected from pinion nose was analyzed in meshing orders of gear pair. Based on modal test results, FEM models correlated and natural frequency analyses were performed for tested components in same boundary conditions. Modal parameters such as damping, mode shapes, and natural frequencies are determined to use in dynamic model. Dynamic analysis results of axle vibrations are compared with test results.

Results showed that vibration levels on pinion nose of the rear axle in meshing orders of gear pair are quite high. In addition, higher vibration region is varying with tested axles, which have different transmission error values. Nonetheless, acoustic performances of the tested axles are quite similar and whine noise is not audible in vehicle cabin based on microphone data. Additionally, tooth mesh stiffness curves of the tested axles are calculated nearly same though their transmission errors are different from each other. So creating a correlated experimental and numerical whine model was not completed for this vehicle and powertrain variant. Thus, it was determined that performing the test with same procedures on different vehicle variant, which detected as whine critical according to customer and quality team

reports. Similarly, multi-body dynamic model are rebuilt with new powertrain components and vehicle systems.

REFERENCES

[1] **Rahnejat, H.** (1998). Multi-body dynamics: vehicles, machines and mechanisms, PEP(IMECHE) and SAE Co-publishers, London, UK / Warrendale Pa, USA.

[2] **Kanda, Y., Saka, T., Fujikawa, M. & Ando, K. (**2005). Experimental transfer path analasis of gear whine. *Noise and Vibration Conference and Exhibition*, no. 2005-01-2288.

[3] **Colabawala, M., Sorenson, J. Houser, D.** (2003). An experimental procedure for characterization of gear whines noise in a variety of vehicle applications. *SAE*, 2003-01-1488.

[4] **Becker, S. and Yu, S.** (1999). Objective noise rating of gear whine. *SAE*, 1999-01-1720.

[5] **Jacobson, M.F., Singh, R and Oswald, F.B.**(1996). Acoustic radiation efficiency models of a simple gearbox, NASA Technical Memorandum 107226.

[6] **Kahraman, A. and Singh, R.**(1991). Interaction between time-varying mesh stiffness and clearance non-linearity's in a geared system, Journal of sound and vibration 146(1):135-156.

[7] **Robinette, D., Beikmann, R. S., Piorkowski, P, and M. Powell.**(2009). Characterizing the onset of manual transmission gear rattle part 1: experimental results, SAE Paper 2009-01-2063.

[8] **Singh, R., He, S., Povic, G.**(2007). Improved gear whine model with focus on friction-induced structure borne noise, NOISE-CON 2007.

[9] **Akerblom, M.**(2002). Gear noise and vibration – influence of gear finishing method and gear deviations, Licentiate thesis, Royal Institute of Technology, Stockholm.

[10] **Maheedhara, S.S. and Pourboghrat, F.** (2007). Finite element analysis of composite worm gears, Journal of Thermoplastic Composite Materials,Vol, 20-January 2007.

[11] **Houser, D., Harianto, J.** (2004). Determining the source of gear whine noise, http://www.gearsolutions.com/media//uploads/assets/PDF/Articles/2004-02-01_Determining_the_Source_of_Gear_Whine_Noise.pdf, [Accessed 10 March 2019]

[12] **Curtis, S., Pears, J., Palmer, D., Eccles, M., Poon, A., Kim, M., Jeon, G., Kim, J., Joo, S.** (2005). An analytical method to reduce gear whine noise, including validation with test data, SAE Technical Paper 01 (1819) (2005) 1-10.

[13] **Dunn, A.L., Houser, D. & Lim, T.C.** (1999). Methods for researching gear whine in automotive transaxles, SAE paper 1999-01-1768.

[14] **Welbourn, D. B.** (1998). Fundamental knowledge of gear noise - a survey, Proc. Noise &Vib. of Eng. and Trans., I Mech E., Cranfield, UK, July 1979, pp 9–14.

[15] **MackAldener, M.** (2001). Tooth interior fatigue fracture & robustness of gears", royal institute of technology, Doctoral Thesis, ISSN 1400-1179, Stockholm.

[16] **Houser, D.** (1967). *Dudley's Gear Handbook,* 2nd edn, Lewis Research Center, NASA.

[17] **Sun, Z., Steyer, G. & Ranek, M.** (2002). FEA studies of axle system dynamics, *World Congress*, no. 2002-01-1190.

[18] **Hirasaka, N., Sugita, H., Asai, M.**(1991). A simulation method of rear axle gear noise, Journal of Passenger Cars 100, 1383–1387.

[19] **Donley, M.G., Lim, T.C., Steyer, G.C.**(1992). Dynamic analysis of automotive gearing systems, Journal of Passenger Cars 101 (1992) 77–87.

[20] **Tadashi, T. & Kazuhide, T.** (2004). Gear whine analysis with virtual power train, *Mitsubishi Motors Technical Review,* vol. 16.

[20] **Campbell, B.** (1997). Gear noise reduction of an automatic transmission through finite element dynamic simulation, no. 971996

[22] **Özgüven, H., Houser, D.**(1988). Dynamic analysis of high speed gears by using loaded transmission error, Journal of Sound and Vibration 125 (1) (1988) 71-83.

[23] **Lee, S., Go, S., Yu, D., Lee, J. & Kim, S.** (2005). Identification and reduction of gear whine noise of the axle system in a passenger van, *Noise and Vibration Conference and Exhibition*, no. 2005-01-2302.

[24] **Chung, C., Steyer, G., Takeshi, A., Clapper, M. & Shah, C.** (1999). Gear noise reduction through transmission error control and gear blank dynamic tuning, *Noise and Vibration Conference and Exhibition,* no. 1999-01-1766.

[25] **Harris, S.L.** (1958). Dynamics loads on the teeth of spur gears, Proc. Insdt. Mech. Eng., Vol 172, 1958, pp87-112.

[26] **Maki, H.** (1999). A study on optimum tooth modifications of helical gears under various loads, *International Congress and Exposition*, no. 1999-01-1053.

[27] **Newland, D.E.** (1984). An introduction to random vibrations and spectral analysis, 2nd edition, Longman, London & New York.

[28] **LMS Test Lab**. (2018). Digital signal processing training, Training Documents, Istanbul.

[29] **Ewins, D. J.** (2000). *Modal testing: theory, practice and applications (2nd Ed.),* Research Studies Press LTD, Hertfordshire, England.

[30] **Url-1** <*http://www.community.plm.automation.siemens.com*>, date retrieved 29.03.2019.

[31] **Url-2** <*http://www. fordtrucks.com.tr*>, date retrieved 10.04.2019.

[32] **Url-3** <*http://www.fuwa.cn*>, date retrieved 15.04.2019.

[33] **Url-4** <*http://www.fordotosan.com.tr*>, date retrieved 15.04.2019.

[34] **Url-5** <*http://www.kistler.com*>, date retrieved 15.04.2019.

[35] **Url-6** <*http://www.bksv.com*>, date retrieved 16.04.2019.

[36] **Url-7** <*http://www.fluke.com*>, date retrieved 16.04.2019.

[37] **Url-8** <*http://www.dytran.com*>, date retrieved 18.04.2019.

[38] **Url-9** <*http://www.plm.automation.siemens.com*>, date retrieved 18.04.2019.

[39] **Dunn, A., Lim, T.** and **Houser, D.** (1999). Methods for researching gear whine in automotive transaxles, *SAE,* 1999-01-1768, 1999.

CURRICULUM VITAE

Name Surname **:** Mehmet DEMIREL

Place and Date of Birth **:** Tokat, 30.08.1987

E-Mail **:** mehmetdemirel30@gmail.com

EDUCATION **:**

- **B.Sc.** **:** 2012, Istanbul Technical University, Mechanical Enginering Faculty, Mechanical Engingineering Department

PROFESSIONAL EXPERIENCE AND REWARDS:

- **Work Experience** **:** Ford Otosan Product Development Engineer **2013-**